

Galaxy Distances, Peculiar Motions, and 3-D Structure in the Nearby Universe

John Blakeslee

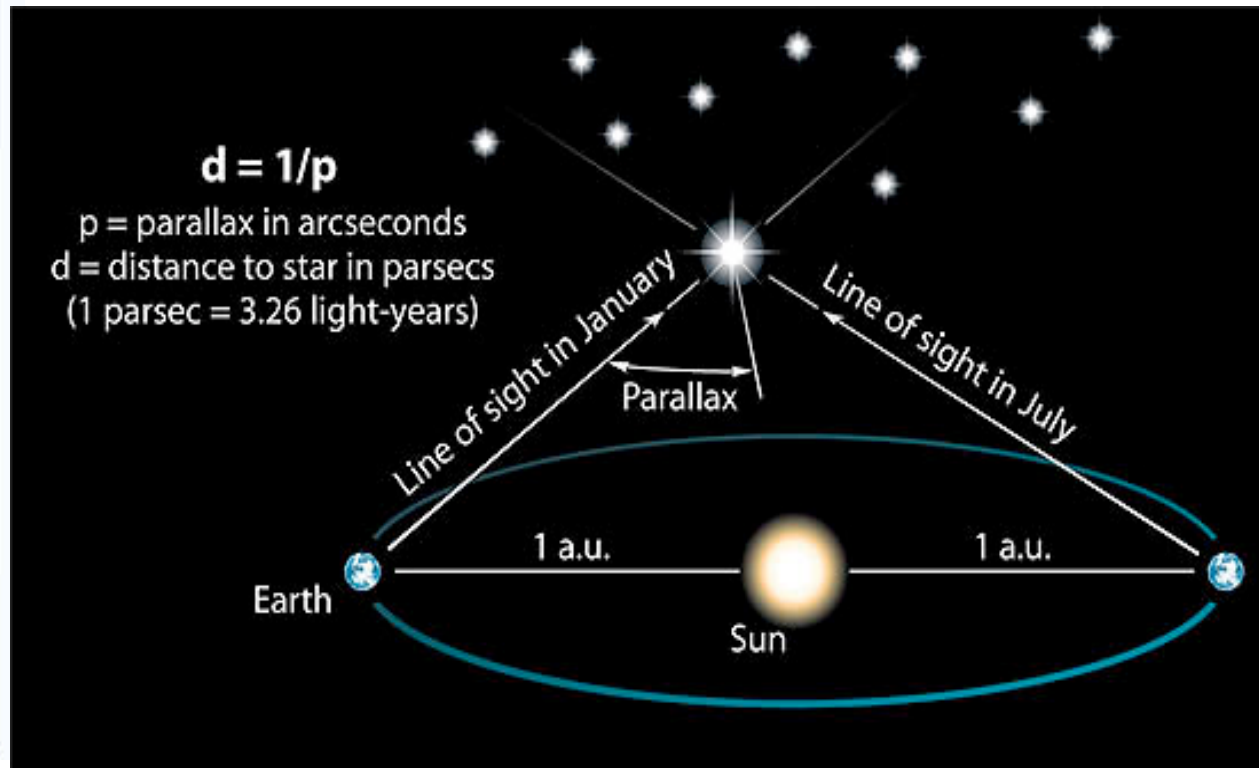
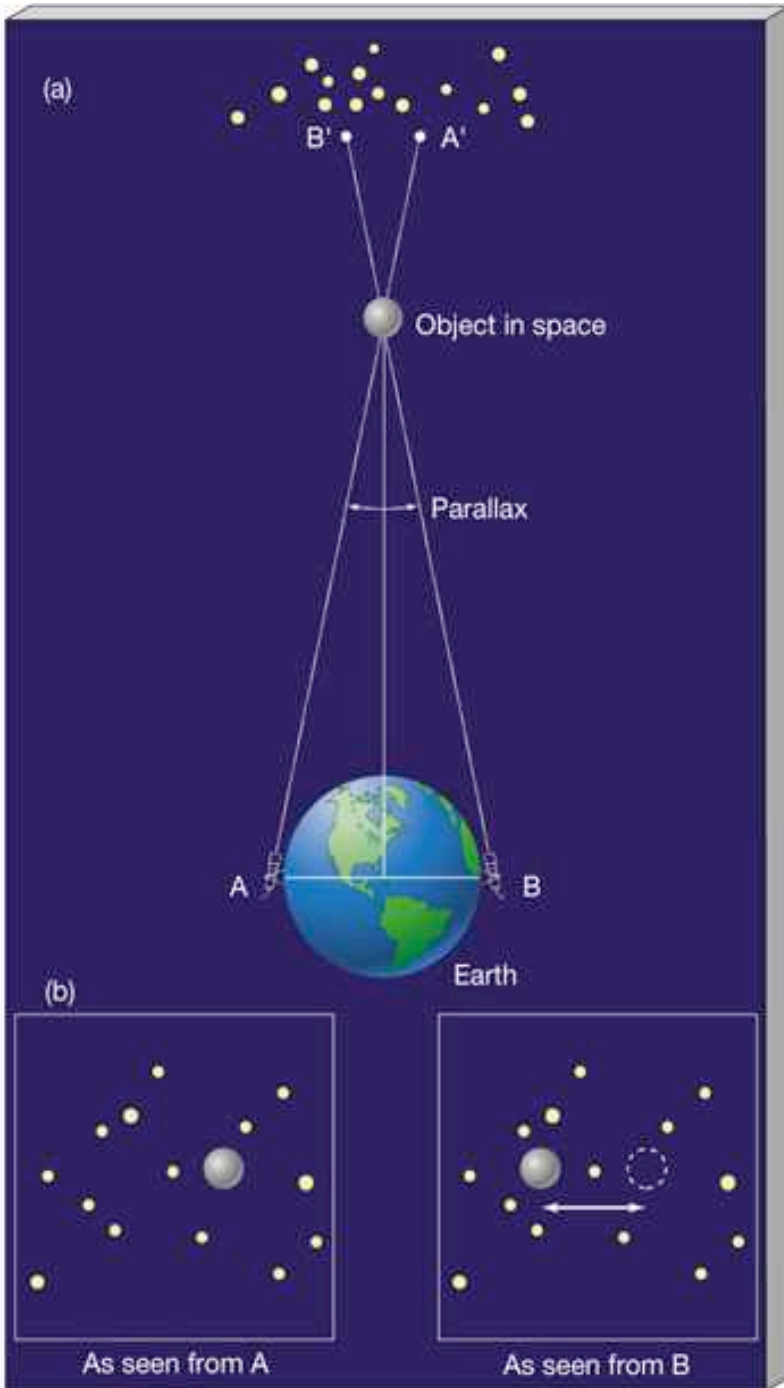
NRC Herzberg Institute of Astrophysics

Talk Overview

- An quick review of distance measurement.
- The “Hubble Law” and peculiar velocities.
- Some popular distance indicators.
- The SBF method in detail.
- A digression on interpolation kernels
- SBF in the ACS Virgo and Fornax Surveys
- SBF in the near-Infrared & Adaptive Optics
- Peculiar Motions and Bulk Flows

Parallax

Because even the nearest stars are very far away, we need the longest possible baseline: two opposite locations on the Earth's surface can give the distance to a satellite, but two widely separated points during the Earth's orbit are needed for measure stellar parallaxes.



Parallax

★ It is useful to define the **parsec** as a unit of distance:

- 1 parsec (1 pc) = distance a star must have for its annual *parallax* to be 1 **arcsec**:

$$\begin{aligned}1 \text{ pc} &= 206,265 \text{ A.U.} \\ &= 3.1 \times 10^{18} \text{ cm} \\ &= 3.26 \text{ light years}\end{aligned}$$

(# arcsec/radian)

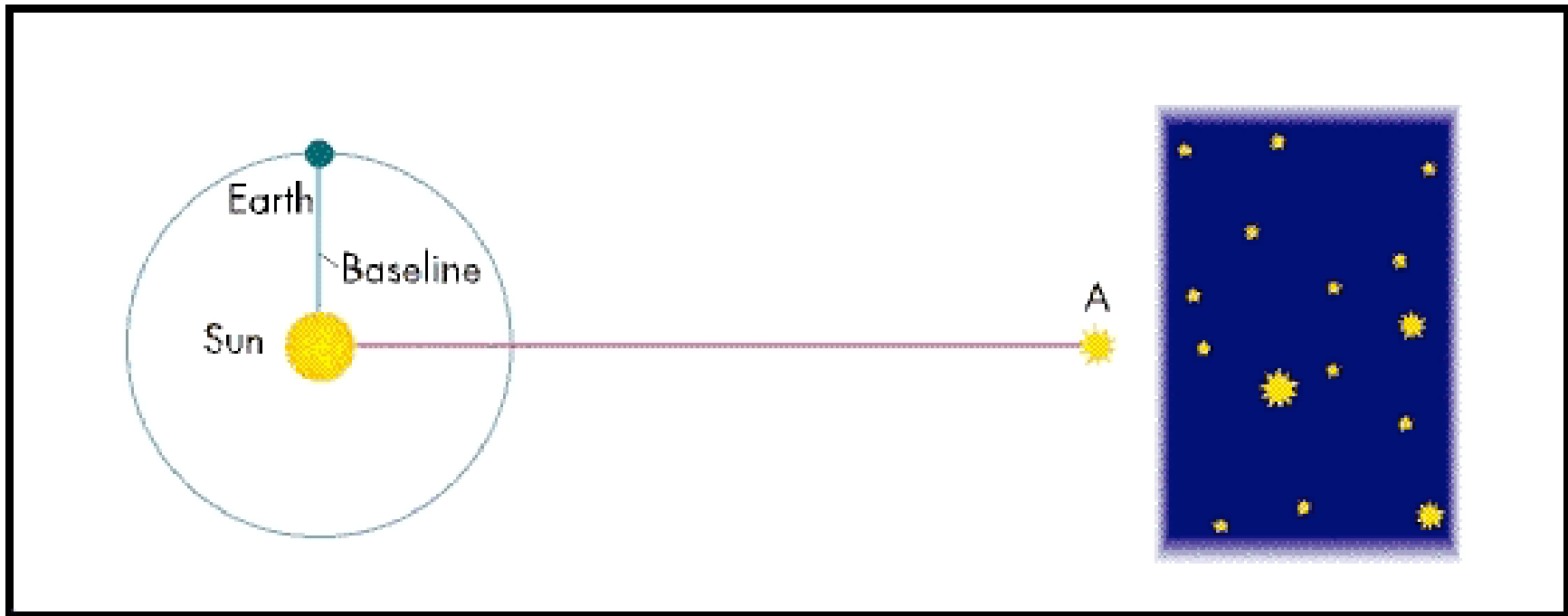
★ It follows that if the parallax is measured in arcseconds (″), and the distance is measured in parsecs (pc), then:

$$p = \frac{1}{d}$$

Parallax

- ★ If the **parallax** (p) is given in arcsec, then the **distance** (d) in *parsec* can be found very simply from:

$$d = \frac{1}{p}$$



If only Earth's orbit were bigger!

Parallax

- ★ Because even the nearest stars are very far away, the largest stellar parallaxes are very small:
 - The nearest star *Alpha Centauri* has a parallax of just 0.76 arcsec. Stellar parallaxes cannot be measured with the naked eye!
 - So, Alpha Centauri's distance is:
 $d = 1/0.76 = 1.3 \text{ pc} = 4.2 \text{ ly}$
- ★ The first parallax was observed in 1837 (by Friedrich Bessel) for the star 61 Cygni.

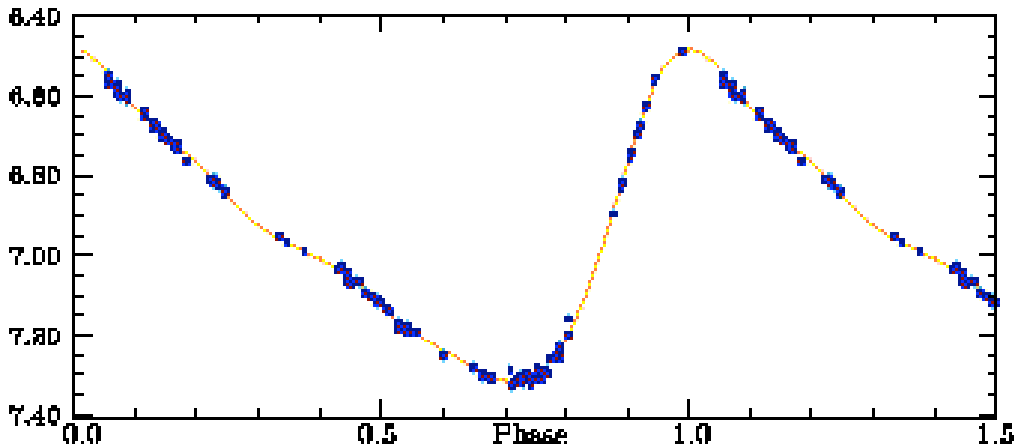


Friedrich Bessel

Measurements of Parallaxes

- ★ Ground-based instruments can measure parallaxes to 0.01 arcsec.
 - *This is like measuring a quarter from a distance of about 40 miles.*
 - Therefore, from the ground we can only measure parallaxes to stars within 100 parsecs. ***This includes only about ~100 stars.***
- ★ The **Hipparcos satellite** (in orbit 1989-1993) measured parallaxes down to 0.001 arcsec, or out to 1000 parsecs = 1 kpc. This included 100,000 stars at 10% accuracy. (HST has similar capability).
- ★ ESA's **GAIA** (Global Astrometric Interferometer for Astrophysics) satellite (to launch in 2011) will measure parallaxes to 10^{-5} arcsec
 - *This requires being able to measure the width of a human hair from a distance of 2500 miles (4000 km)!*
 - Should measure parallaxes for a billion stars (1% of the Milky Way galaxy) and the Magellanic Clouds (50 kpc). ***This would remove the major lingering uncertainty in the Cepheid distance scale.***

Henrietta Swan Leavitt and the Cepheid Period-Luminosity Relationship



Light curve of a Cepheid variable



Large & Small Magellanic Clouds

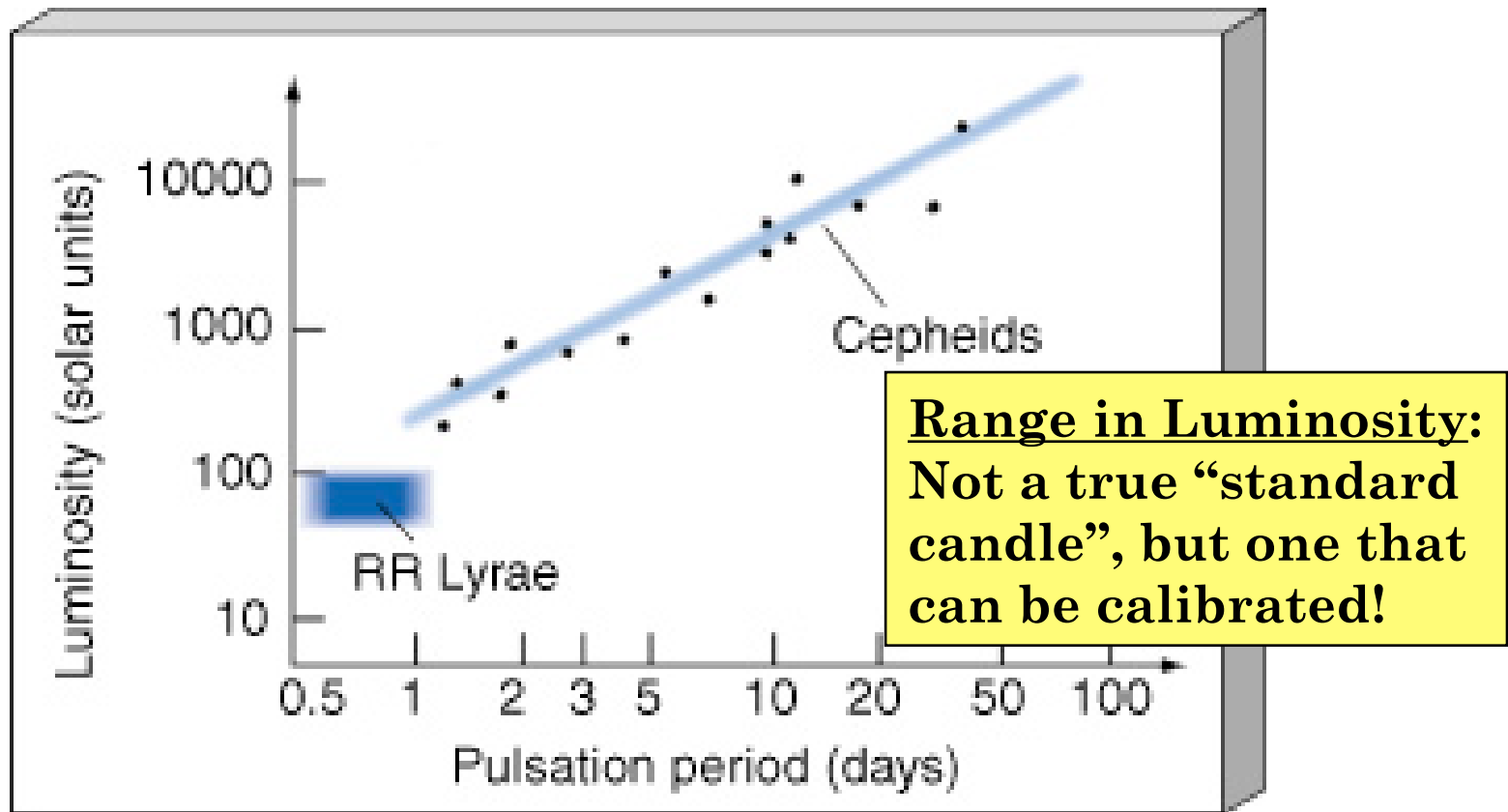
More luminous Cepheid variables take longer to go through one pulsation cycle. This simple observation made possible the discovery that “spiral nebulae” are separate galaxies, and more recently, the value of H_0 to better than 10% accuracy. **It thus unlocked the secret to the vast size and extent of the Cosmos!**

Measuring Distances to Galaxies

- ★ Astronomical objects whose luminosities are known with confidence are called “**Standard Candles.**” Measuring their apparent brightness gives their distance, after some calibration.
- ★ Examples (which can be calibrated locally, except SNe) include:
 - **RR Lyrae variables** can be used within the Local Group and out to about 5 Mpc; luminosities depend on metallicity or color
 - **Cepheid variables** have been used out to about 30 Mpc (about 2x Virgo); luminosities depend on the period (+ metallicity?)
 - **Classical novae** (up to 50-100 Mpc?): peak luminosity depends on decline rate, the time it takes for the nova to fade by ~ 2 mag.
 - **Globular clusters** (up to 100 Mpc): mean luminosity is roughly the same in all galaxies; some metallicity + age dependence.
 - **Type I supernovae** (out to many Gpc): maximum luminosity depends on the decline rate.

Example: Cepheid P-L Relation

- ★ Suppose we measure the period of a Cepheid variable. We can then use the **period-luminosity relation** to find its luminosity.



- ★ We measure the Cepheid’s apparent magnitude m directly; armed with its luminosity, or absolute magnitude M , we know: $(m-M) = 5 \log(d) + 25$, where d is distance in Mpc.

Galaxy Velocities from Redshifts

We measure the velocities of galaxies from the shift of their spectral lines:

$$(\lambda_{obs} - \lambda_0) / \lambda_0 = v / c$$

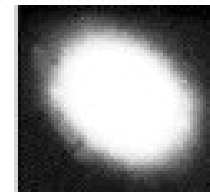
$$v = c (\lambda_{obs} - \lambda_0) / \lambda_0 = cz$$

where v is the galaxy's **velocity**.

As Hubble found, almost all galaxies (beyond the Local Group) are *redshifted*, and thus moving away from us with positive velocity. With Sloan, 2dF, etc, we now have v 's for millions of galaxies, but distances are harder to measure.

Plotting galaxy *distance* (from Cepheids, etc, but not parallax!) vs *velocity* gives a **Hubble diagram**.

GALAXIES in



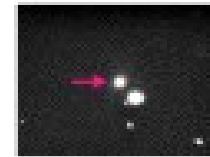
Virgo



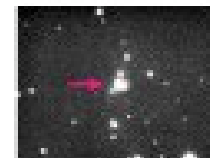
Ursa Major



Corona Borealis

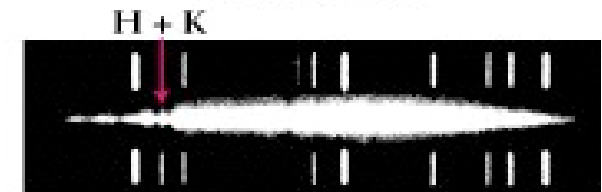


Boötes



Hydra

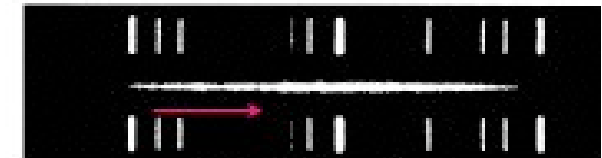
REDSHIFTS



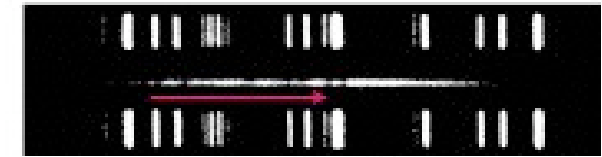
1,200 km/s



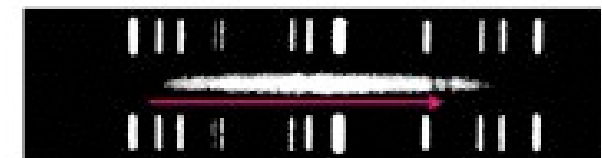
15,000 km/s



22,000 km/s



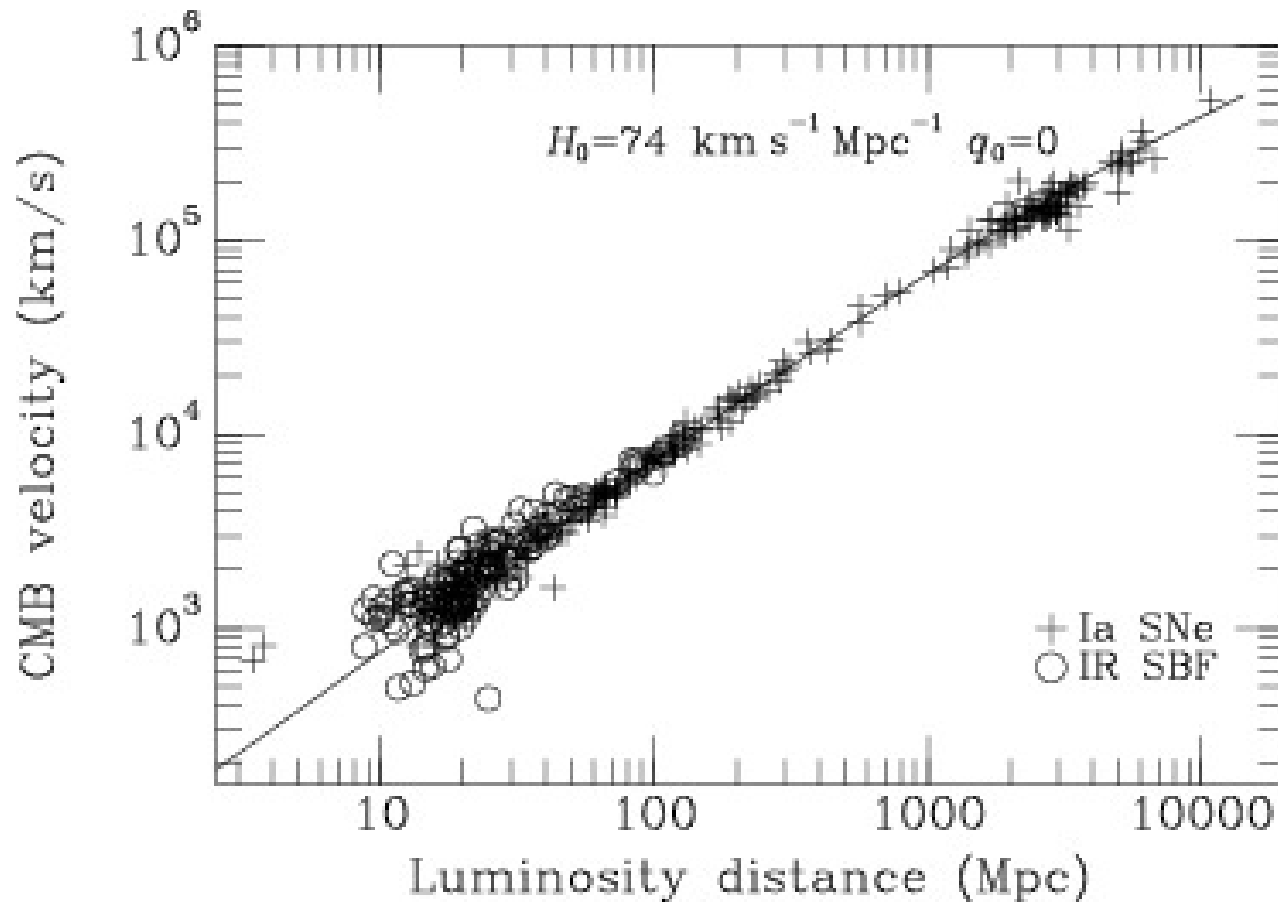
39,000 km/s



61,000 km/s

Doppler shifts tell us the galaxy velocities.

Example Hubble diagram, out to $d = 10$ Gpc, $z = 1.7$



The Hubble Law

- ◆ Hubble's law can be summarized as:

$$v = H_0 \times d + v_p$$

$$d = (v - v_p) / H_0$$

- ◆ where v is the observed velocity, v_p is the peculiar velocity, d is the distance, and H_0 is the Hubble constant, the rate at which the local Universe is expanding.
- ◆ Best current estimate: $H_0 = 72 \pm 6$ km/s/Mpc.
 - ➔ **This means that for every 1 Mpc increase in distance, a galaxy's velocity will increase by about 73 km/sec.**
- ◆ The problem of course is v_p , *the unknown peculiar velocity*.
- ◆ *You have to go out to at least 50 Mpc for v_p to be less than 10% of the observed velocity, and at least 100 Mpc if you really want it to be negligible (assuming the galaxy isn't in a cluster with velocity dispersion $\sigma \approx 1000$ km/s).*

TABLE III. How key cosmological parameter constraints depend on data used and on assumptions about other parameters. The columns compare different theoretical priors indicated by numbers in *italics*. w_c denotes dark energy that can cluster as in [7]. Rows labeled “+SDSS” combine WMAP3 and SDSS LRG data.

	Data	Vanilla	Vanilla + Ω_{tot}	Vanilla + r	Vanilla + α	Vanilla + ω_ν	Vanilla + w	Vanilla + w_c
Ω_{tot}	WMAP	1	$1.054^{+0.064}_{-0.046}$	1	1	1	1	1
	+SDSS	1	$1.003^{+0.010}_{-0.009}$	1	1	1	1	1
Ω_Λ	WMAP	$0.761^{+0.032}_{-0.037}$	$0.60^{+0.14}_{-0.17}$	$0.805^{+0.038}_{-0.042}$	$0.708^{+0.051}_{-0.060}$	$0.651^{+0.082}_{-0.086}$	$0.704^{+0.071}_{-0.100}$	$0.879^{+0.064}_{-0.168}$
	+SDSS	$0.761^{+0.017}_{-0.018}$	$0.757^{+0.020}_{-0.021}$	$0.771^{+0.018}_{-0.019}$	$0.750^{+0.020}_{-0.022}$	$0.731^{+0.024}_{-0.030}$	$0.757^{+0.019}_{-0.020}$	$0.762^{+0.020}_{-0.021}$
Ω_m	WMAP	$0.239^{+0.037}_{-0.032}$	$0.46^{+0.23}_{-0.19}$	$0.195^{+0.042}_{-0.038}$	$0.292^{+0.060}_{-0.051}$	$0.349^{+0.086}_{-0.082}$	$0.30^{+0.10}_{-0.07}$	$0.12^{+0.17}_{-0.06}$
	+SDSS	$0.239^{+0.018}_{-0.017}$	$0.246^{+0.028}_{-0.025}$	$0.229^{+0.019}_{-0.018}$	$0.250^{+0.022}_{-0.020}$	$0.269^{+0.030}_{-0.024}$	$0.243^{+0.020}_{-0.019}$	$0.238^{+0.021}_{-0.020}$
ω_m	WMAP	$0.1272^{+0.0082}_{-0.0080}$	$0.1277^{+0.0082}_{-0.0079}$	$0.1194^{+0.0096}_{-0.0092}$	$0.135^{+0.010}_{-0.009}$	$0.139^{+0.011}_{-0.011}$	$0.1274^{+0.0083}_{-0.0082}$	$0.1269^{+0.0082}_{-0.0080}$
	+SDSS	$0.1272^{+0.0044}_{-0.0043}$	$0.1260^{+0.0056}_{-0.0054}$	$0.1268^{+0.0043}_{-0.0042}$	$0.1271^{+0.0045}_{-0.0044}$	$0.1301^{+0.0048}_{-0.0044}$	$0.1248^{+0.0063}_{-0.0059}$	$0.1264^{+0.0075}_{-0.0079}$
ω_b	WMAP	$0.0222^{+0.0007}_{-0.0007}$	$0.0218^{+0.0008}_{-0.0008}$	$0.0233^{+0.0011}_{-0.0010}$	$0.0210^{+0.0010}_{-0.0010}$	$0.0215^{+0.0009}_{-0.0009}$	$0.0221^{+0.0007}_{-0.0007}$	$0.0222^{+0.0008}_{-0.0007}$
	+SDSS	$0.0222^{+0.0007}_{-0.0007}$	$0.0222^{+0.0007}_{-0.0007}$	$0.0229^{+0.0009}_{-0.0008}$	$0.0213^{+0.0010}_{-0.0010}$	$0.0221^{+0.0008}_{-0.0008}$	$0.0223^{+0.0007}_{-0.0007}$	$0.0224^{+0.0008}_{-0.0007}$
ω_ν	WMAP	0	0	0	0	<0.024 (95%)	0	0
	+SDSS	0	0	0	0	<0.010 (95%)	0	0
M_ν	WMAP	0	0	0	0	<2.2 (95%)	0	0
	+SDSS	0	0	0	0	<0.94 (95%)	0	0
w	WMAP	-1	-1	-1	-1	-1	$-0.82^{+0.23}_{-0.19}$	$-1.69^{+0.88}_{-0.85}$
	+SDSS	-1	-1	-1	-1	-1	$-0.941^{+0.087}_{-0.101}$	$-1.00^{+0.17}_{-0.19}$
σ_8	WMAP	$0.758^{+0.050}_{-0.051}$	$0.732^{+0.051}_{-0.046}$	$0.706^{+0.064}_{-0.072}$	$0.776^{+0.056}_{-0.053}$	$0.597^{+0.085}_{-0.075}$	$0.736^{+0.054}_{-0.052}$	$0.747^{+0.066}_{-0.066}$
	+SDSS	$0.756^{+0.035}_{-0.035}$	$0.747^{+0.046}_{-0.044}$	$0.751^{+0.036}_{-0.036}$	$0.739^{+0.036}_{-0.035}$	$0.673^{+0.056}_{-0.061}$	$0.733^{+0.048}_{-0.043}$	$0.745^{+0.057}_{-0.056}$
r_{002}	WMAP	0	0	<0.65 (95%)	0	0	0	0
	+SDSS	0	0	<0.33 (95%)	0	0	0	0
n_s	WMAP	$0.954^{+0.017}_{-0.016}$	$0.943^{+0.017}_{-0.016}$	$0.982^{+0.032}_{-0.026}$	$0.871^{+0.047}_{-0.046}$	$0.928^{+0.022}_{-0.024}$	$0.945^{+0.017}_{-0.016}$	$0.947^{+0.019}_{-0.017}$
	+SDSS	$0.953^{+0.016}_{-0.016}$	$0.952^{+0.017}_{-0.016}$	$0.967^{+0.022}_{-0.020}$	$0.895^{+0.041}_{-0.042}$	$0.945^{+0.017}_{-0.017}$	$0.950^{+0.016}_{-0.016}$	$0.953^{+0.018}_{-0.017}$
α	WMAP	0	0	0	$-0.056^{+0.031}_{-0.031}$	0	0	0
	+SDSS	0	0	0	$-0.040^{+0.027}_{-0.027}$	0	0	0
h	WMAP	$0.730^{+0.033}_{-0.031}$	$0.53^{+0.15}_{-0.10}$	$0.782^{+0.058}_{-0.047}$	$0.679^{+0.044}_{-0.040}$	$0.630^{+0.065}_{-0.065}$	$0.657^{+0.085}_{-0.086}$	$1.03^{+0.46}_{-0.37}$
	+SDSS	$0.730^{+0.019}_{-0.019}$	$0.716^{+0.047}_{-0.043}$	$0.744^{+0.022}_{-0.021}$	$0.713^{+0.022}_{-0.022}$	$0.695^{+0.025}_{-0.028}$	$0.716^{+0.031}_{-0.029}$	$0.727^{+0.037}_{-0.034}$
t_{now}	WMAP	$13.75^{+0.15}_{-0.16}$	$16.0^{+1.5}_{-1.8}$	$13.53^{+0.21}_{-0.25}$	$13.98^{+0.20}_{-0.20}$	$14.31^{+0.24}_{-0.33}$	$13.96^{+0.34}_{-0.28}$	$13.44^{+0.49}_{-0.27}$
	+SDSS	$13.76^{+0.15}_{-0.15}$	$13.93^{+0.59}_{-0.58}$	$13.65^{+0.17}_{-0.18}$	$13.90^{+0.19}_{-0.19}$	$13.98^{+0.22}_{-0.20}$	$13.80^{+0.18}_{-0.17}$	$13.77^{+0.26}_{-0.24}$
τ	WMAP	$0.090^{+0.029}_{-0.029}$	$0.083^{+0.029}_{-0.029}$	$0.091^{+0.031}_{-0.032}$	$0.101^{+0.031}_{-0.031}$	$0.082^{+0.029}_{-0.030}$	$0.087^{+0.030}_{-0.031}$	$0.087^{+0.030}_{-0.030}$
	+SDSS	$0.087^{+0.028}_{-0.030}$	$0.088^{+0.029}_{-0.031}$	$0.085^{+0.029}_{-0.031}$	$0.101^{+0.032}_{-0.032}$	$0.087^{+0.028}_{-0.029}$	$0.090^{+0.030}_{-0.031}$	$0.089^{+0.030}_{-0.032}$
b	WMAP							
	+SDSS	$1.896^{+0.074}_{-0.069}$	$1.911^{+0.092}_{-0.086}$	$1.919^{+0.078}_{-0.072}$	$1.853^{+0.081}_{-0.077}$	$2.03^{+0.11}_{-0.10}$	$1.897^{+0.076}_{-0.072}$	$1.92^{+0.10}_{-0.08}$
Q_{nl}	WMAP							
	+SDSS	$30.3^{+4.4}_{-4.1}$	$30.0^{+4.6}_{-4.2}$	$30.9^{+4.5}_{-4.1}$	$34.7^{+6.1}_{-5.4}$	$34.9^{+6.9}_{-5.3}$	$31.0^{+4.7}_{-4.3}$	$31.0^{+5.0}_{-4.4}$
$\Delta\chi^2$	WMAP	0.0	-2.0	0.0	-3.6	-1.0	-1.0	0.0
	+SDSS	0.0	0.0	-0.5	-2.4	-0.5	-0.9	-0.3

Tegmark et al. 2006

The Hubble Space Telescope Key Project on the Distance Scale (“ H_0 Key Project”)

- Series of papers measuring Cepheid distances to spiral galaxies with HST and then recalibrating various distance indicators to get the value of H_0
- Culminated in **Freedman et al. (2001, ApJ, 553, 47)**, which averaged H_0 results from the following 5 methods:
 - Type Ia supernovae (all galaxy types)
 - Tully-Fisher method (spirals)
 - Surface Brightness Fluctuations (ellipticals, S0s, bulges)
 - Type II supernovae (late-type, star-forming galaxies)
 - Fundamental plane (early-type galaxies)

The Hubble Space Telescope Key Project on the Distance Scale (“ H_0 Key Project”)

- In an earlier paper, **Ferrarese et al. (2000, ApJ, 529, 745)**, besides calibrating the SBF method, also calibrated the following distance indicators:
 - Tip of the Red Giant Branch (‘Pop II’ systems)
 - Globular Cluster Luminosity Function (mostly gE’s)
 - Planetary Nebula Luminosity Function (all types, more or less, but can have problems with HII regions in spirals)
- but these were deemed not “far-reaching” enough (TRGB and PNLF) or not reliable enough (GCLF) for useful H_0 estimates.
- For additional info on distance methods, see the big review article by: **Jacoby et al. (1992), PASP, 104, 599**
(including C. Pritchett)

Comments on selected distance methods

- TRGB, Cepheids, SBF, and SNe Ia have the best internal accuracies, all better than 10%, or 0.2 mag, per galaxy
- TRGB is great, but barely gets you to Virgo, even with HST
- Cepheids are the gold standard, but intensely observationally demanding, and require HST for distances beyond a few Mpc
- SNe Ia reach cosmological distances with good accuracy, but *cannot target individual galaxies*, e.g., for peculiar velocities
- T-F and FP can target very large samples of galaxies, but the internal accuracy per galaxy is only about 20%, or 0.4 mag
- GCLF has uncertain universality; GC mean size (Jordan et al. 2005, ApJ, ACSVCS X) is an interesting new method, but much more observationally demanding & requires HST.
- SBF: what we'll consider in detail for most of this lecture...

A NEW TECHNIQUE FOR MEASURING EXTRAGALACTIC DISTANCES^{a)}JOHN TONRY^{b)}

Physics Department, Massachusetts Institute of Technology, Cambridge, Massachusetts 02139

DONALD P. SCHNEIDER

Institute for Advanced Study, Princeton, New Jersey 08540

Received 26 April 1988

ABSTRACT

We describe a relatively direct technique of determining extragalactic distances. The method relies on measuring the luminosity fluctuations that arise from the counting statistics of the stars contributing the flux in each pixel of a high-signal-to-noise CCD image of a galaxy. The amplitude of these fluctuations is inversely proportional to the distance of the galaxy. This approach bypasses most of the successive stages of calibration required in the traditional extragalactic distance ladder; the only serious drawback to this method is that it requires an accurate knowledge of the bright end ($M_V < 3$) of the luminosity function. Potentially, this method can produce accurate distances of elliptical galaxies and spiral bulges at distances out to about 20 Mpc. In this paper, we explain how to calculate the value of the fluctuations, taking into account various sources of contamination and the effects of finite spatial resolution, and we demonstrate, via simulations and CCD images of M32 and N3379, the feasibility and limitations of this technique.

I. INTRODUCTION

A basic problem in astrophysics is the measurement of the distance to celestial objects. Truly reliable distances can be derived from radar timing in the solar system and parallax measurements of nearby stars. For more distant sources, we must rely on indirect techniques such as the moving cluster method, statistical parallaxes, or main-sequence fitting (see, for example, Mihalas and Binney 1981). The traditional approach for extragalactic measurements is to construct a distance ladder of ever more luminous and rare beacons that can be seen to enormous distances, stand out from the surrounding background, and which, we trust, have constant or calibratable luminosities. As we bootstrap ourselves up this distance ladder, however, each successive rung is progres-

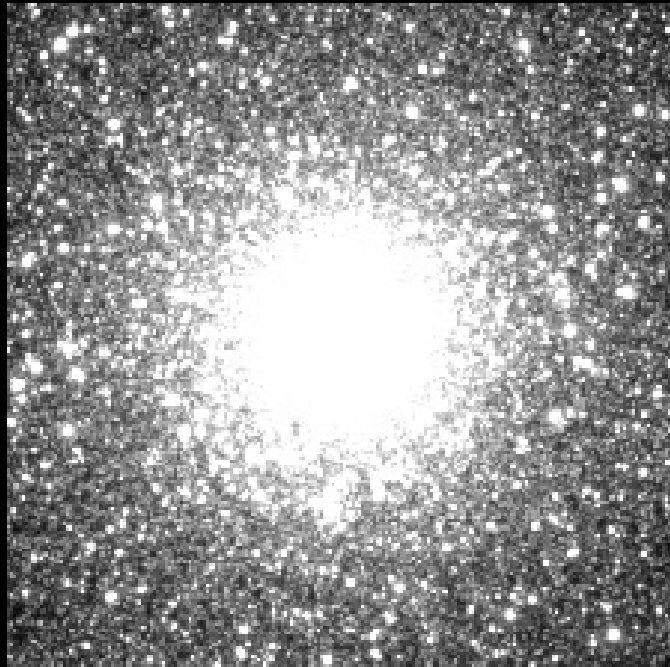
sively more difficult to construct. The primary disadvantages are that the stellar luminosity function must be quite accurately known and that high-signal-to-noise data are required; the latter item demands that the contributors to the noise and fluctuations in the data be well understood. The finite spatial resolution introduced by instrumental and atmospheric blurring, while setting the ultimate limits for the technique, is actually an asset to the method in some respects.

The following section investigates the sources and amplitudes of luminosity fluctuations and describes the steps required for data processing. Section III illustrates the expected behavior of galaxies at different distances, and shows the results of this technique when applied to simulated data. Observations of M32 and N3379 are presented in Sec. IV. In Sec. V we discuss the results and implications, and suggest

Surface Brightness Fluctuations (SBF)

- SBF is the brightness, or intensity, variance in a galaxy image due to the fluctuations in the finite number and luminosity of unresolved stars per pixel in the image.
- The ratio of this brightness variance to the mean galaxy surface brightness is called \overline{f} and it scales inversely with the square of the galaxy distance.
- \overline{f} has units of flux and is usually converted to a *magnitude* called \overline{m} . The distance modulus: $(m-M) = (\overline{m} - \overline{M})$ follows once \overline{M} is known.
- In practice, \overline{M} depends on both the bandpass & stellar population. In the optical, the stellar pop dependence is well calibrated, and the zero point has been tied to the Cepheid distance scale to accuracy of ~ 0.08 mag.

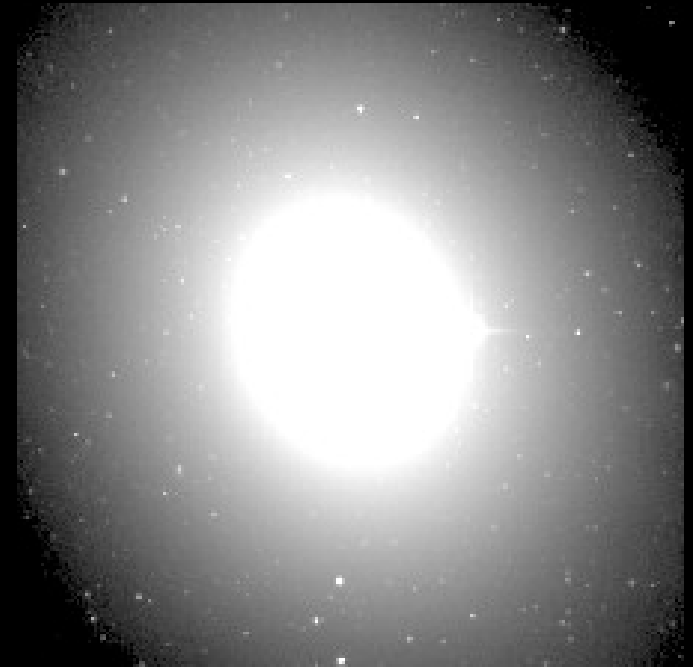
SBF: Galaxy surface brightness is independent of distance, but the variance (measured in Fourier space) goes as d^{-2}



globular star cluster
 $N \sim 10^6$ stars
 $d \sim 10$ kpc



M32 (Andromeda)
 $N \sim 10^9$ stars
 $d \sim 770$ kpc



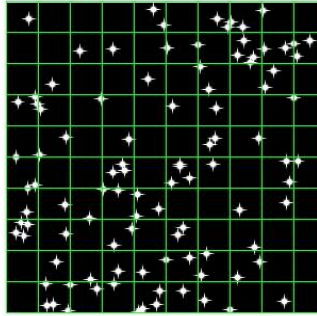
M49 (Virgo)
 $N \sim 10^{12}$ stars
 $d \sim 16$ Mpc

Surface Brightness Fluctuations illustrated

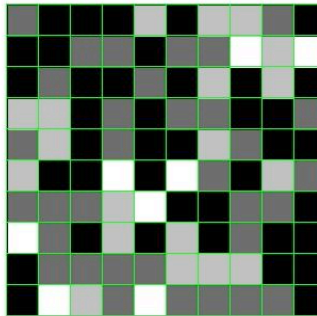
$$\bar{L} = \frac{\langle L_*^2 \rangle}{\langle L_* \rangle}$$

This is the luminosity corresponding to flux \bar{f} and absolute mag \bar{M} .

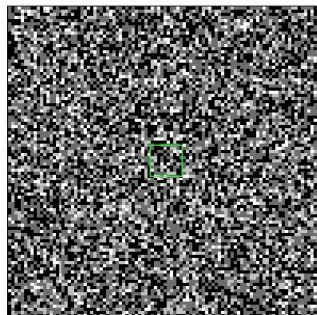
Nearby Galaxy



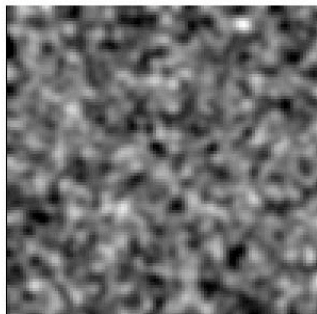
Galaxy star field



What the CCD sees

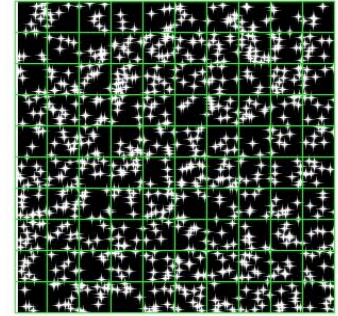


More CCD pixels

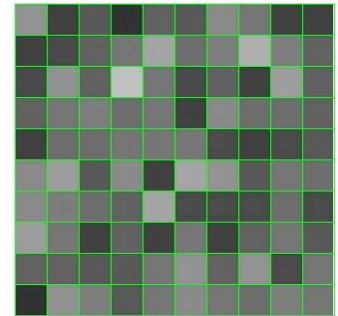


Blurred by atmosphere

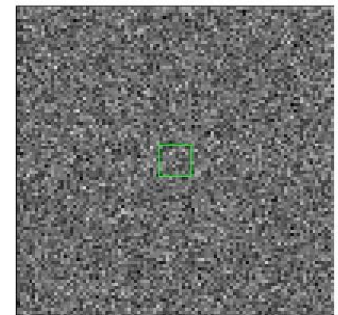
Same Galaxy
Three times the distance



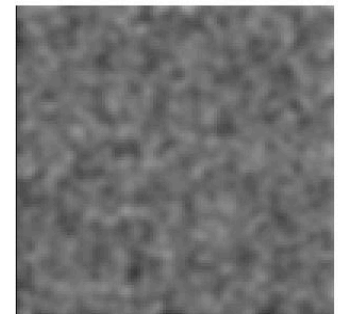
Galaxy star field



What the CCD sees



More CCD pixels



Blurred by atmosphere

\bar{f} Star flux $\bar{f}/9$

n Star density $9n$

Surface Brightness

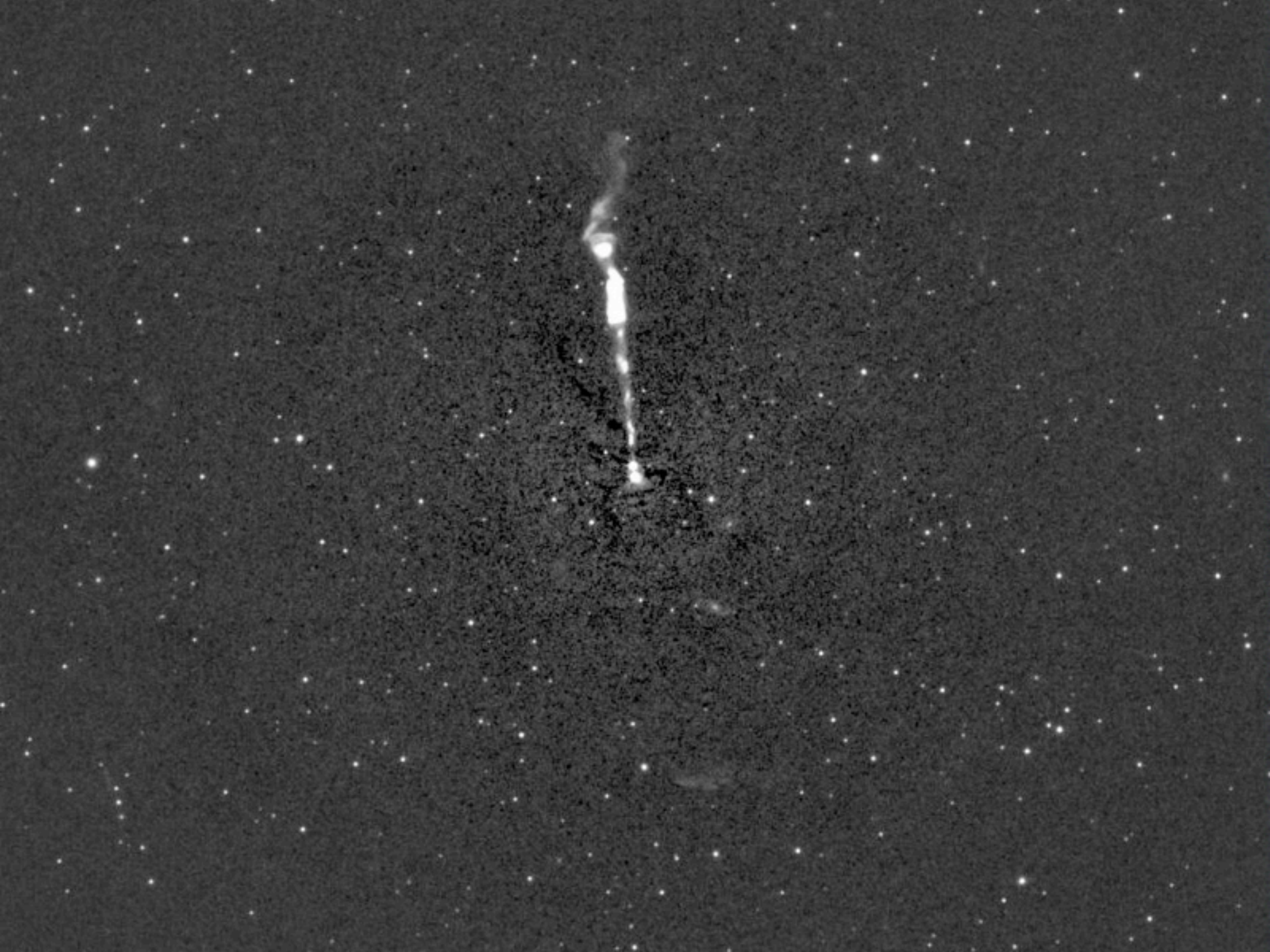
$n\bar{f}$ $n\bar{f}$

Rms fluctuation
(inversely prop. to distance)

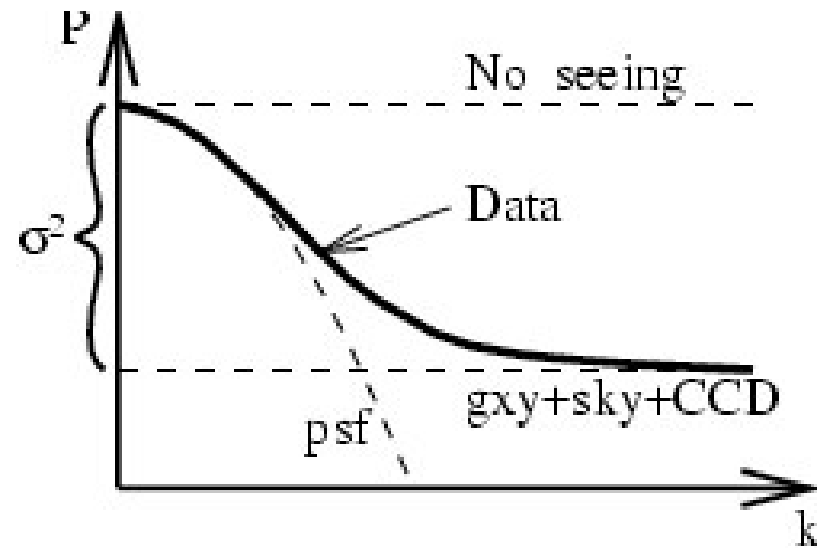
$$\sqrt{n} \bar{f} \quad \sqrt{9n} \bar{f}/9 \\ = \frac{1}{3} \sqrt{n} \bar{f}$$

Variance divided by Mean
(Star flux)

$$\bar{f} = \frac{(\text{rms})^2}{\text{mean}} \quad \bar{f}/9 = \frac{(\text{rms})^2}{\text{mean}}$$



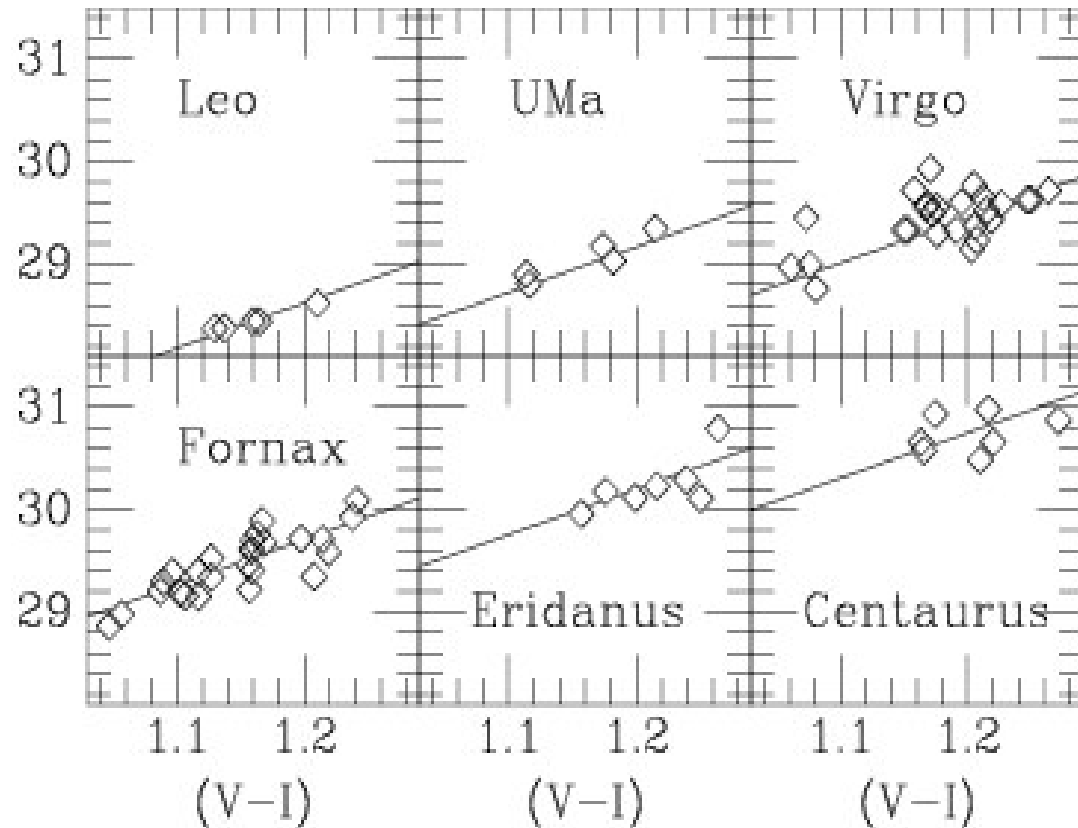
Measure amplitude of the fluctuations in Fourier space (variance convolved with PSF)



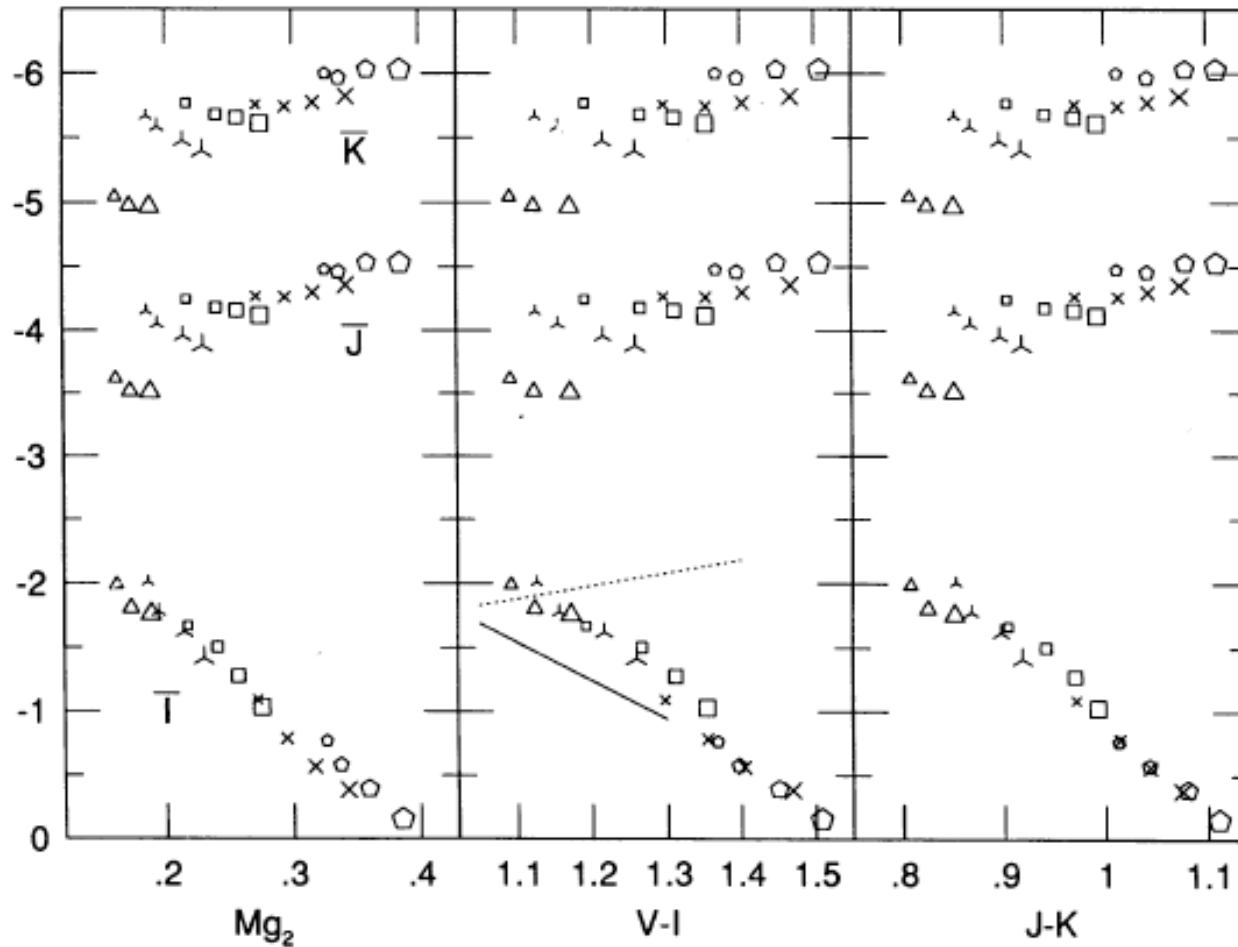
Convert to magnitudes and calibrate dependence on stellar pop (color, Mg_2 , etc) for galaxies at same distance:
 normalized fluctuations (SBF) fainter in redder galaxies.

Set zero point from Cepheid distances to these groups.

Or, if you're bold, from stellar population models.

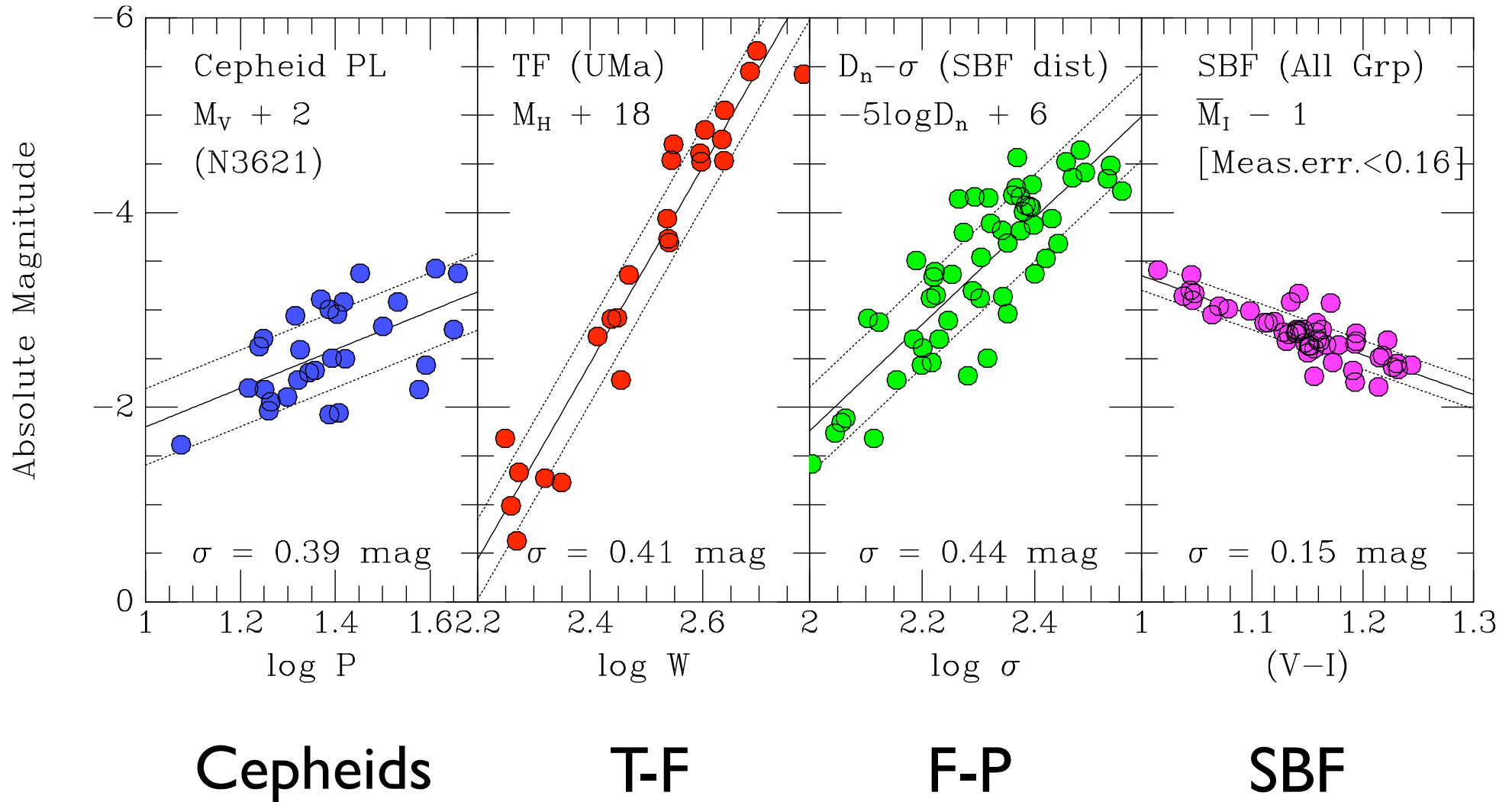


First Good SBF Models: Worthey 1993, Buzzoni 1993



2.—The same as Fig. 1, for fluctuation magnitudes \bar{I} , \bar{J} , and \bar{K} . An empirical calibration for \bar{I} as a function of $V-I$ (Tonry 1991) is shown as a solid line, theoretical calibration from TAL90 (not empirically shifted to agree with the distance of M32) is shown as a dotted line.

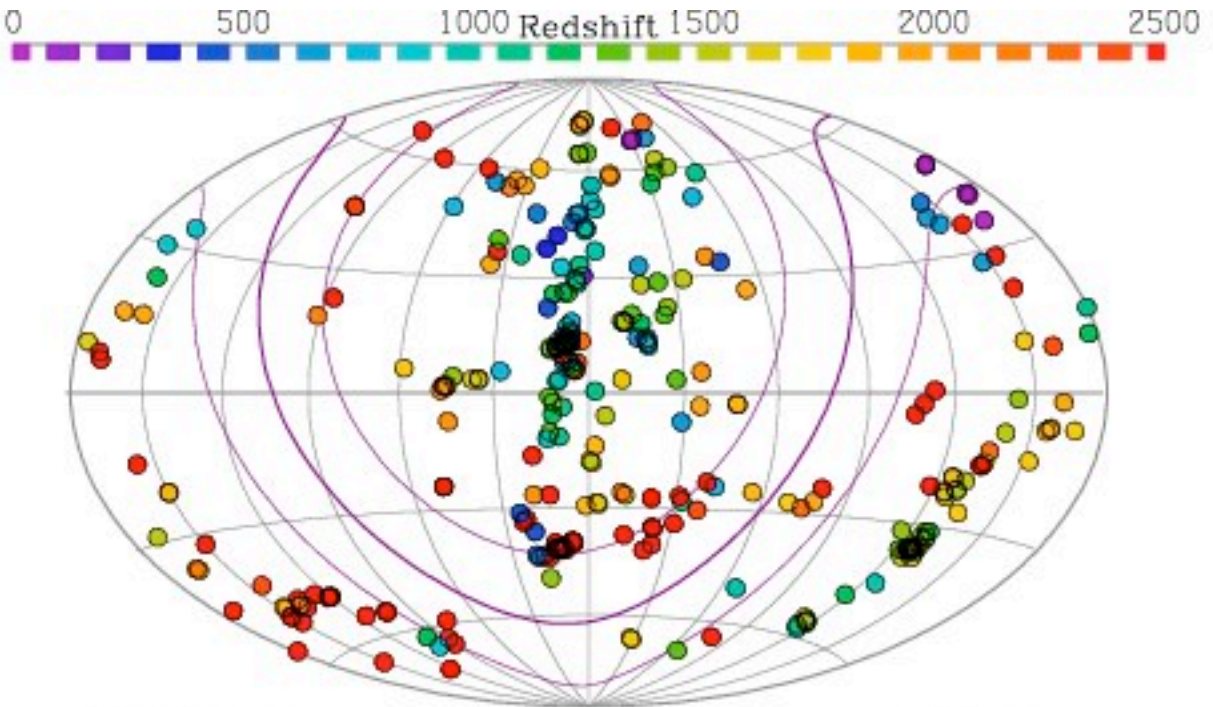
Comparison of Distance Indicators



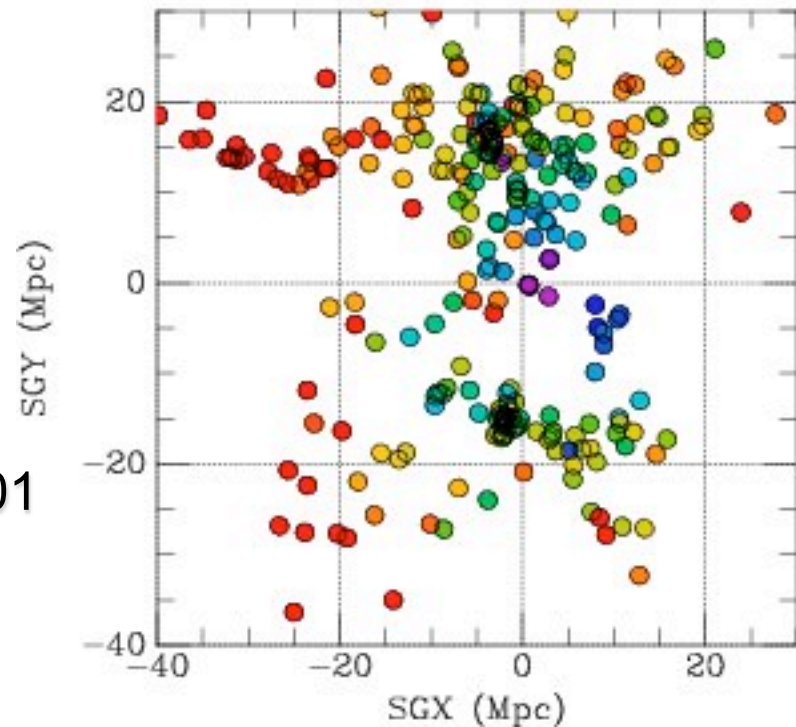
SBF in the 90's:
Ground-based *I*-band
survey of ~ 300 galaxies.

SBF distances
used to constrain
peculiar velocities,
Virgo infall,
 $H_0 \approx 73$ km/s/Mpc
 $\beta = \Omega^{0.6}/b \approx 0.45$
 $\Omega \approx 0.25$

Tonry et al. 1997, 2000, 2001
Blakeslee et al. 1999, 2002

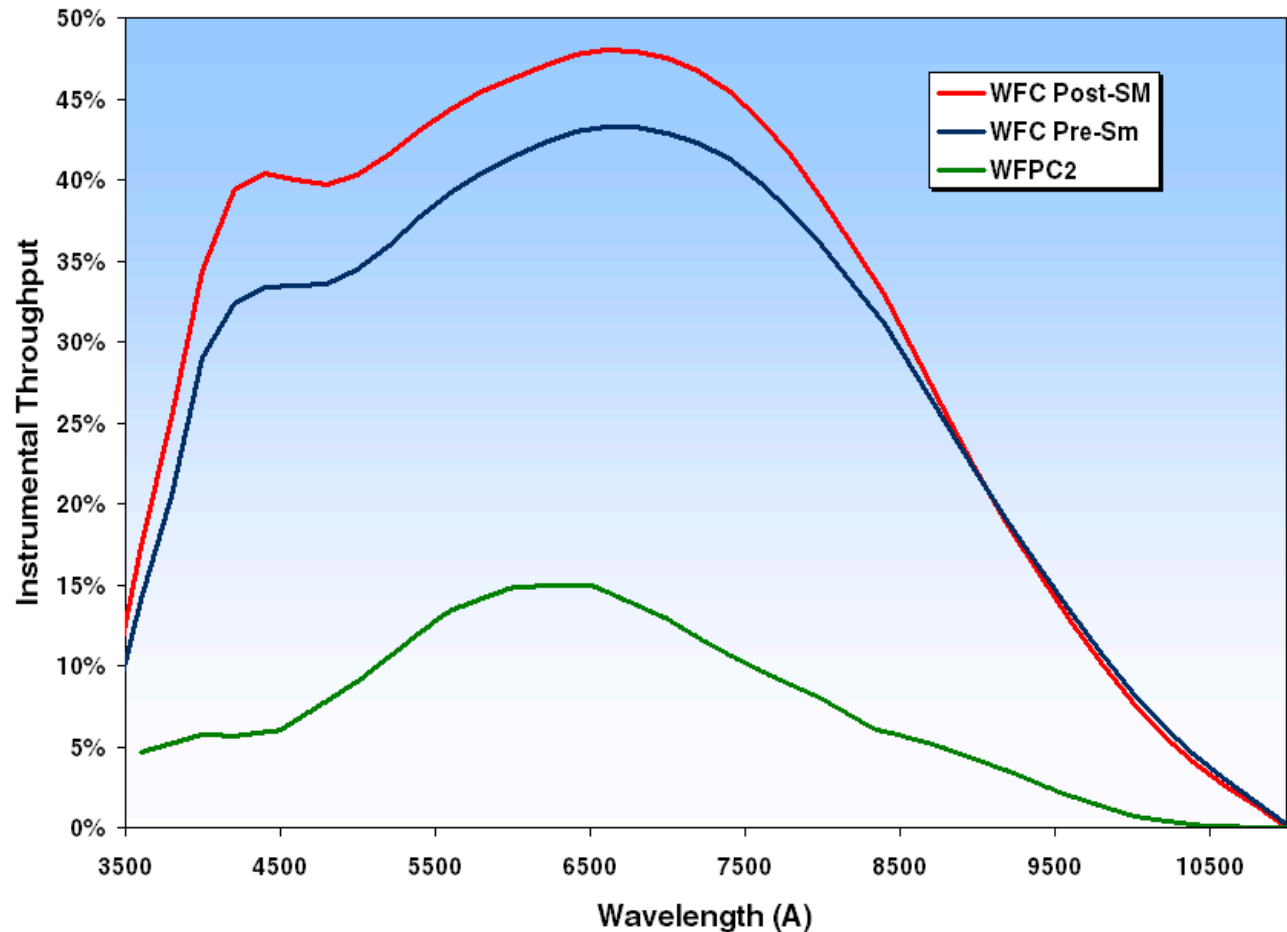
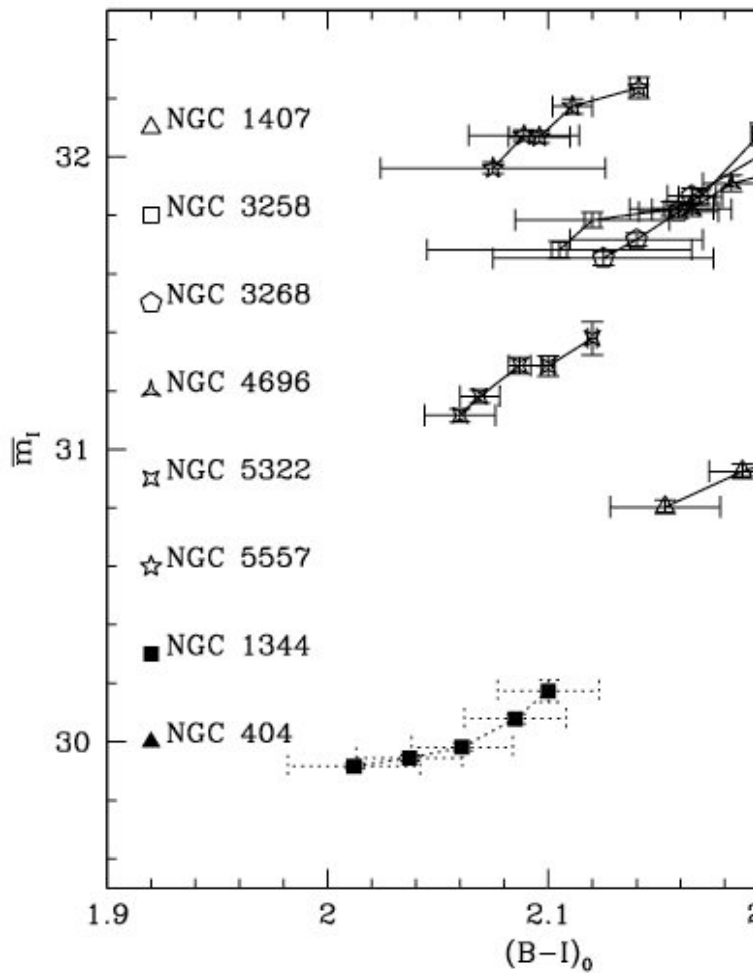


The SBF Survey of Galaxy Distances



Data from:
MDM, CTIO,
KPNO, LCO, CFHT

On to the New Era . . .



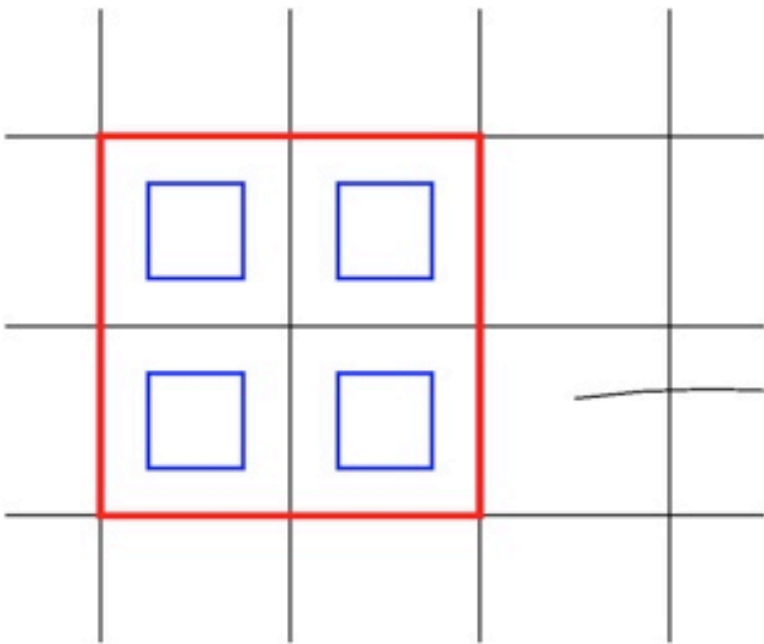
Radial SBF gradients in eight galaxies at various distances

SBF fainter in (red) galaxy centers.

Measurements from archival HST/ACS data.

(Cantiello, Blakeslee, Raimondo, Brocato et al. 2005, 2007)

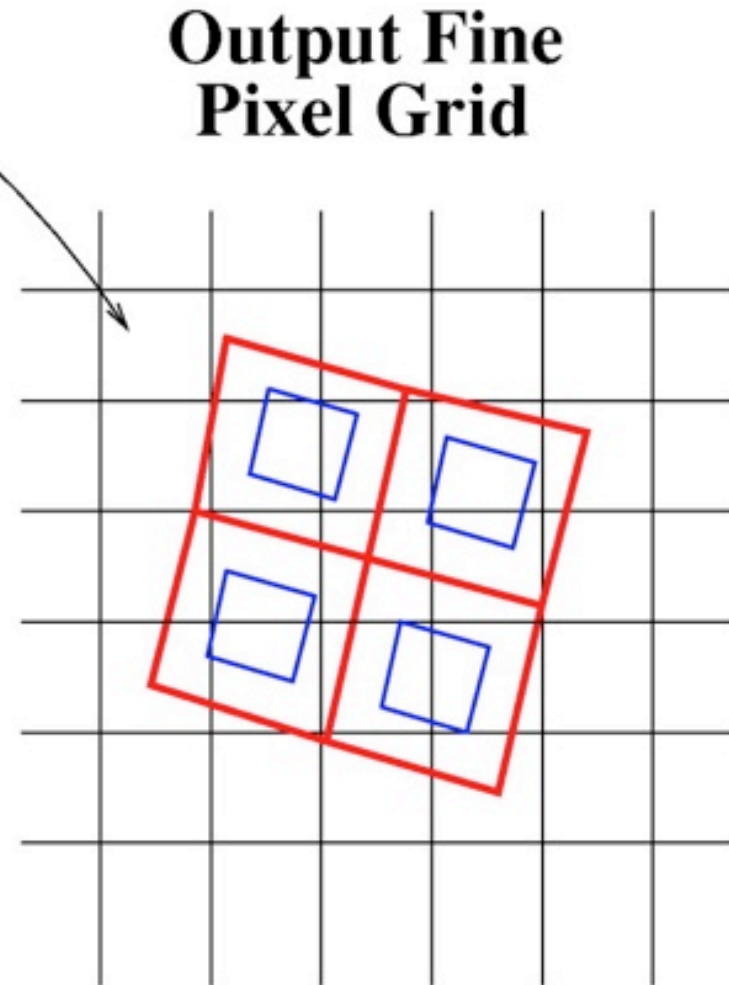
See: Fruchter & Hook
2002, PASP, 114, 144



**Original Coarse
Pixel Grid**

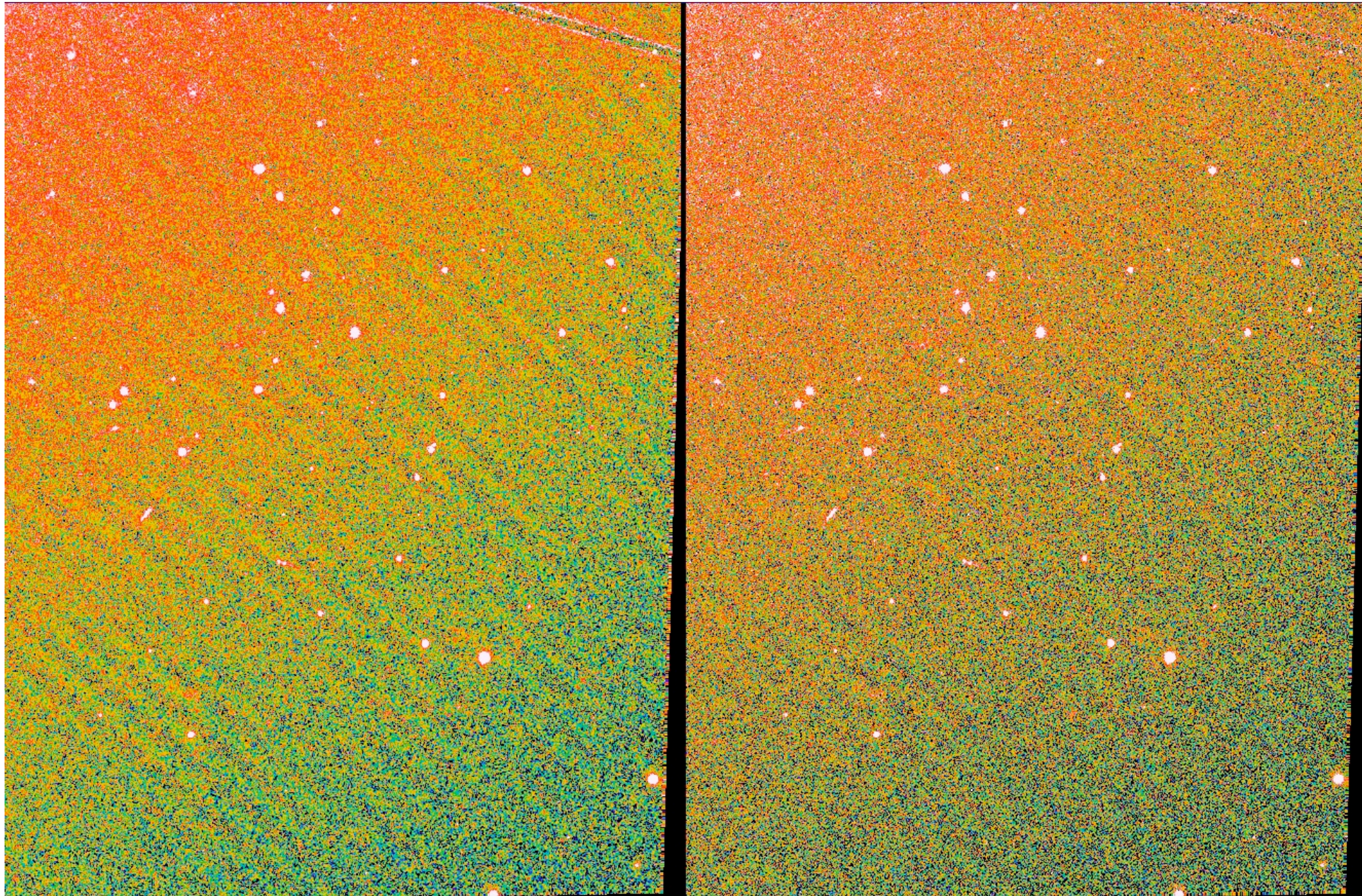
**Geometrical
Transformation**

“Drizzle” is a program for correcting
geometric distortion in HST images.

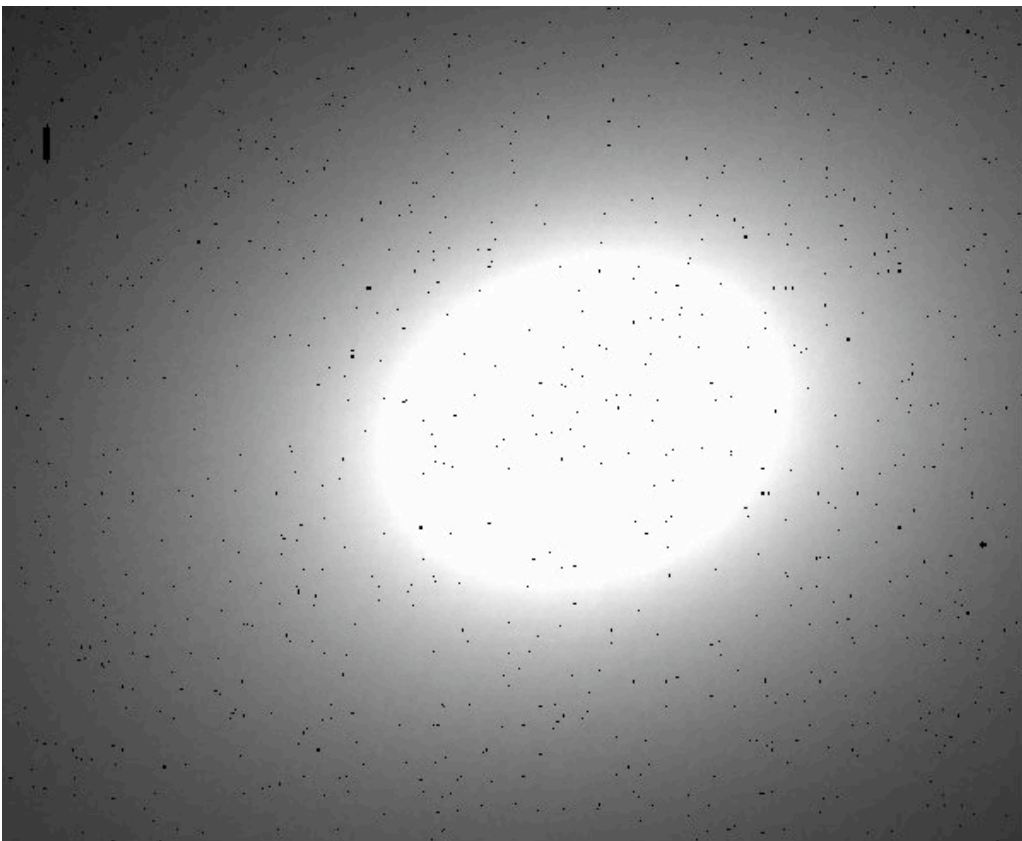


**Output Fine
Pixel Grid**

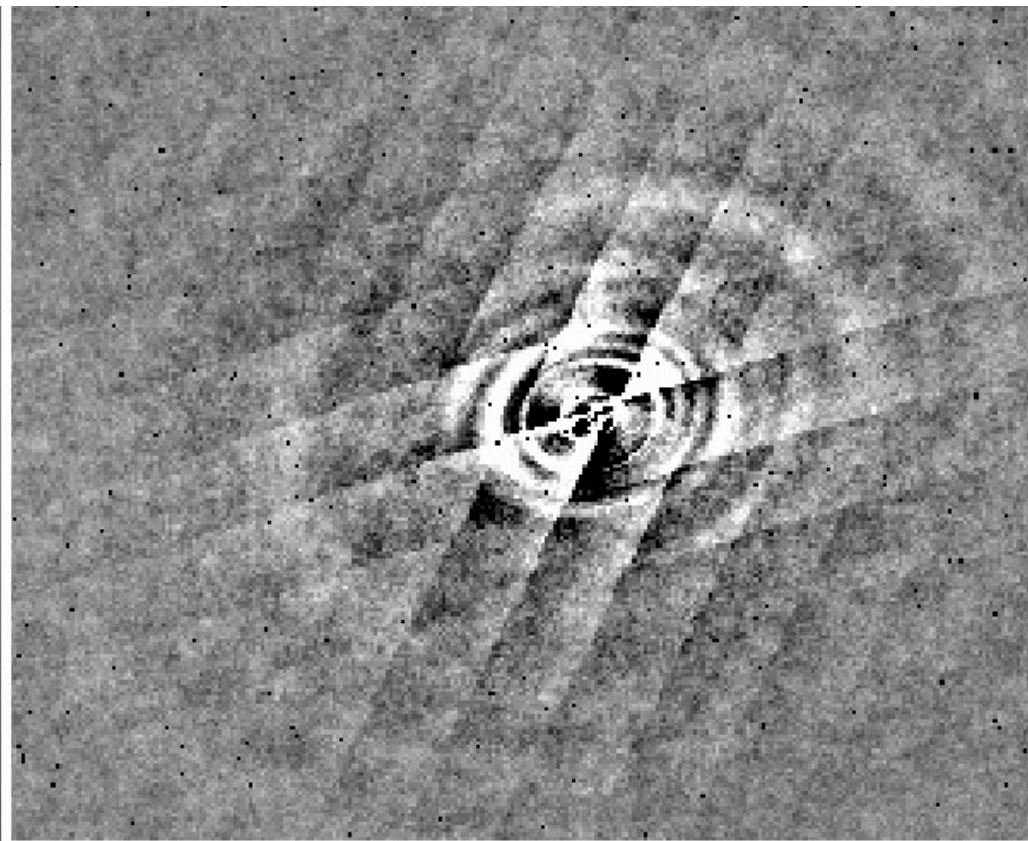
M87 drizzled with Guassian (left) and Lanczos3 (right) kernels.



The point kernel is great for preserving noise properties, but not for small-scale structure.
(Unless you have very many images and can subpixelize, e.g., UDF.)



single-pointing image
drizzled with point kernel

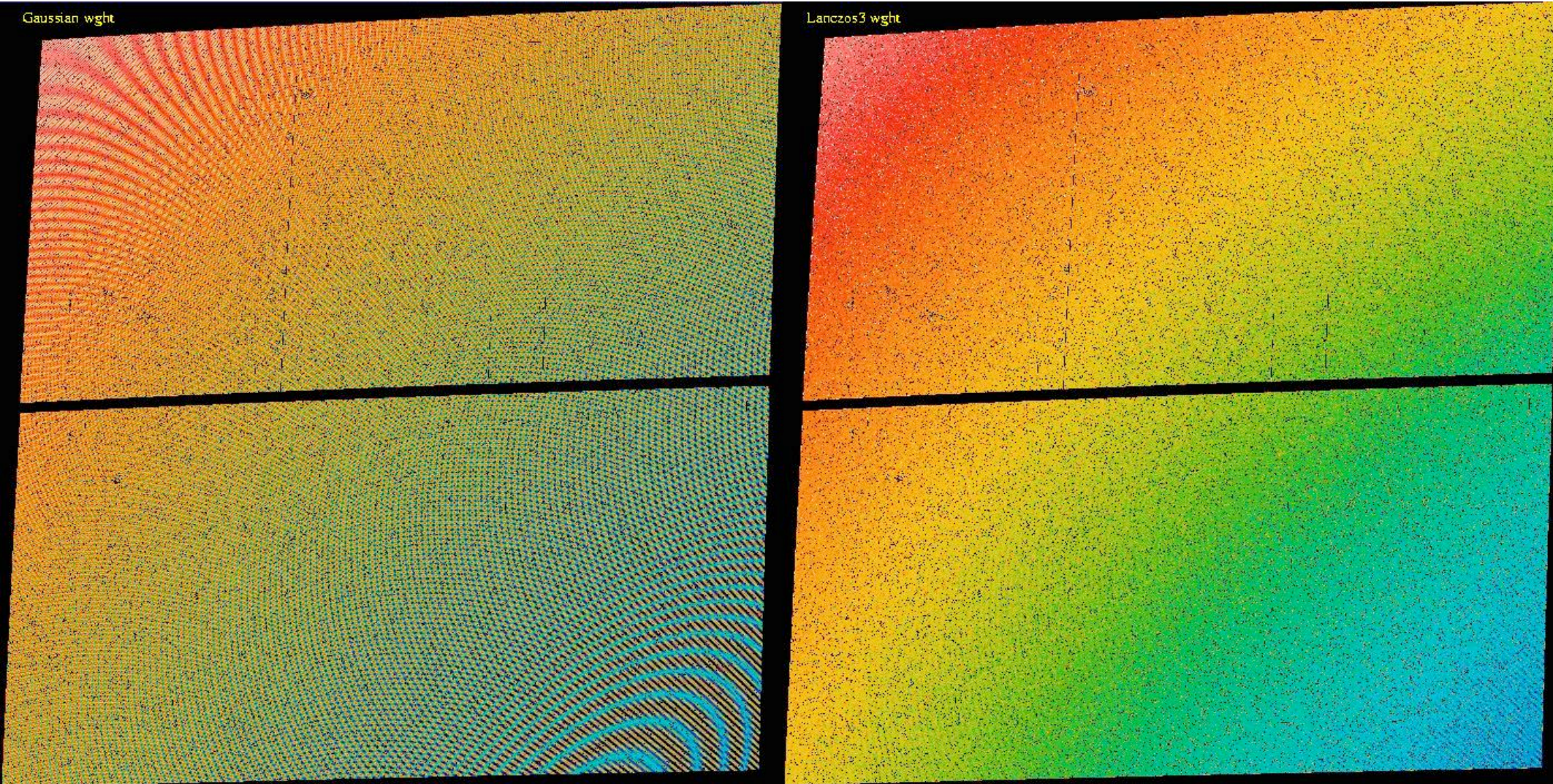


residual after smooth
model subtraction

Drizzle weight maps for different kernels

Gaussian kernel (similar to linear)

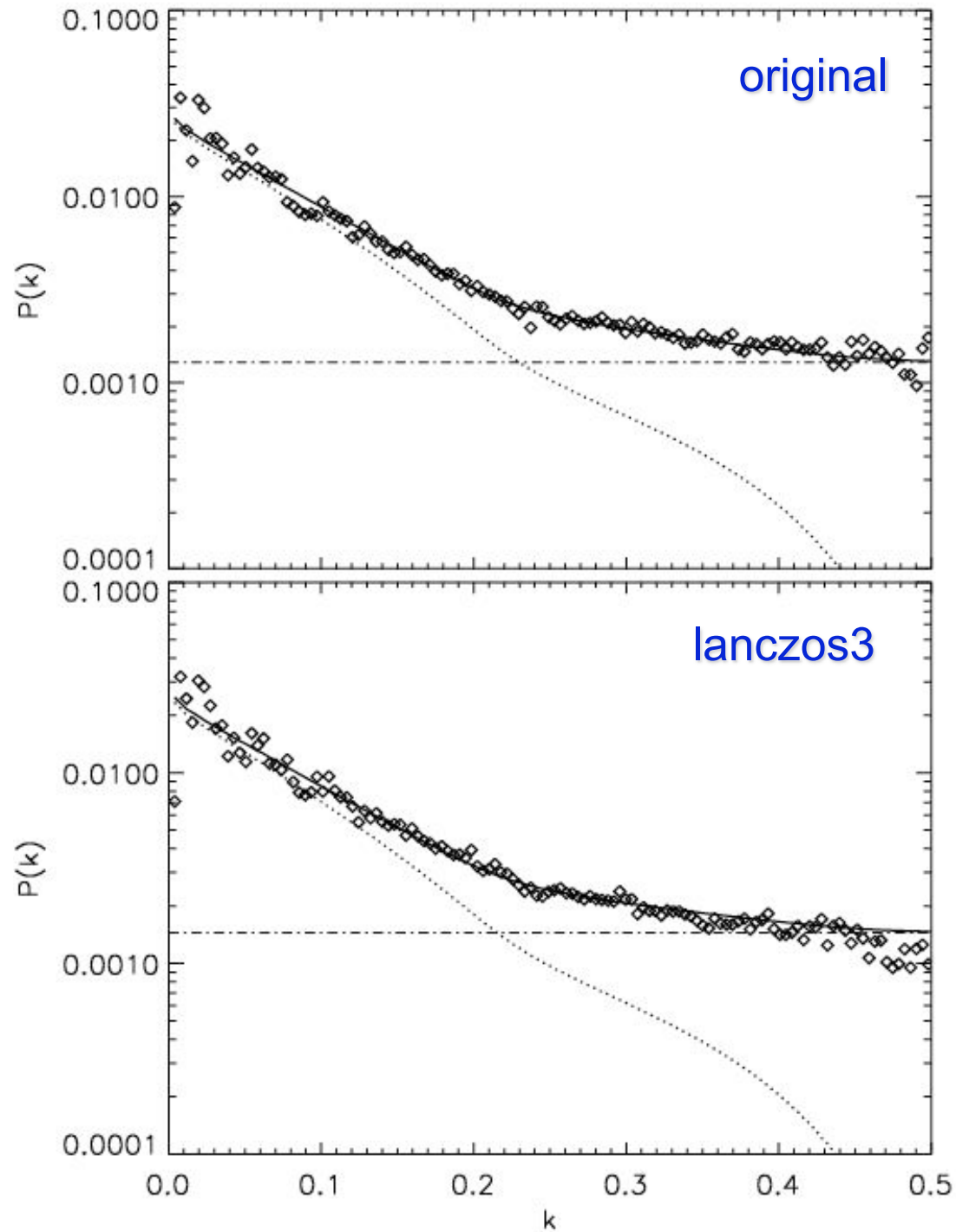
Lanczos3 kernel



Overall gradient is due to variable pixel area in original (distorted) image.

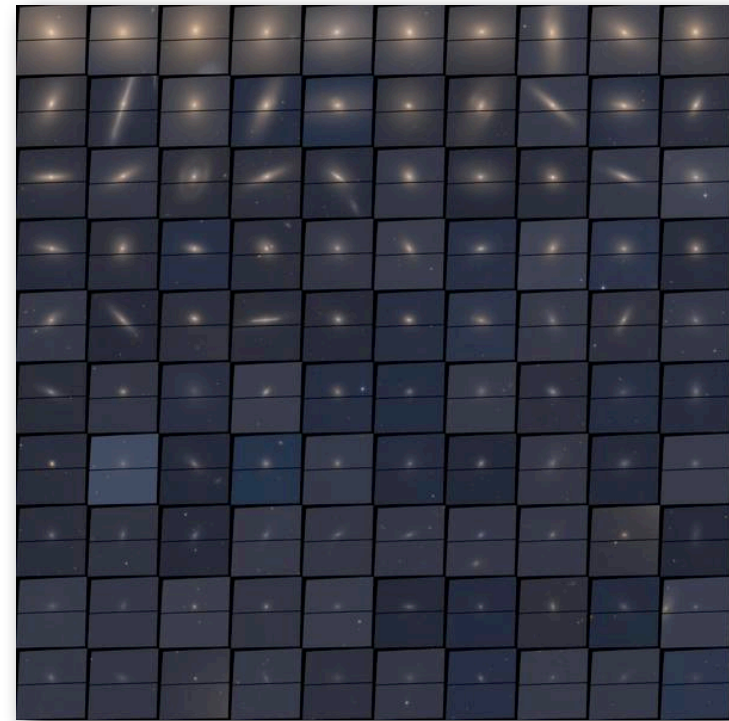
Simulations indicate we can get unbiased measurement of the power spectrum amplitude using the lanczos3 kernel, though may need to omit the highest wavenumbers from the fit.

Mei, Blakeslee, Tonry,
& ACS Virgo Team 2005

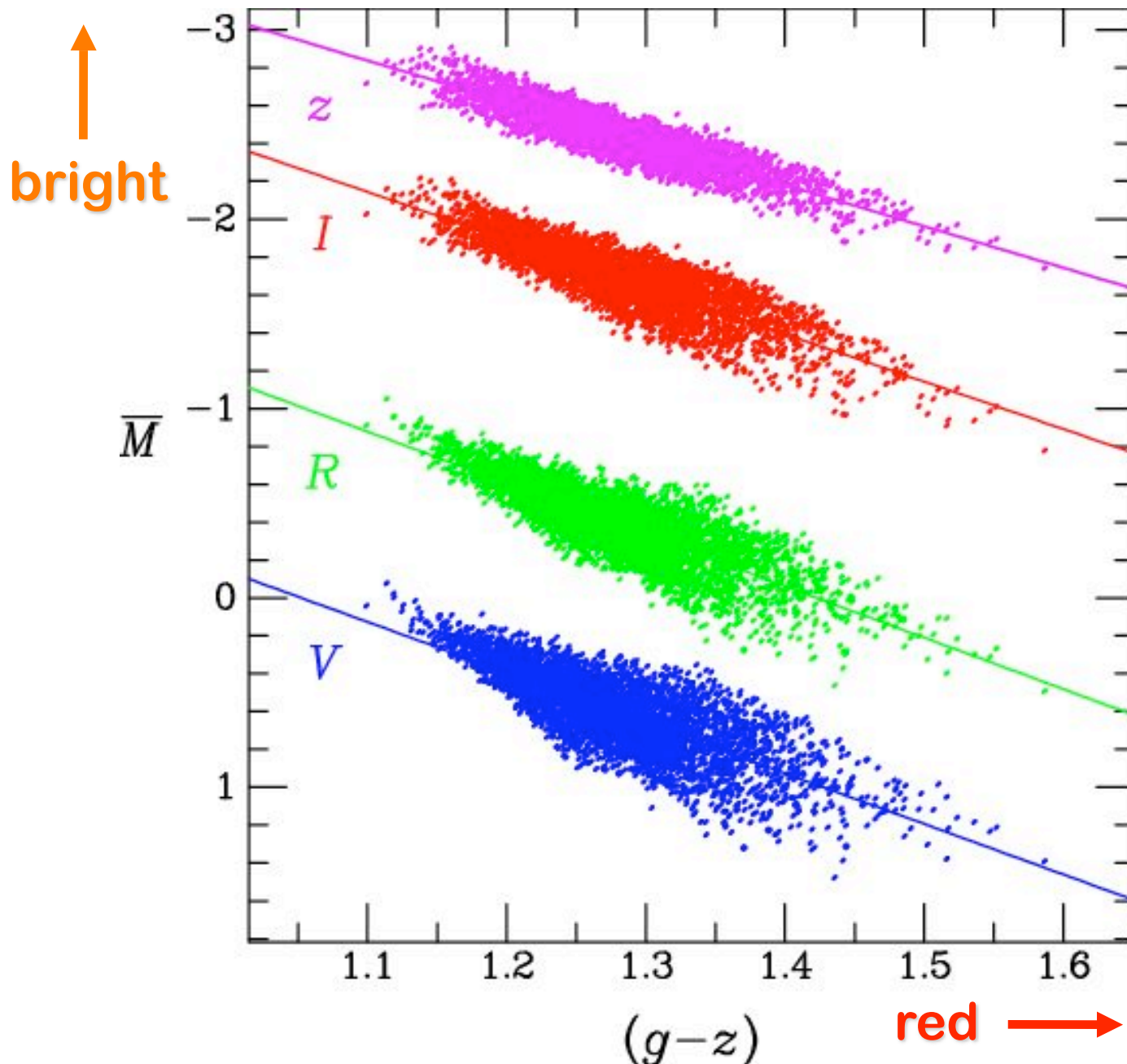


ACS Virgo + Fornax Surveys

- * Imaging surveys of 100 [+43] early-type galaxies in the Virgo [+Fornax] clusters with **g+z** bandpasses of the *Advanced Camera for Surveys* (ACS) on HST
- * **ACSVCS** (Cycle 11) and **ACSFCS** (Cycle 13)
- * Scientific Objectives Include:
 - * Properties of **globular clusters** (GCs) in early-type galaxies: half-light radii (Jordán et al. 2005), colors (Peng et al. 2006), masses (Jordán et al. 2006; 2007), LMXB connection (Jordán et al. 2004, Sivakoff et al. 2006), CMDs (Mieske et al. 2006), frequencies and formation efficiencies (Peng et al. 2007)
 - * **Central structure** of early-type galaxies and their **nuclei** and **black holes** [Ferrarese et al. 2006ab; Côté et al. 2006, 2007]
 - * Calibration of the **Surface Brightness Fluctuations** method in ACS **z**-band, derivation of distances and mapping of the **3-D galaxy distribution** in Virgo; exploration of effects from stellar population variation [Mei, Blakeslee, Tonry, et al. 2005ab, 2007]



SBF “fluctuation magnitude” versus (g-z) color: elliptical galaxy stellar population **VRIz** predictions



z-band SBF bright;
~ 0.06 mag scatter.

Blakeslee, Vazdekis,
& Ajhar 2001
composite stellar
population models.

Other SBF models:

Worthey 1993

Buzzoni 1993

Liu et al. 2000

Cantiello et al. 2003

Mouhcine et al. 2005

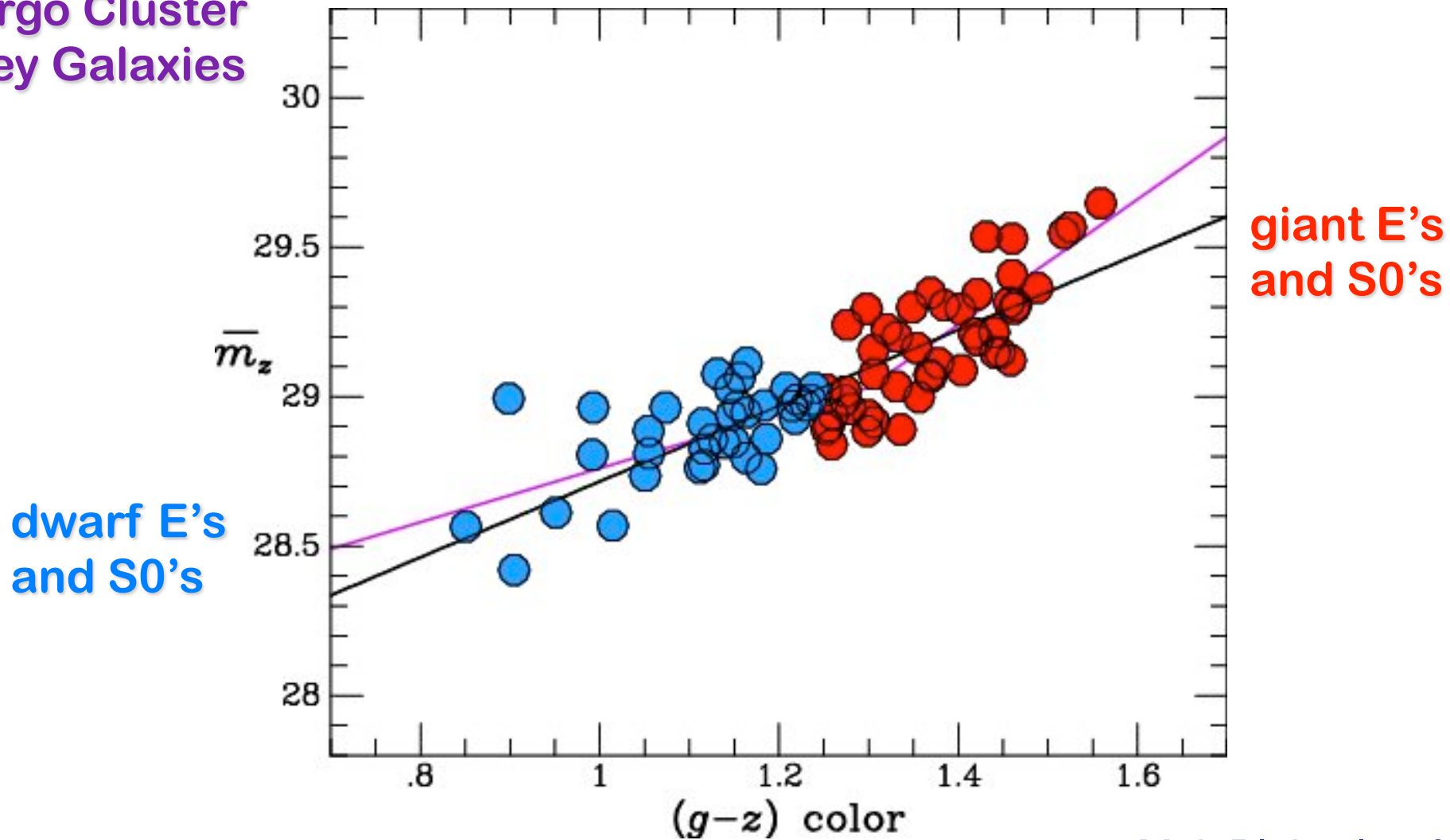
Raimondo et al. 2005

Marin-Franch &
Apparicio 2006

Lee et al. 2008

z-band SBF magnitude versus (g-z) color: The Empirical Distance Calibration

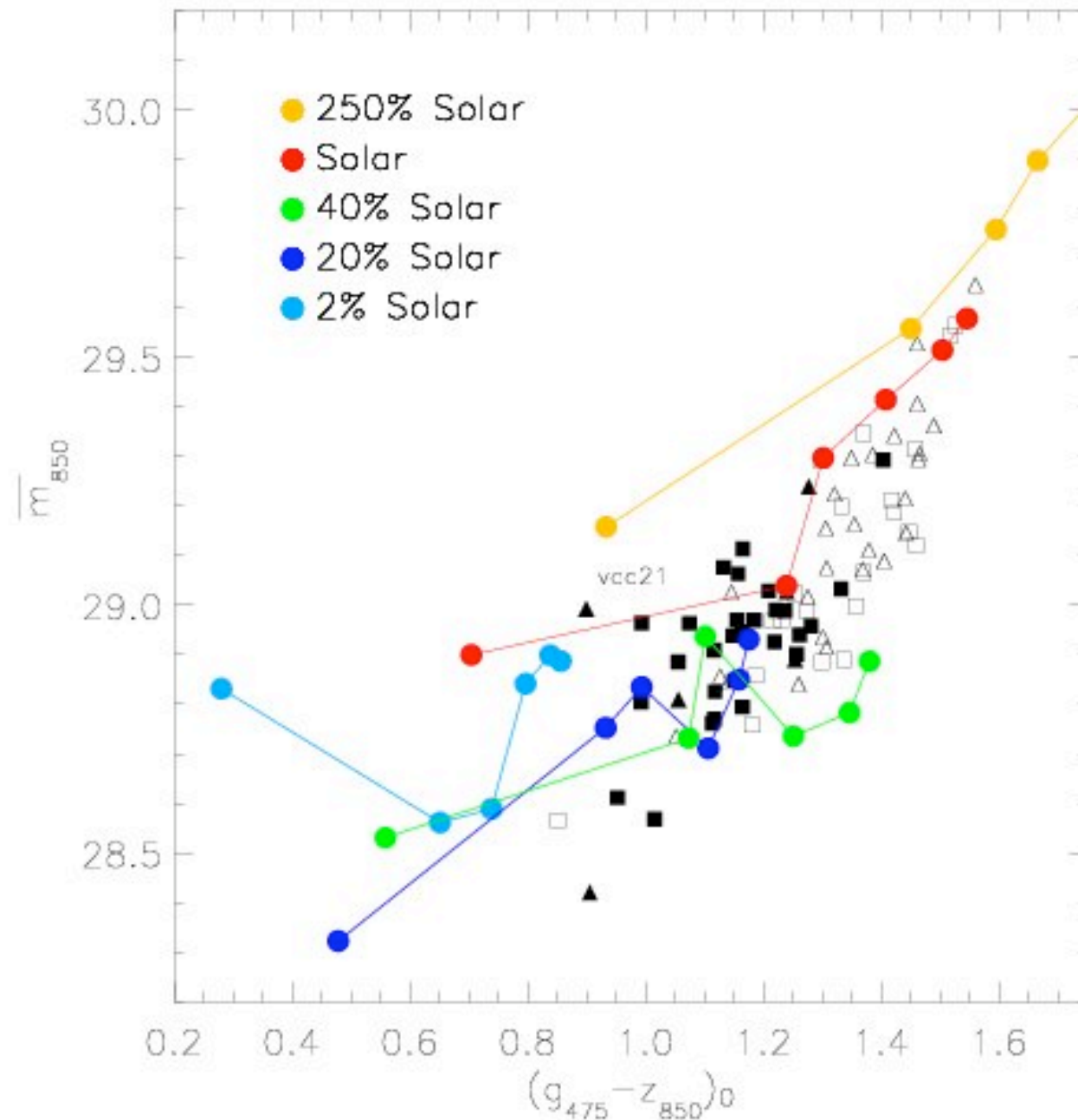
85 Virgo Cluster
Survey Galaxies



(Omitting background W' galaxies)

Mei, Blakeslee &
ACS Virgo Team
2005, ApJ.

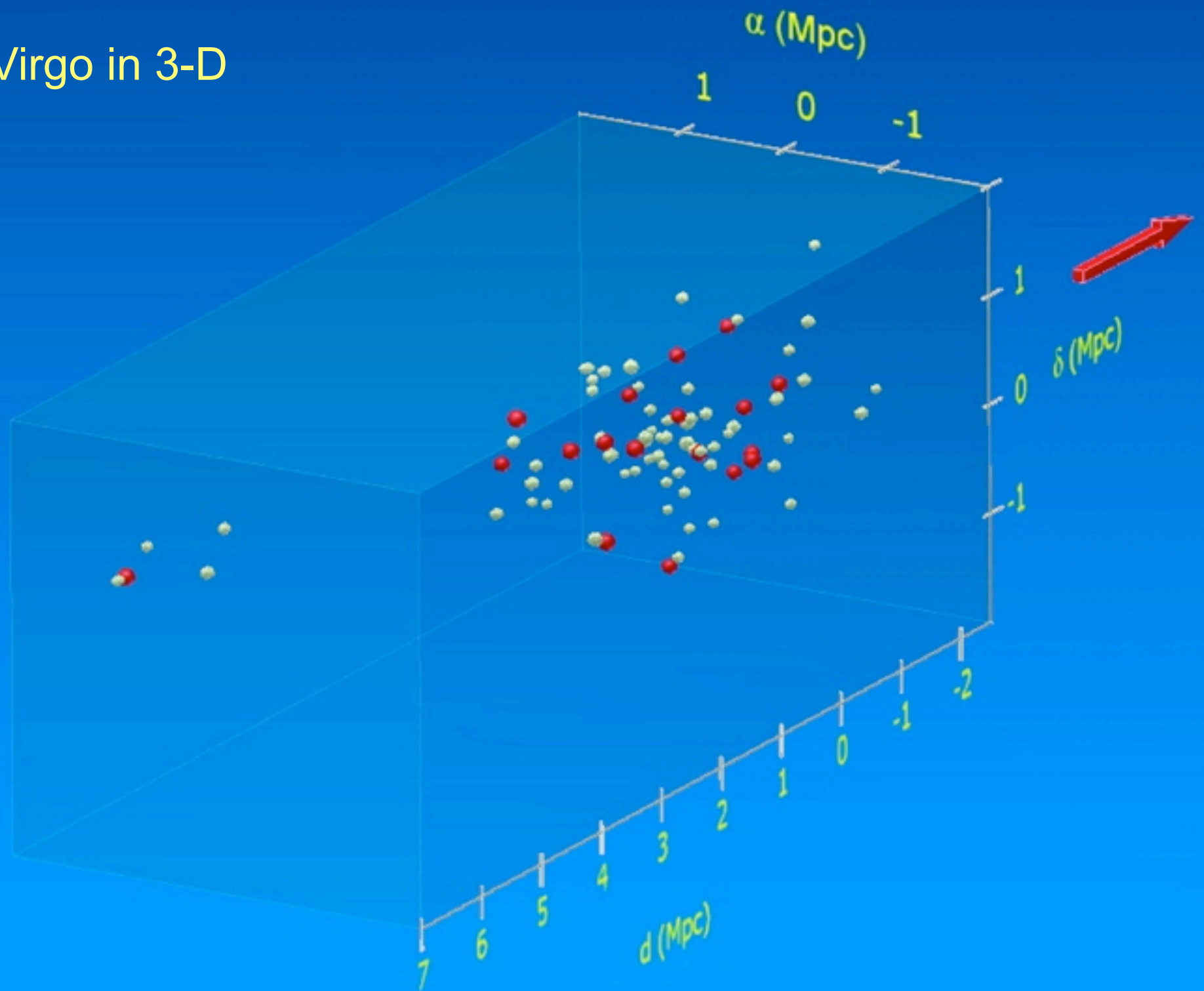
ACSVCS SBF measurements compared to BC2003 stellar population model predictions



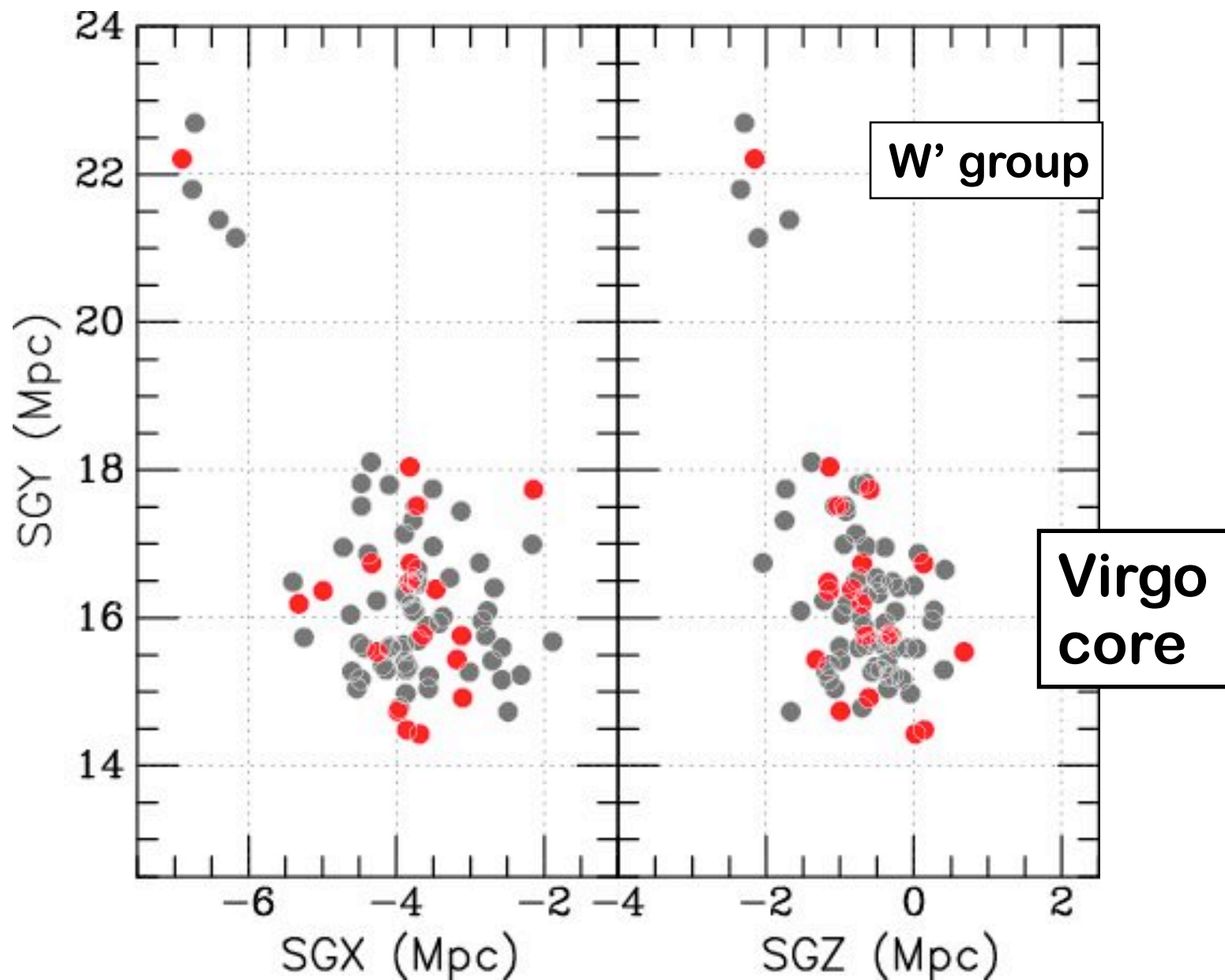
Theoretically-calibrated SBF Virgo distance of 15.5 Mpc (but some uncertainty in model zero-point luminosity).

See also the comparison to Raimondo et al. (2005) models in Biscardi et al. (2008).

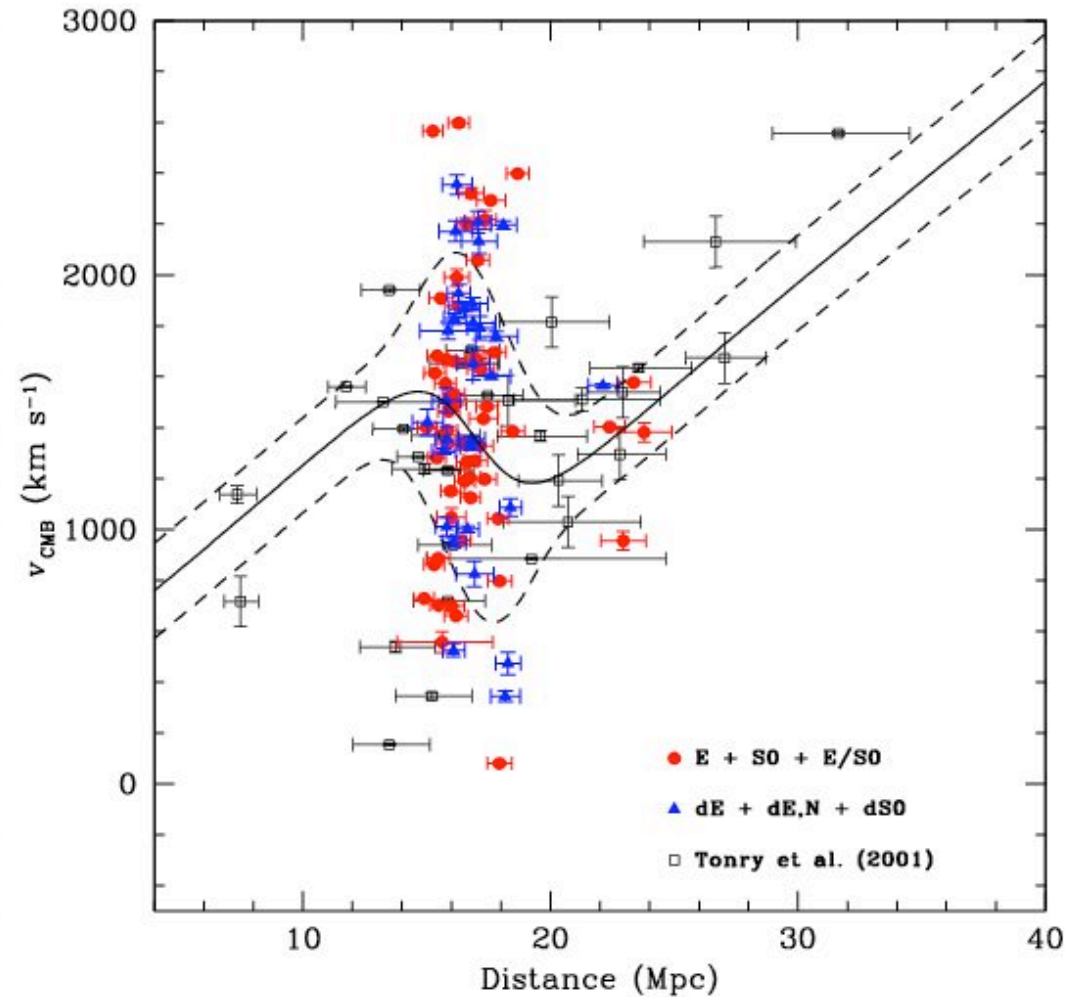
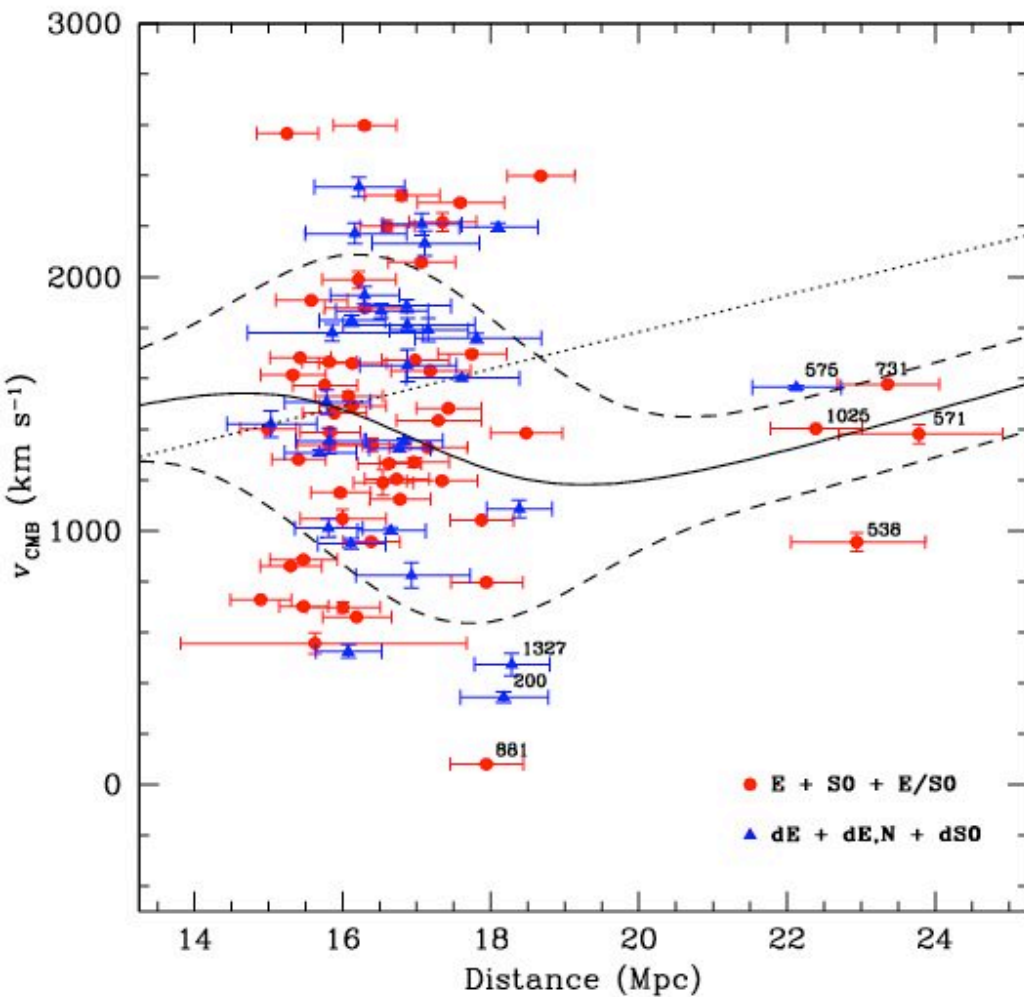
Virgo in 3-D



The 3-D Structure of Virgo: Projections in the Supergalactic Plane



Velocity-distance relation from the ACS Virgo Cluster Survey



3-D Structure of Virgo

- Mean error per galaxy: $\sigma (m-M) = 0.07$ mag, or ≈ 0.5 Mpc.
- Triaxial structure, with axial ratios about **1 : 0.7 : 0.5**
- Line-of-sight depth of main cluster = 2.4 ± 0.4 Mpc (i.e., $\pm 2\sigma$ intrinsic distribution).
- Spatial distribution of dwarfs follows that of giants.
- Group of galaxies associated with NGC 4365 (W' Cloud) about 6.5 Mpc behind main cluster and infalling at ~ 450 km/s.
- Other substructure evident, e.g., the high-velocity galaxy M86 (NGC4406) and companions are ~ 1 Mpc beyond the core.
- M87 and M49 subclusters at essentially identical $D \approx 16.5$ Mpc.

“Next Generation Virgo Survey”

Approved CFHT
Large Survey
Programme,
PI: L. Ferrarese

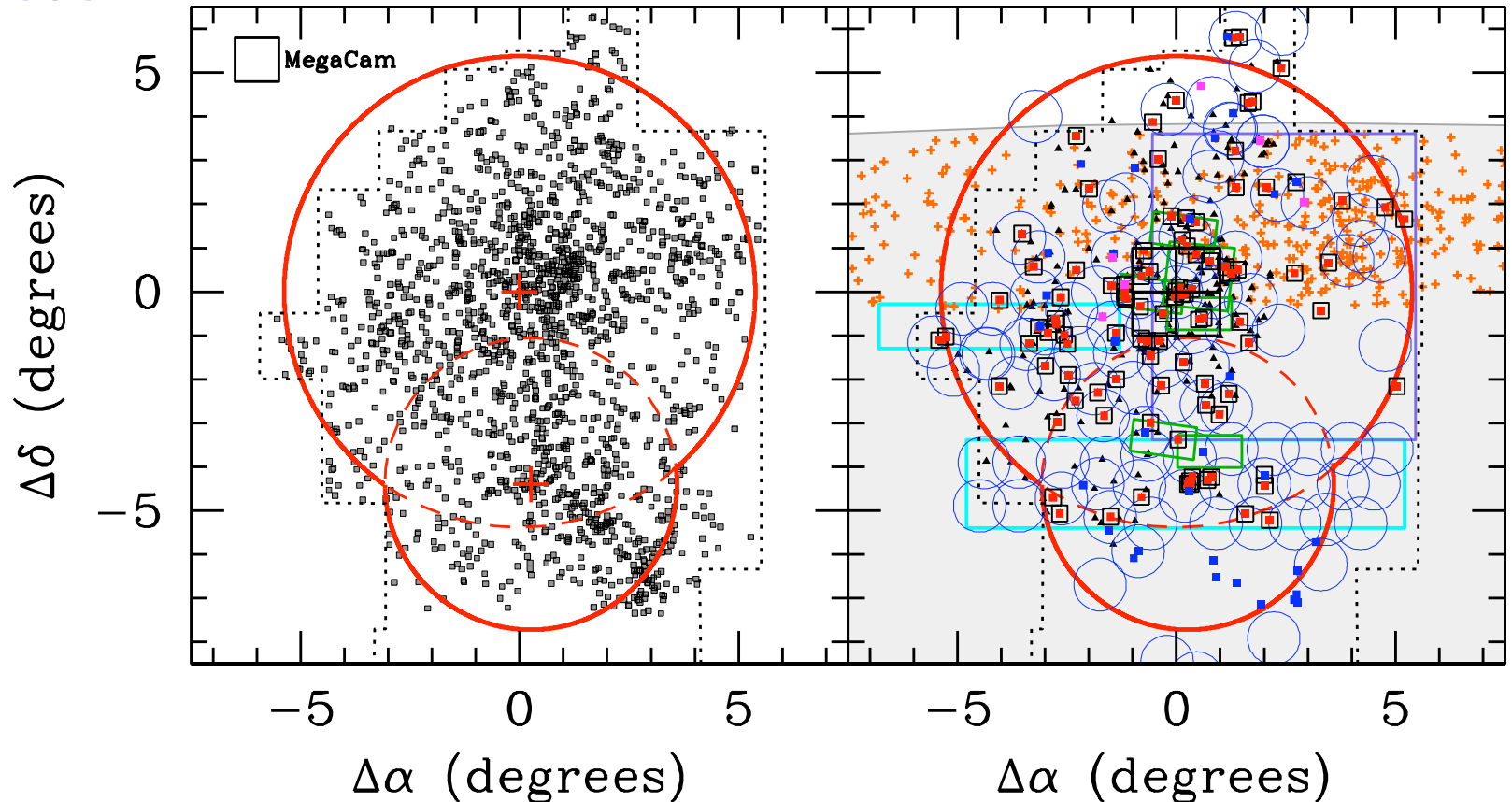
- Virgo Cluster Catalog (Binggeli et al. 1985)
- + Subcluster A and B centers
- ACS Virgo Cluster Survey
 - Cote et al. (2004, 2008) (ACS,WFP2,NIC1,WIRCam)
 - Treu et al. (2007) (Chandra, Spitzer)
 - Kenny/Axon et al. (2008) (VLA)
- GALEX fields
- CWR Intracluster Light Survey
- Arcibo Galaxy Environment Survey (AGES)
- Herschel Virgo Cluster Survey (HeViCS)
- UKIDSS/LAS (UKIRT Infrared Deep Sky Survey)

<http://www.astrosci.ca/NGVS>

Pilot

▲ MacDonald et al. (2008) H-band Survey

— NGVS Survey - R_{200} for Subclusters A and B



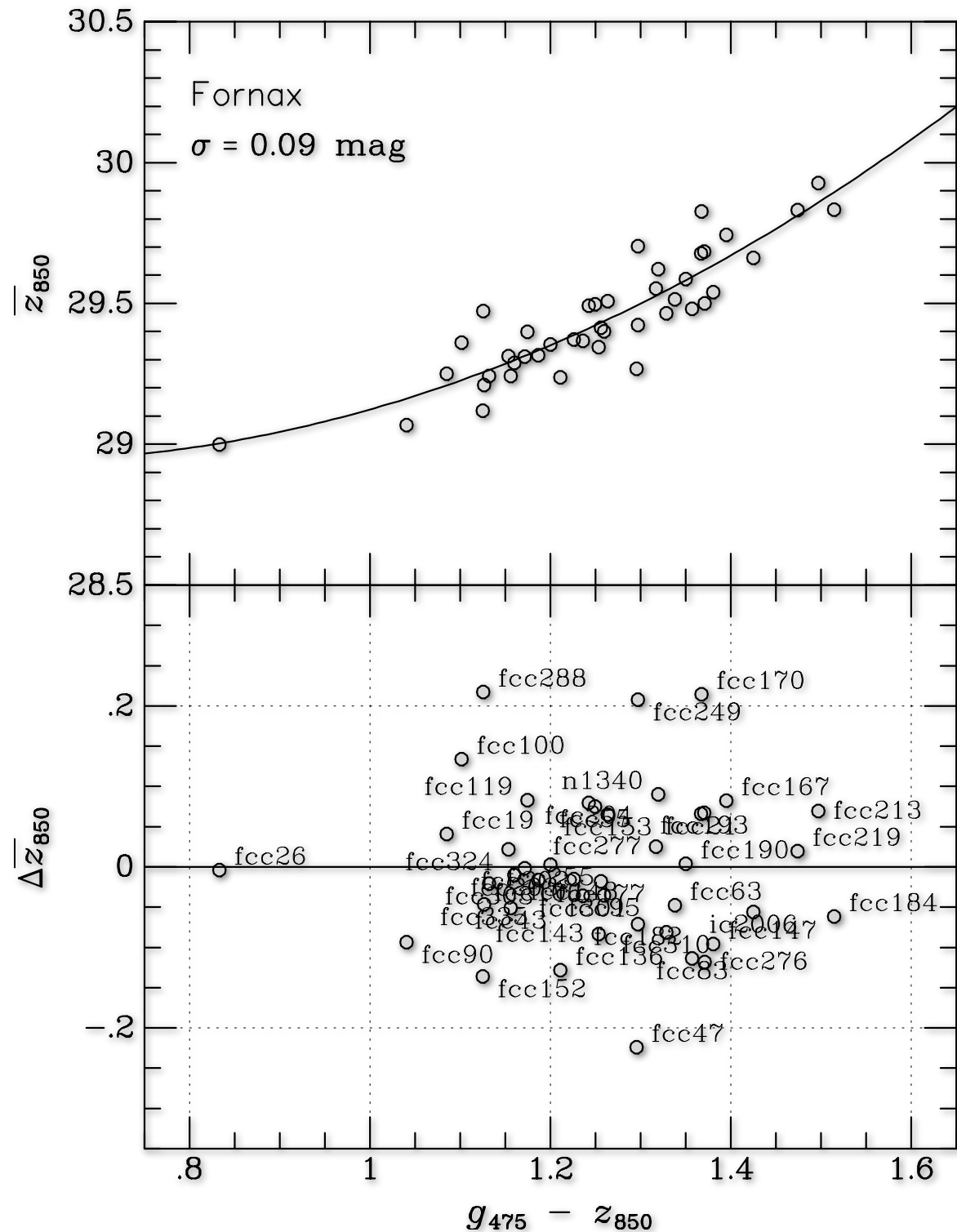
What about Fornax?

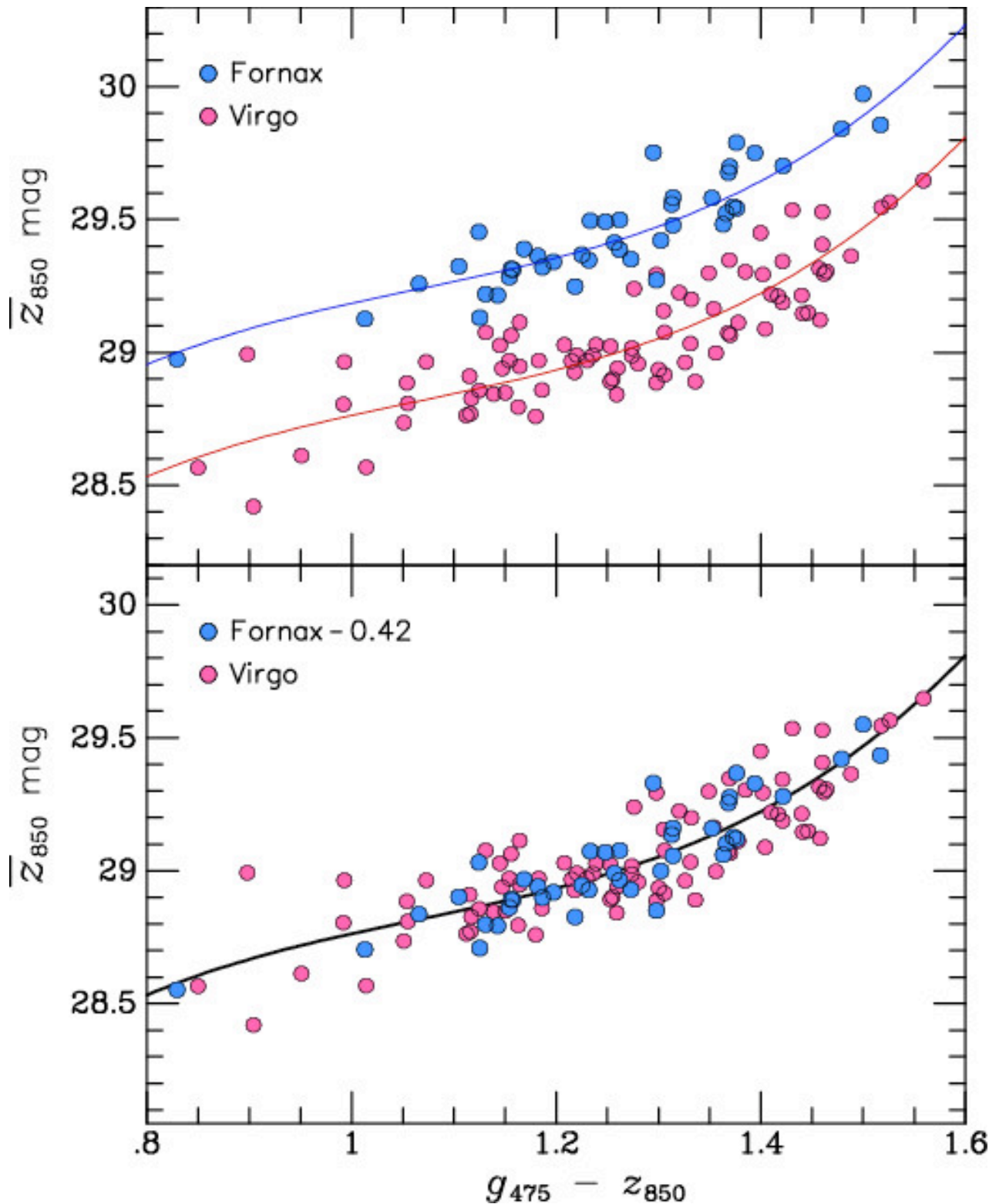
The Fornax Cluster:

- more regular and dynamically evolved than Virgo
- core radius $\approx 40\%$ that of Virgo
- central density ($\approx 500 \text{ Mpc}^{-3}$) twice that of Virgo
- velocity dispersion ($\approx 370 \text{ km s}^{-1}$) half that of Virgo
- order of magnitude higher collision rate
- compact structure ideal for distance calibration
 - will allow us to improve work on Virgo structure

SBF results for Fornax

Scatter about 20% less than in Virgo, despite ~20% larger distance.

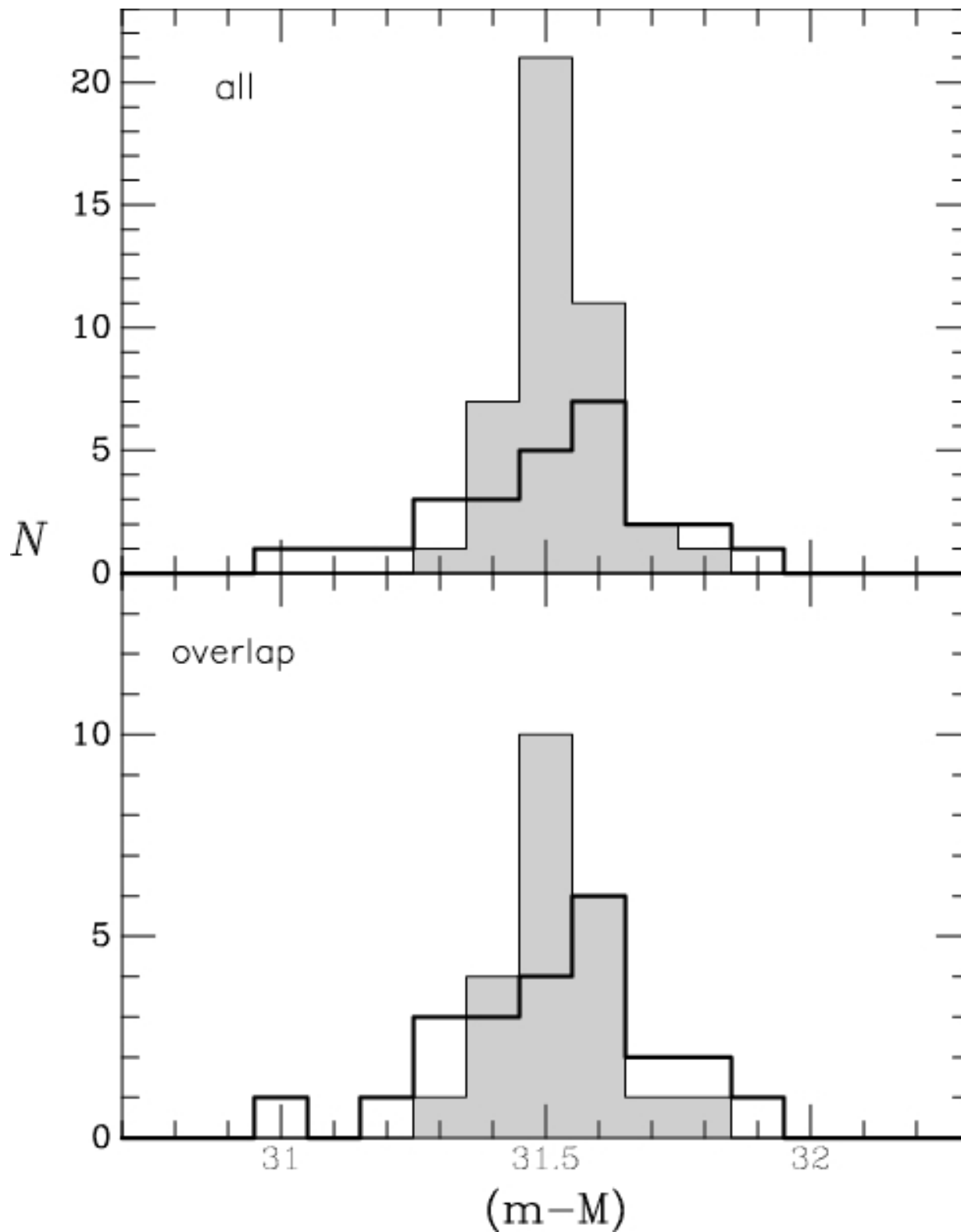




SBF Results from ACS Fornax + Virgo Surveys

Fornax cluster
is $21 \pm 1\%$ more
distant than
Virgo cluster.

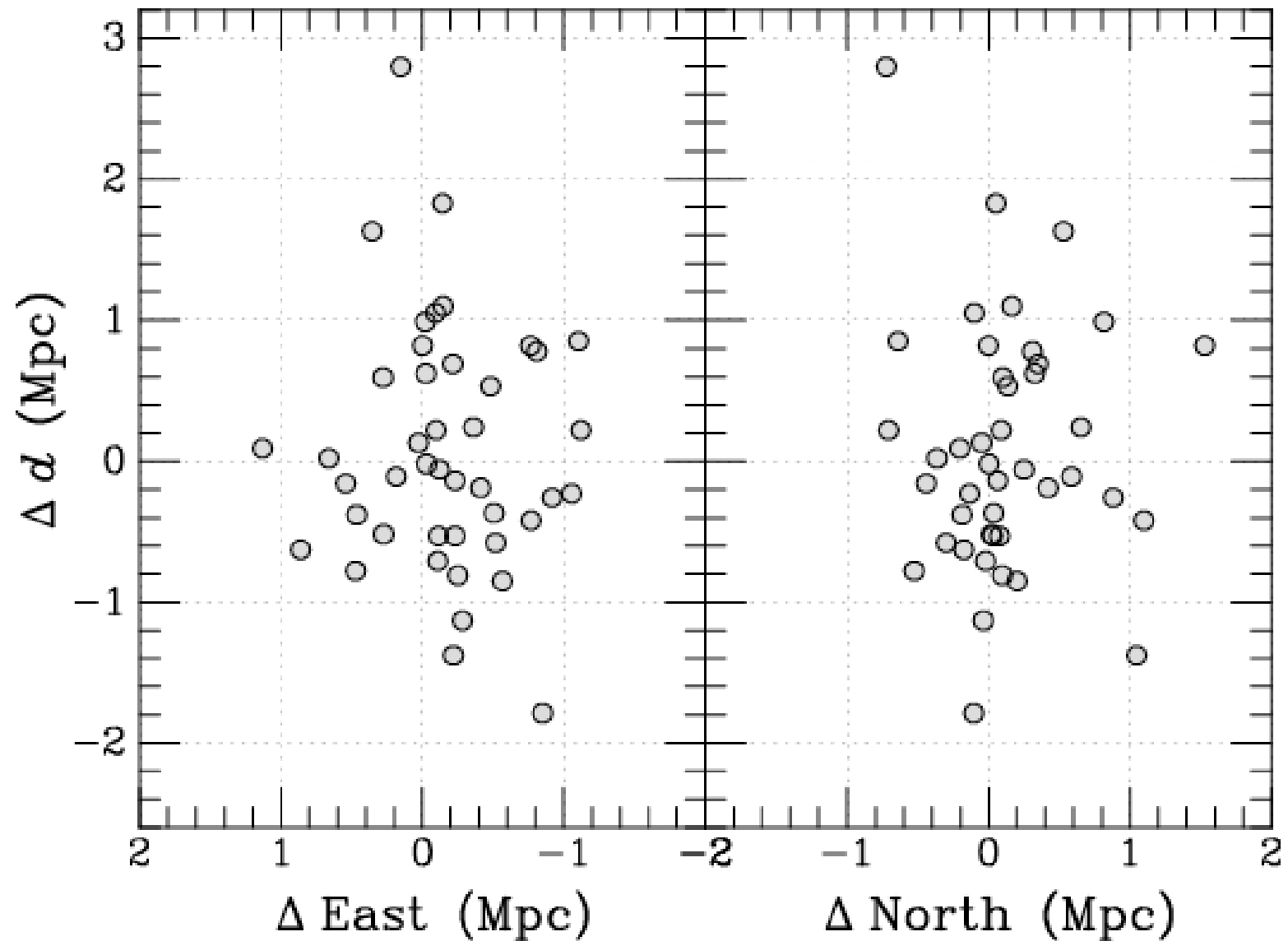
JPB et al 2008,
ApJ, submitted.



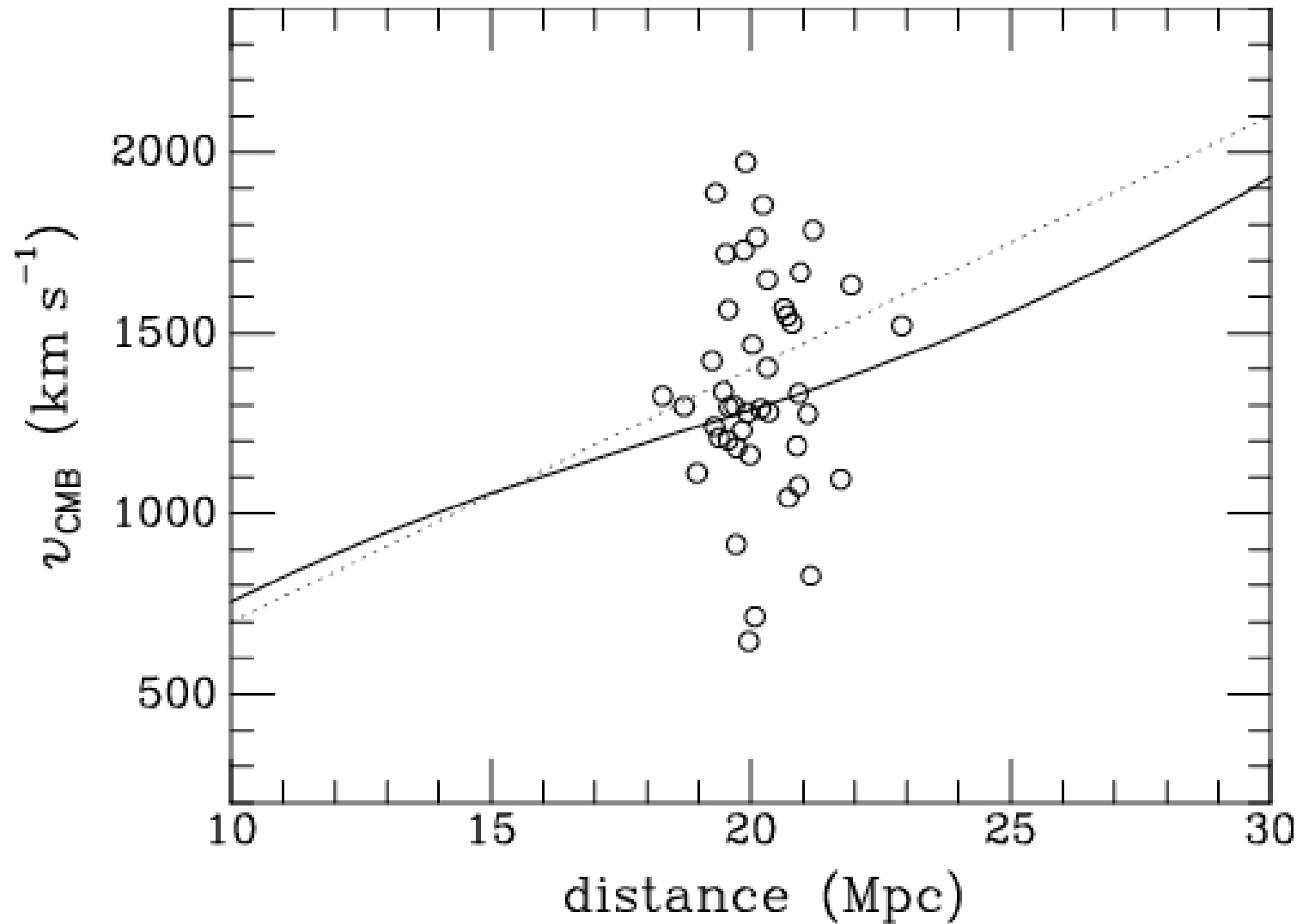
ACS Fornax Survey
compared to Tonry
et al. 2001 distances

3x improvement in
measurement error;
2x improvement in
distance uncertainty.

Structure of Fornax (or lack thereof)



Fornax Hubble Diagram



No sign of velocity-distance relation, unlike in Virgo

Infrared SBF

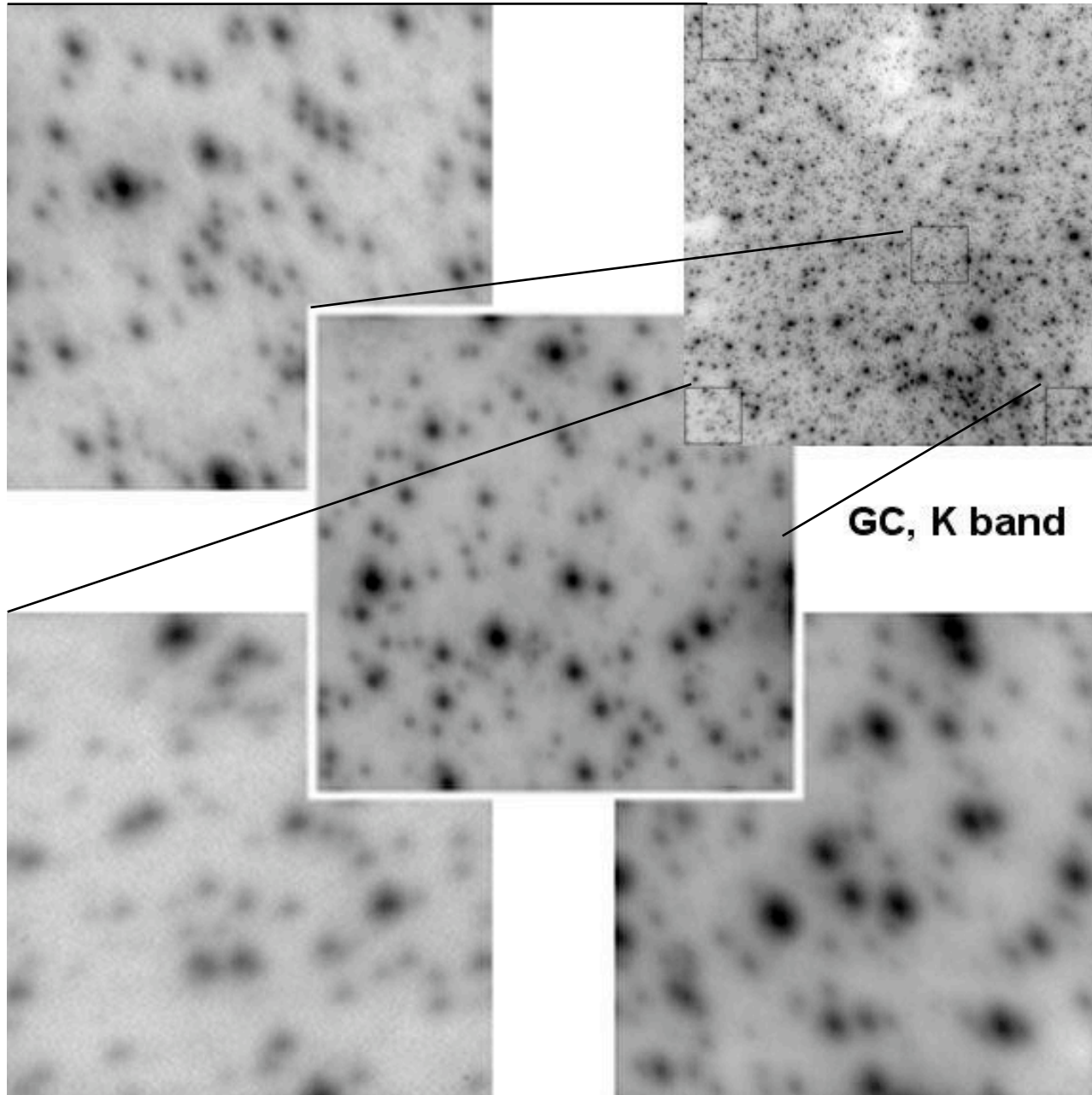
- SBF is $\sim 30\times$ more luminous at K than at I
 - ◆ Dominated by luminous RGB stars
- Increased contrast with (less contamination from) globular clusters & background galaxies
- Seeing is better in the near-IR
- Extinction is much lower than in the optical
- Sensitive to young populations and AGB stars
- Age-metallicity degeneracy is broken
 - IR SBF can reach greater distances
 - IR SBF can reveal young and intermediate components in unresolved stellar populations

IR SBF with Adaptive Optics

- SBF measurements rely on photometric PSF fitting in Fourier space.
- Temporal and spatial variations of the PSF in AO images have limited their usefulness for SBF measurements to date.



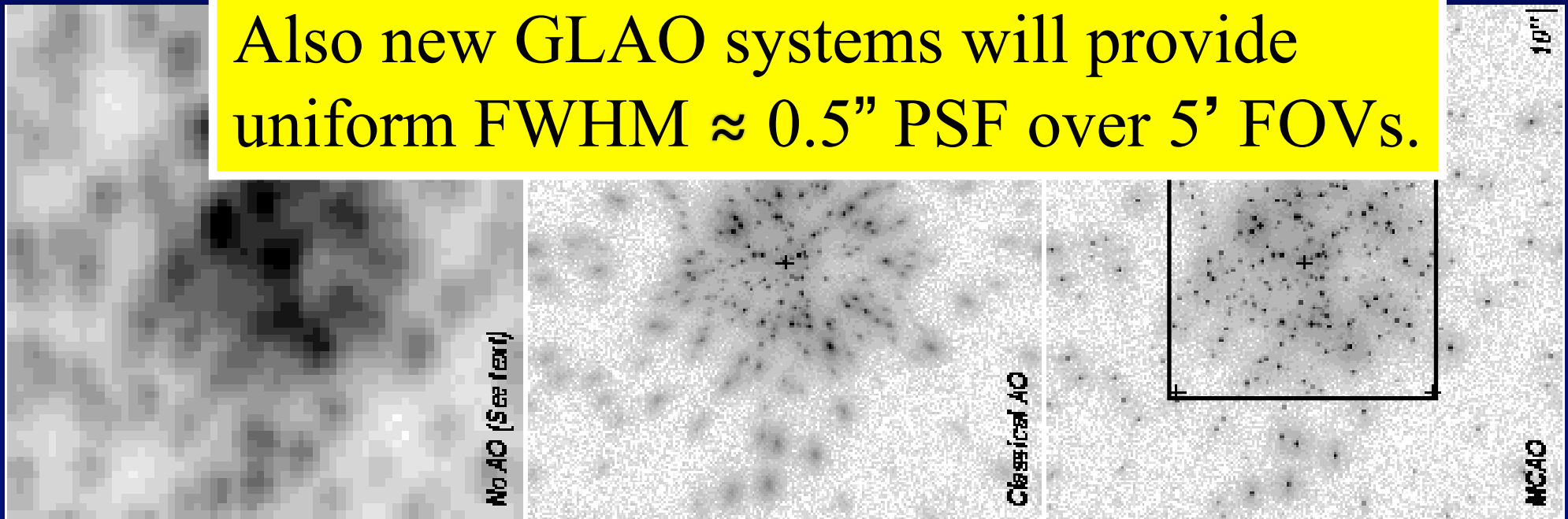
Anisoplanatism



Multi-conjugate AO

- Gemini MCAO + GSAOI
 - ◆ Provides a uniform PSF across a 1.4×1.4 arcmin field
 - ◆ 3 DMs, 5 laser guide stars, 3 natural tip-tilt guide stars
 - ◆ 4096×4096 with 0.02 arcsec pixels, 2 arcmin^2
 - ◆ Will be deployed on Gemini-South in 2009 (fingers crossed)

Also new GLAO systems will provide uniform FWHM $\approx 0.5''$ PSF over $5'$ FOVs.



IR SBF: looking ahead . . .

JWST NIRCam

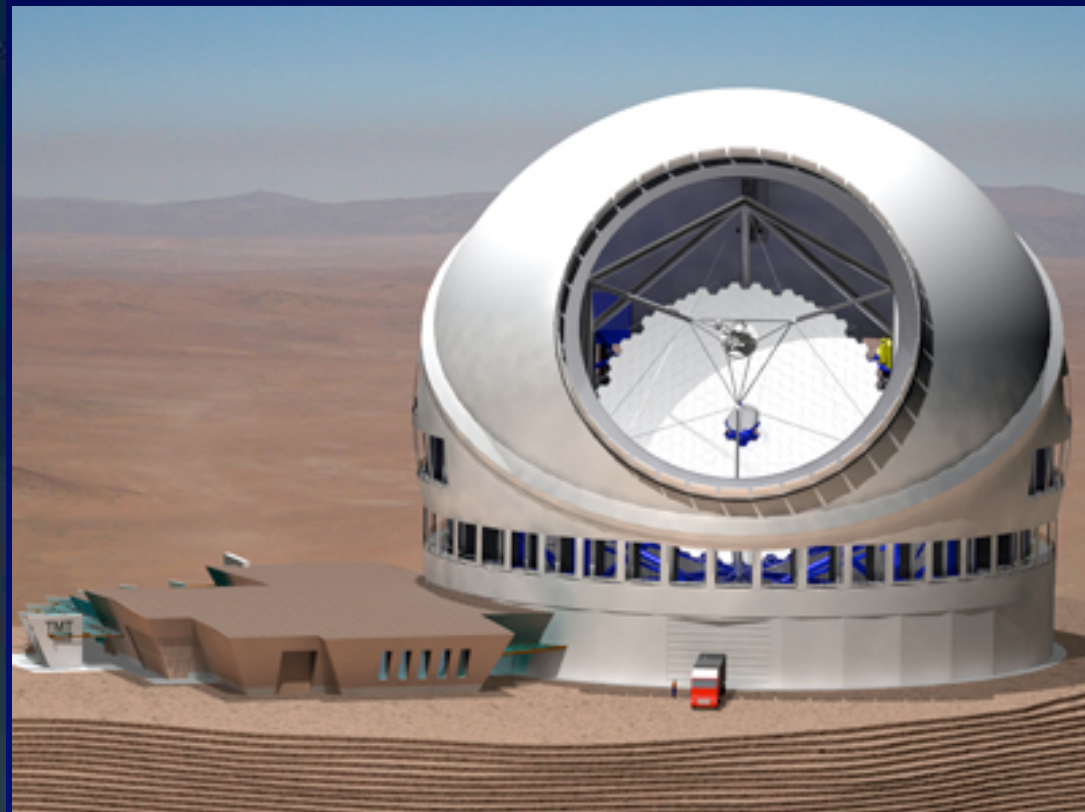
- Very low background
- Extremely stable PSF



10× further than Gemini
or HST/NICMOS

TMT IRIS

- Enormous collecting area
- Very high spatial resolution
diffraction-limited images



50× faster than Gemini

Peculiar Velocity Surveys and Large-Scale Flows



The density and peculiar velocity fields of nearby galaxies

Michael A. Strauss^a, Jeffrey A. Willick^b

^a *School of Natural Sciences, Institute for Advanced Study, Princeton, NJ 08540, USA*

^b *Observatories of the Carnegie Institution of Washington, 813 Santa Barbara Street, Pasadena, CA 91101-1292, USA*

Received February 1995; editor D.N. Schramm

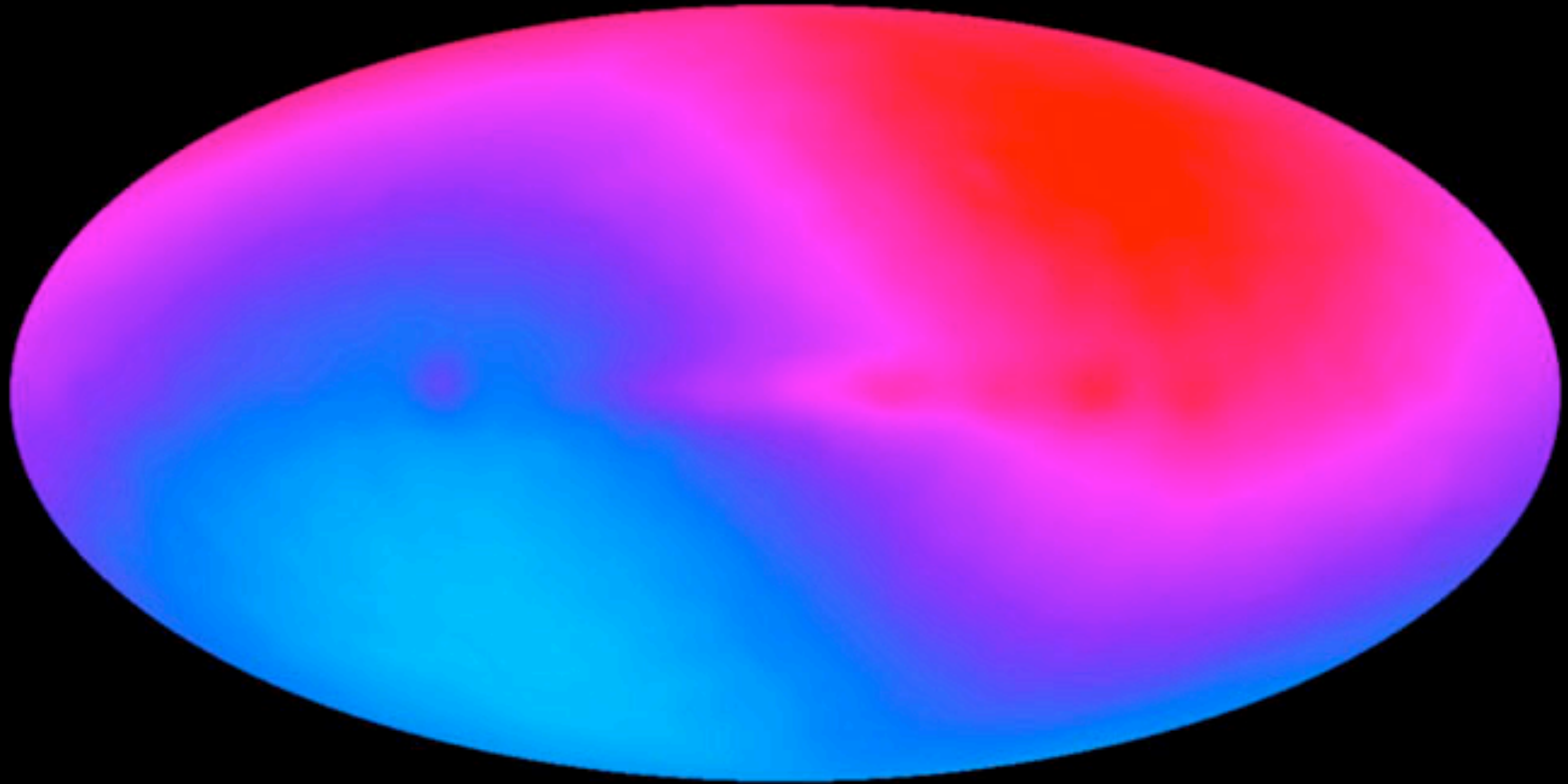
Contents:

1. Introduction	274	5.5. The density distribution function and counts in cells	336
2. Theoretical background	276	5.6. Topology and related issues	338
2.1. The Big Bang model and its parameters	276	5.7. The dipole	339
2.2. The gravitational instability paradigm	280	5.8. Spherical harmonics	341
2.3. Power spectra, initial conditions, and dark matter	283	5.9. Recovering the real space density field	343
2.4. The relation between the mass and galaxy density fields	289	5.10. Clustering of different types of galaxies	345
2.5. Outstanding questions	291	6. Peculiar velocity fields: techniques of measurement and analysis	347
3. Redshift surveys: setting the quantitative groundwork	292	6.1. Galaxian distance indicator relations	349
3.1. The variety of redshift surveys	292	6.2. Universality of the distance indicator relations	357
3.2. History of redshift surveys	294	6.3. Beyond TF and D_n - σ : a look to the future?	358
3.3. The measurement of galaxy redshifts	298	6.4. Statistical bias and methods of peculiar velocity analysis	361
3.4. Determination of the luminosity and selection functions	300	6.5. Quantifying statistical bias	369
3.5. Luminosity functions: scientific results	305	7. Statistical measures of the velocity field	383
3.6. Testing the Hubble law with redshift surveys	306	7.1. A history of observations of large-scale flow	383
3.7. The smoothed density field	307	7.2. Homogeneous peculiar velocity catalogs	390
3.8. Filling in the galactic plane	311	7.3. Velocity correlation function	393
4. Redshift surveys: a cosmographical tour	313	7.4. The cosmic Mach number	394
5. Redshift surveys: galaxy clustering	317	7.5. Reconstructing the three-dimensional	

The CMB Dipole

- Until the 1970's, astronomers pretty much assumed that the Local Group, on average, was “at rest” with respect to the general Hubble expansion
- This changed with the discovery in 1976 of the dipole anisotropy in the Cosmic Microwave Background (CMB) radiation.
- The CMB provides a natural reference frame for the analysis of motions in the universe.
- The dipole in the CMB showed that the Local Group has a significant motion with respect to the overall mass distribution of the universe.

CMB Dipole



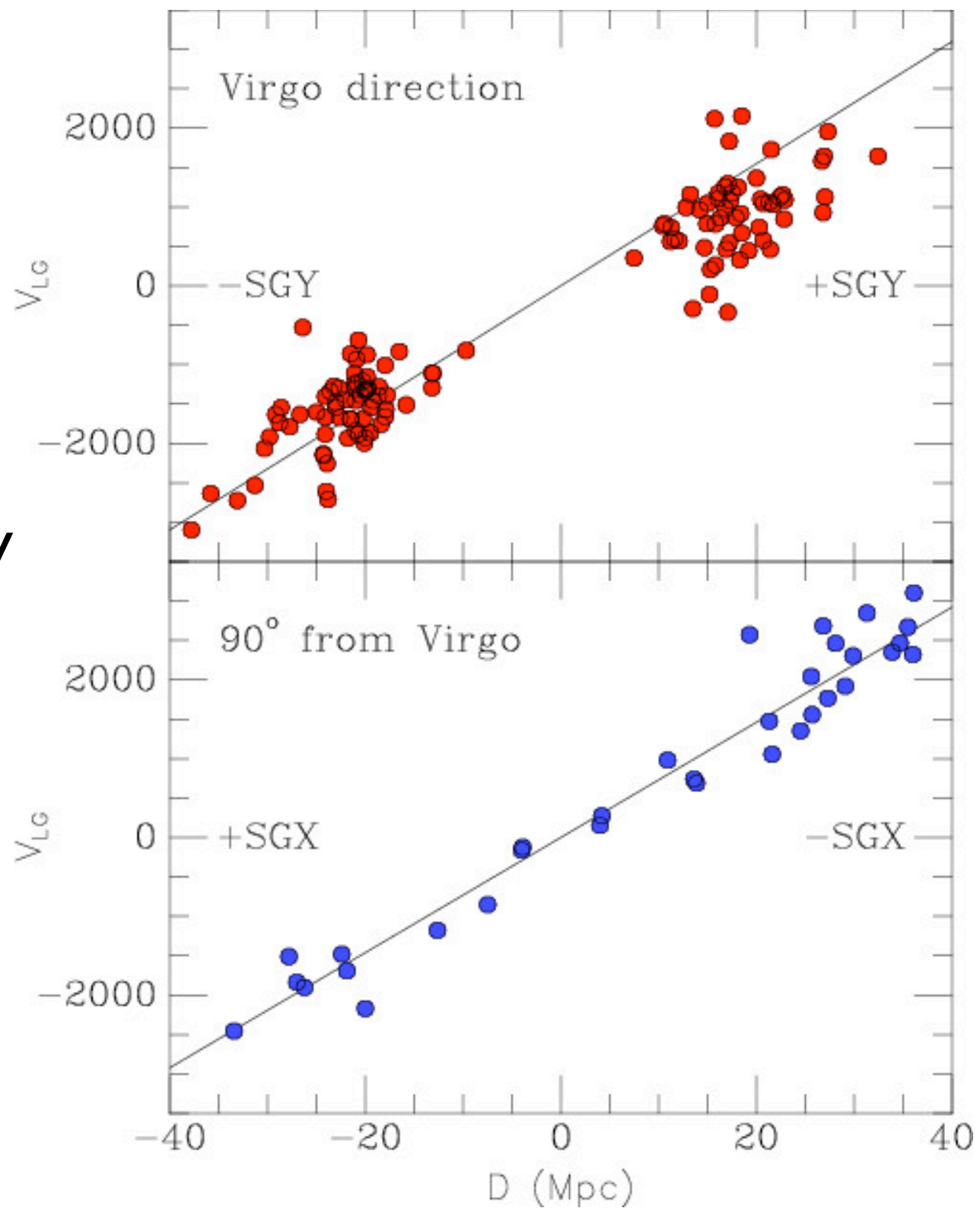
The CMB Dipole

- The solar system moves with a velocity of 370 km/s with respect to the CMB rest frame, known to very high precision from CMB experiments.
- Corrected for the Sun's orbit and the relative motion of the Milky Way and Andromeda, the barycenter of the Local Group is moving at 626 km/s with respect to the CMB in the direction: $(l, b) = 276^\circ, +30^\circ$
- Thus, peculiar velocities of many hundreds of km/s exist in the universe, even for groups in relatively low density regions such as the local volume.

Explaining the CMB Dipole

- Early work on peculiar motions (late '70s & early '80s) concentrated on measuring the infall of the Local Group towards the Virgo cluster, located at $cz \approx 1100$ km/s (or $d \approx cz/H_0 \approx 1100/72 \approx 15$ Mpc).
- Virgo infall velocities of 150-400 km/s were found; this was too low to account for the CMB dipole and not in the right direction, since Virgo is at $(l, b) = 187^\circ, +12^\circ$
- The rest of the LG motion must result from a pull in the direction of the Hydra-Centaurus supercluster. It was assumed that Hydra-Cen, which is at $cz \approx 3000$ km/s ≈ 40 Mpc, was the source of the gravitational attraction.

Virgo Infall as seen from SBF peculiar velocity measurements.



CMB Dipole: Great Attractor?

- However, in the late 1980s, a series of papers by the “Seven Samurai” (Faber, Dressler, Burstein, Lynden-Bell, Davies, Wegner, Terlevich) used the Fundamental Plane distance indicator to measure peculiar velocities for about 400 early-type galaxies.
- They reported that galaxies in the Hydra-Centaurus supercluster also participated in a large-scale flow towards a yet more distant source.
- The 7S group called the source of this motion the “**Great Attractor**”. They found a best-fit Hubble velocity $cz \approx 4500$ km/s for the GA, or about 50% more distant than Hydra-Cen itself (but in same direction).

CMB Dipole: Great Attractor?

- *Still more curiously*, attempts in the 1990s to measure “back-side infall” into the Great Attractor for galaxies at $cz = 5000$ km/s and beyond gave conflicting results. Claimed detections of the back-side infall were highly ambiguous and controversial.
- At the same time, it was also pointed out that the more distant **Shapley Supercluster**, at $cz \approx 14,800$ km/s lay in the same direction. Thus, the proposed GA might really be a combination of Hydra-Cen at 3000 km/s and Shapley at 4-5 times this distance.

Even Larger Scale Flows?

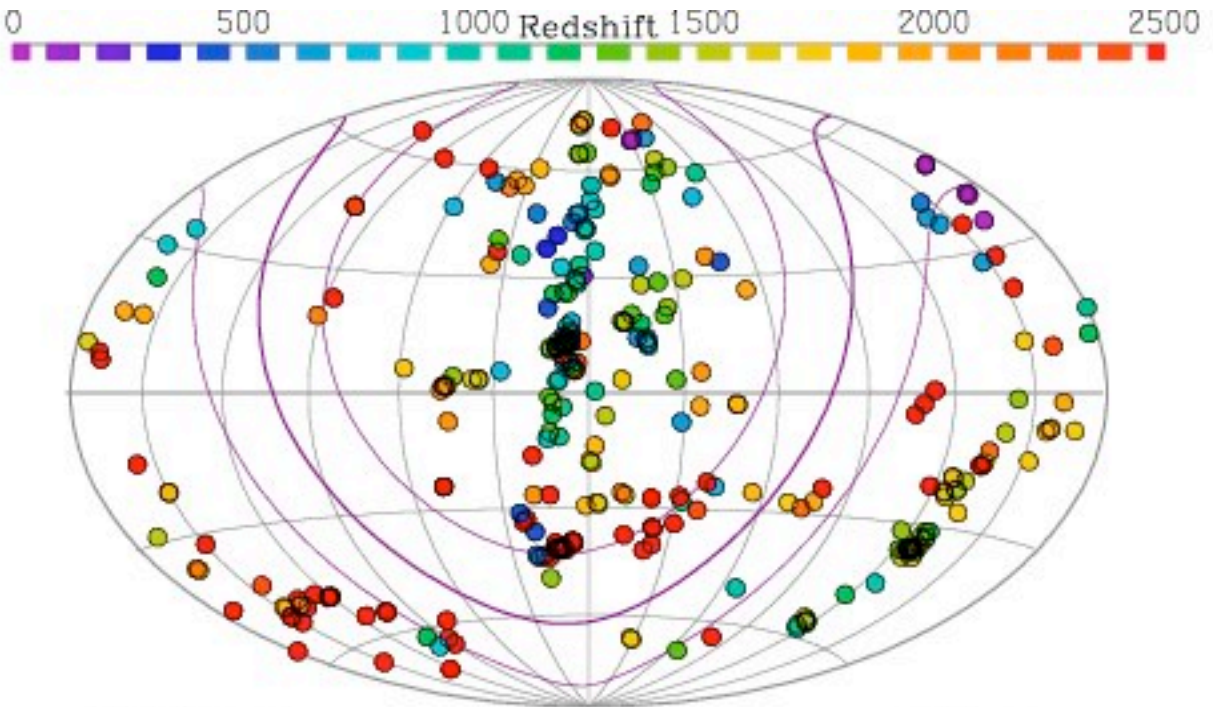
- In the mid-1990s, Lauer & Postman measured the bulk flow for 119 Abell clusters out to $cz = 15,000$ km/s using brightest cluster galaxies (BCGs) as *rough* standard candles (with a luminosity correction based on the galaxy profile).
- They found a similar amplitude bulk motion of ~ 600 km/s, but in an entirely different direction. This result attracted a lot of attention, because such a large amplitude flow, over such a large volume, appeared inconsistent with the smoothness of the CMB radiation. It would be difficult to generate so much power on these large scales, given that the universe appeared so smooth at recombination.
- No subsequent study confirmed the Lauer-Postman result, and most people now consider it incorrect, although no one has identified a major systematic error in their analysis.

(*cf.* Victoria Cosmic Flows conference)

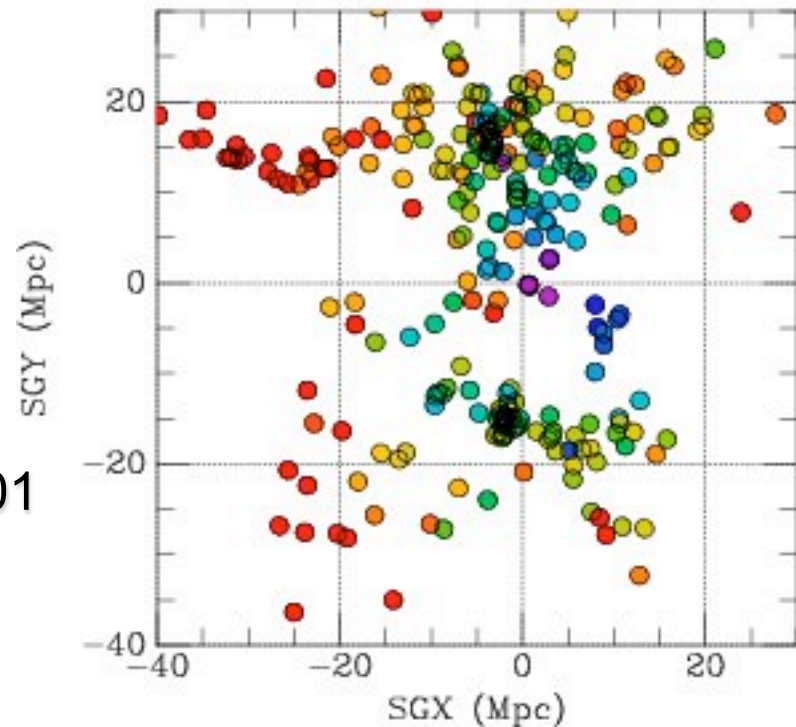
SBF in the 90's:
Ground-based *I*-band
survey of ~ 300 galaxies.

SBF distances
used to constrain
peculiar velocities,
Virgo infall,
 $H_0 \approx 73$ km/s/Mpc
 $\beta = \Omega^{0.6}/b \approx 0.45$
 $\Omega \approx 0.25$

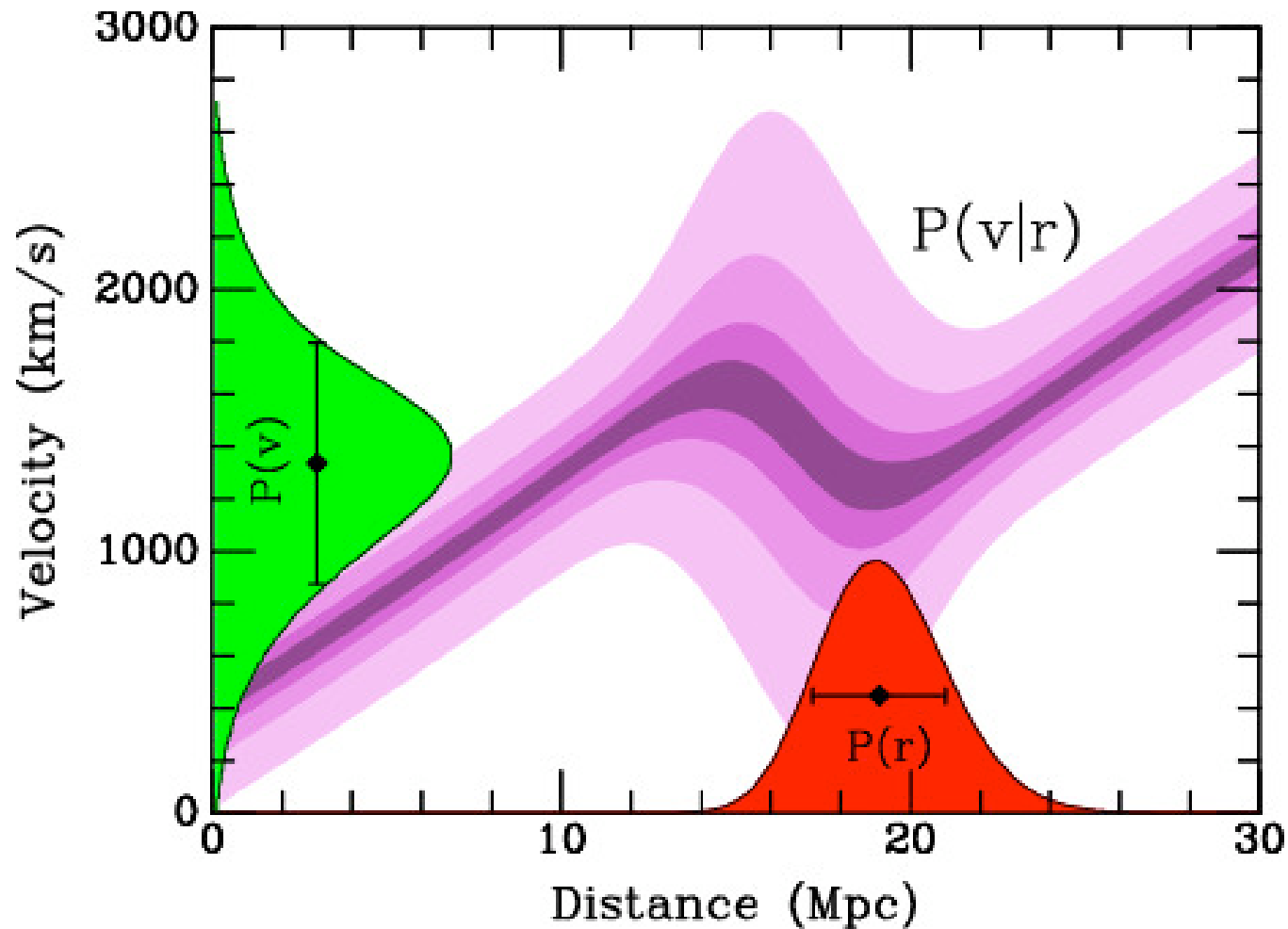
Tonry et al. 1997, 2000, 2001
Blakeslee et al. 1999, 2002



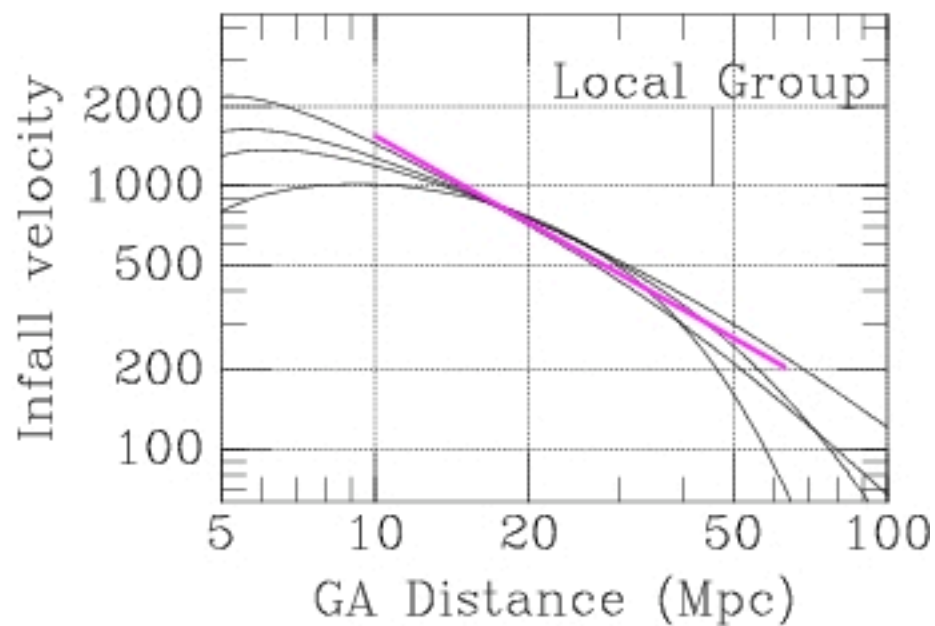
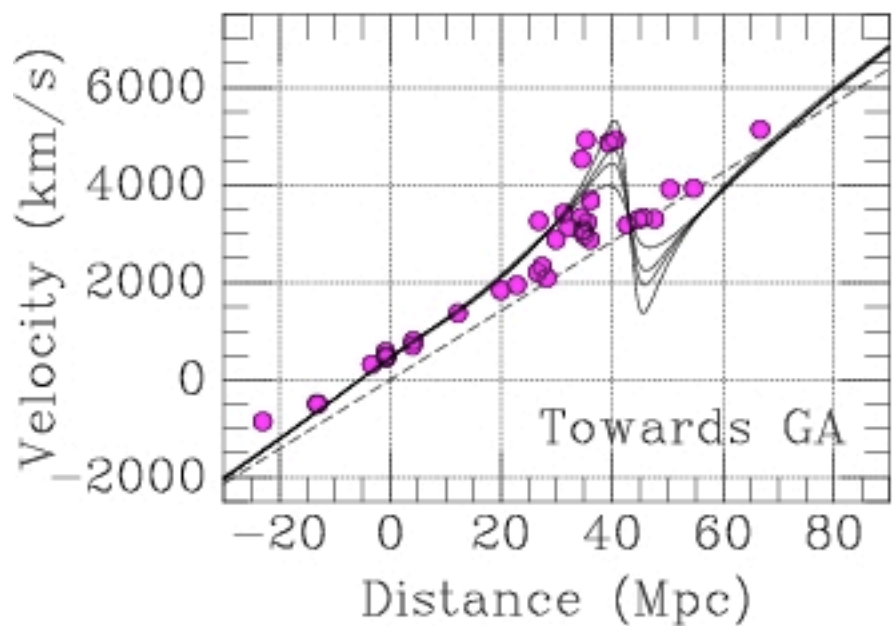
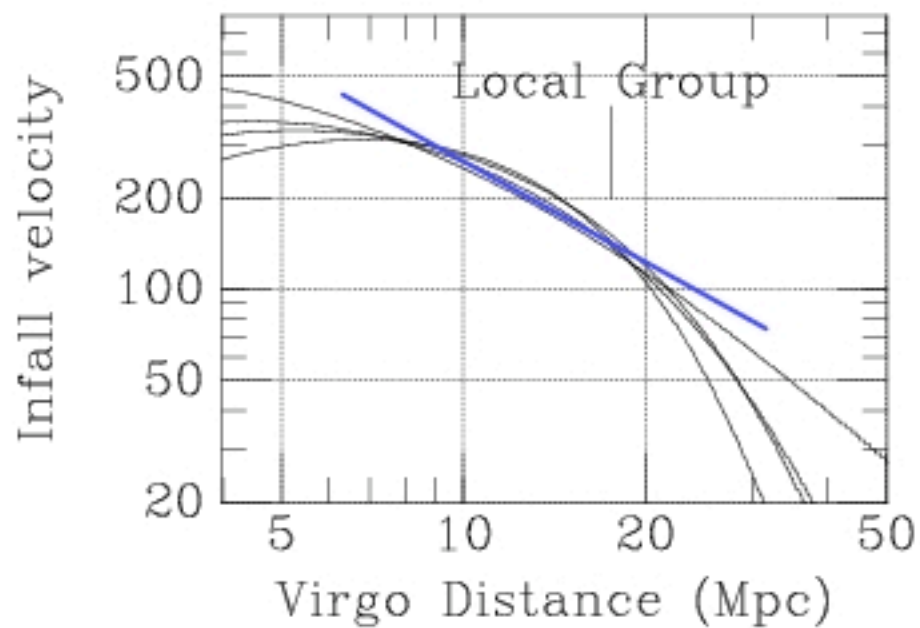
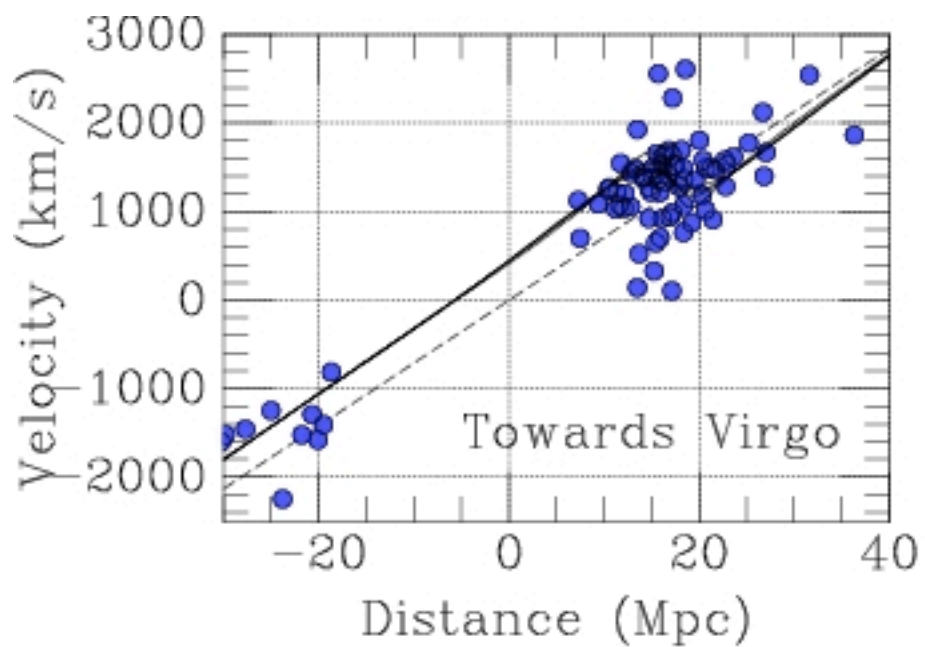
The SBF Survey of Galaxy Distances

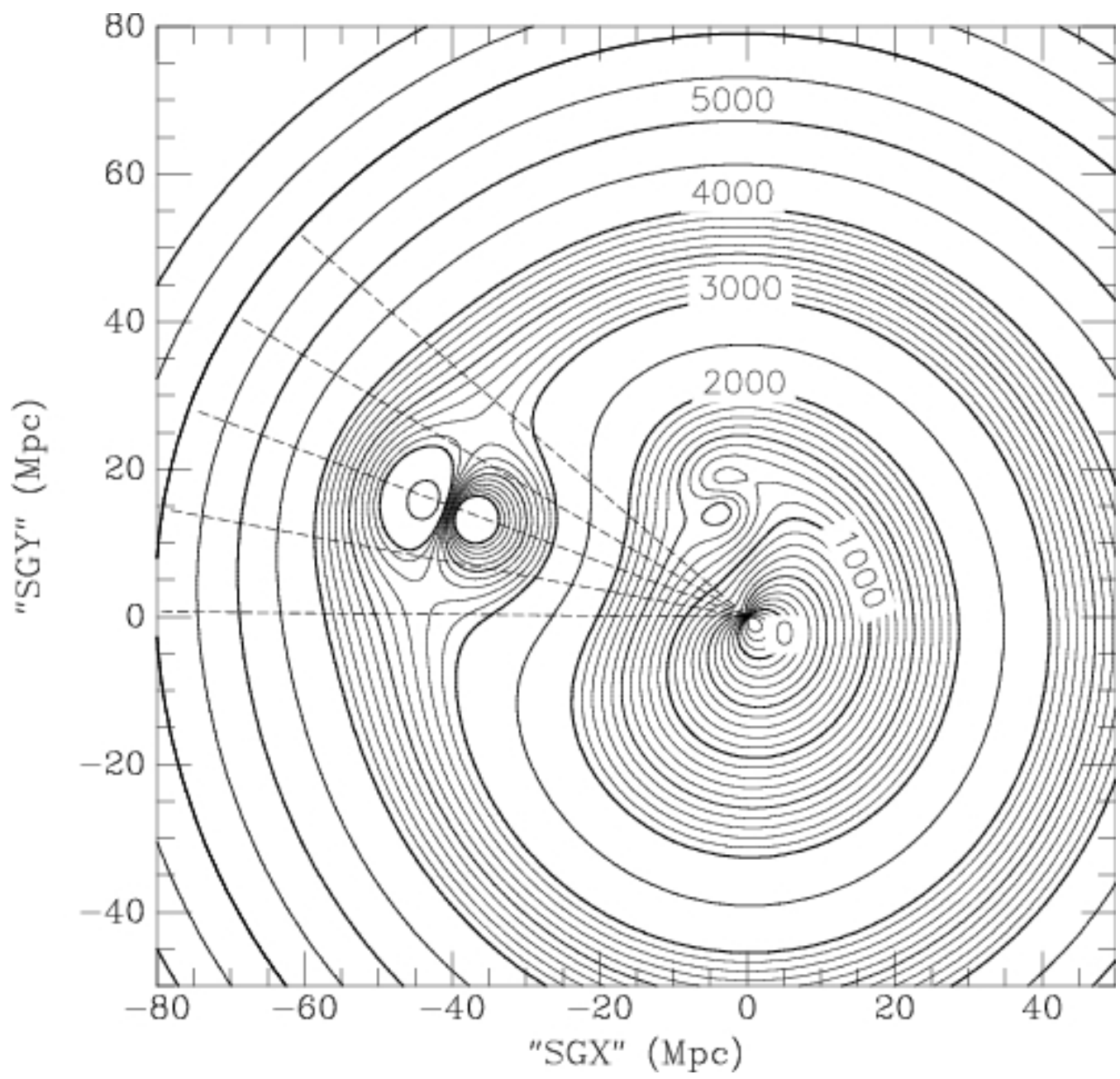


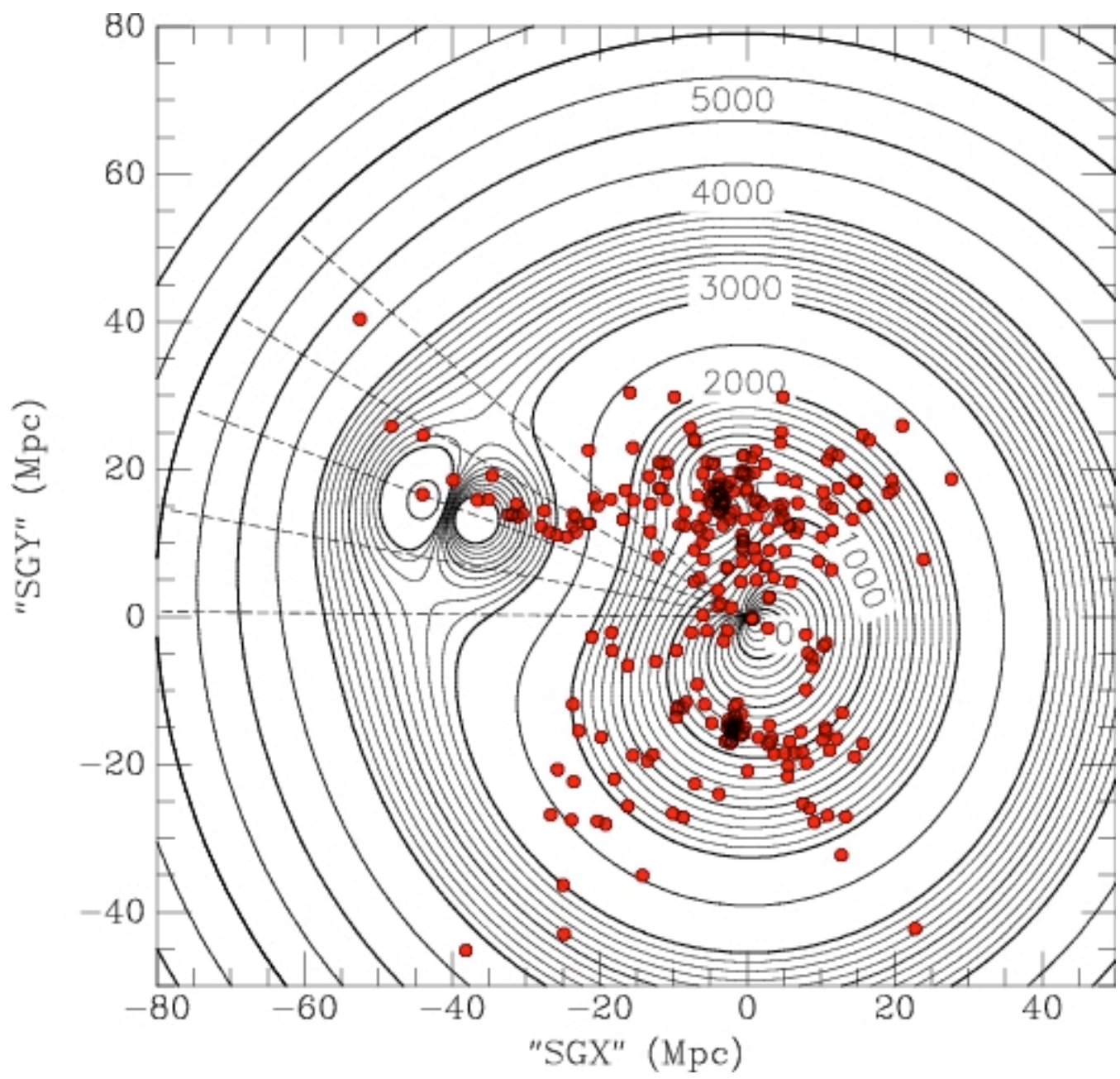
Data from:
MDM, CTIO,
KPNO, LCO, CFHT



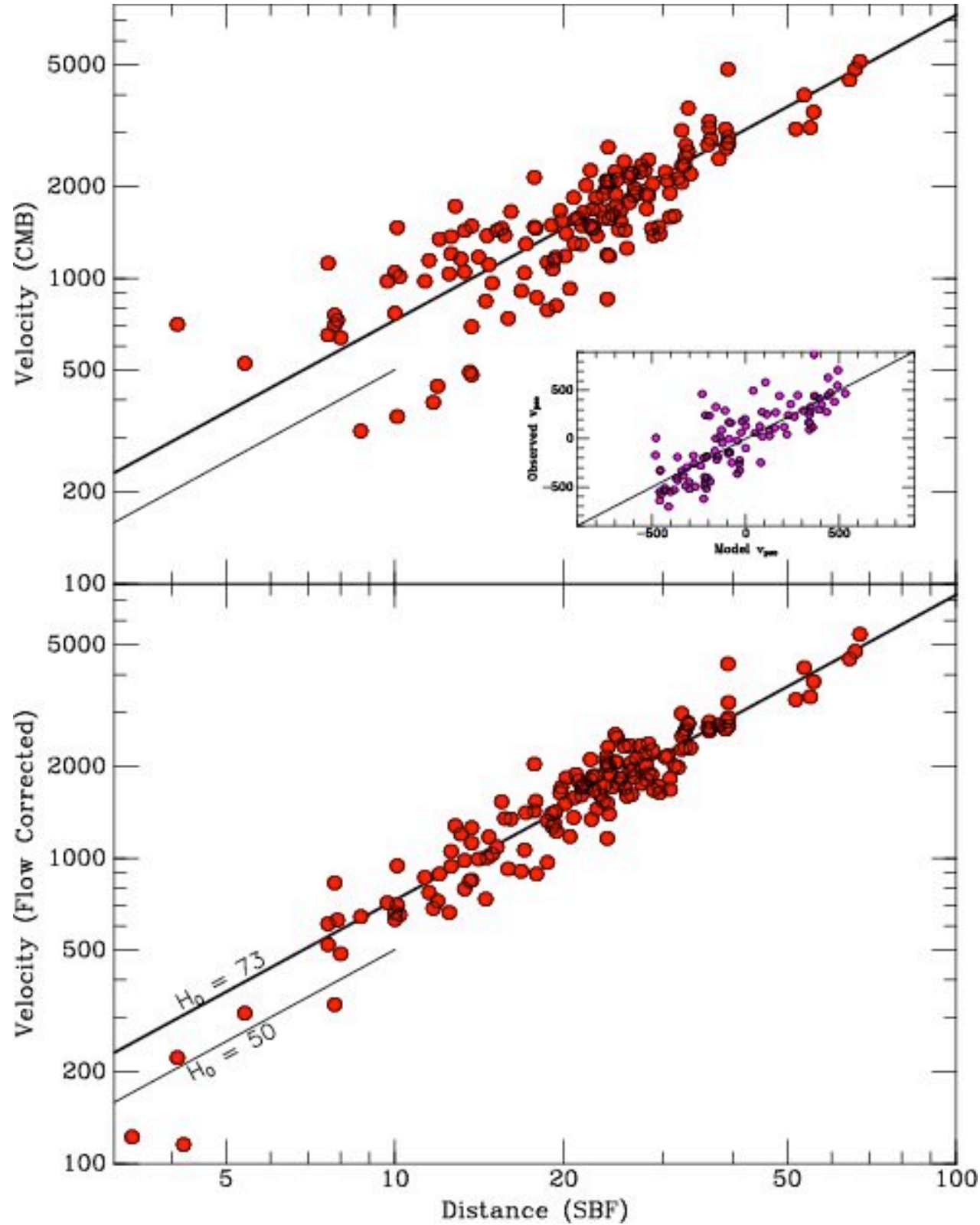
Tonry et al. (2000) used SBF distances and peculiar velocities to model the local velocity field using massive Virgo and Great Attractors, plus a residual dipole and quadrupole from masses outside the survey volume.







Hubble diagram:
raw velocity
versus distance



Hubble diagram
with velocities
corrected by SBF
flow model .

Tonry, Blakeslee, Ajhar
& Dressler 2000

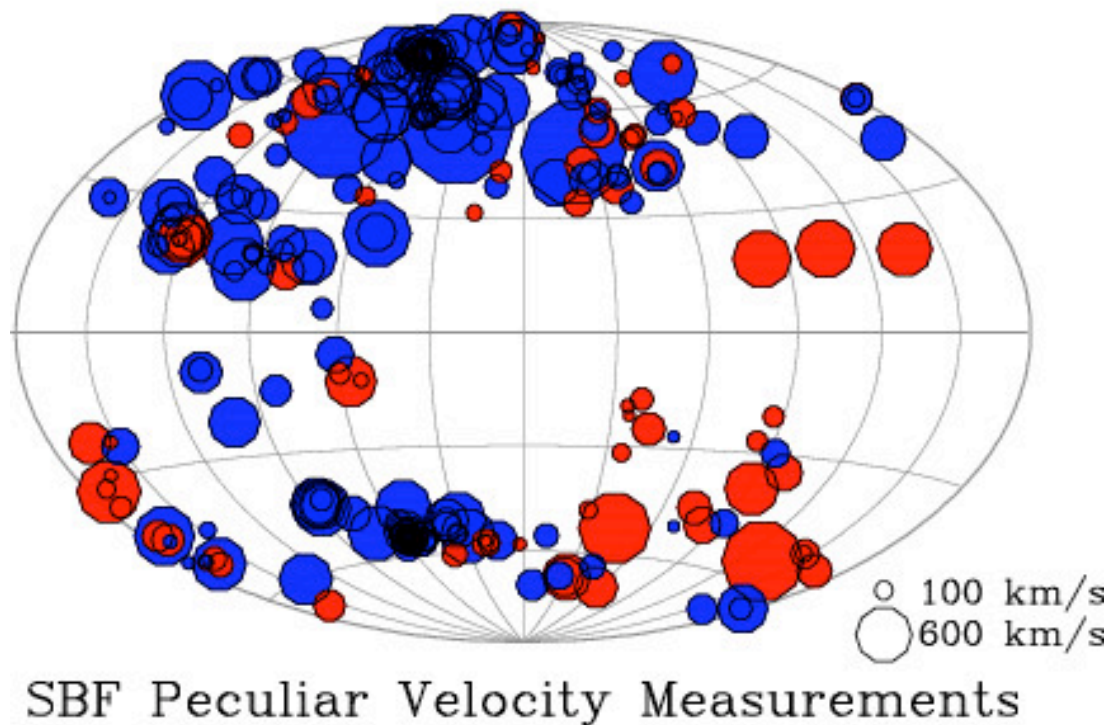
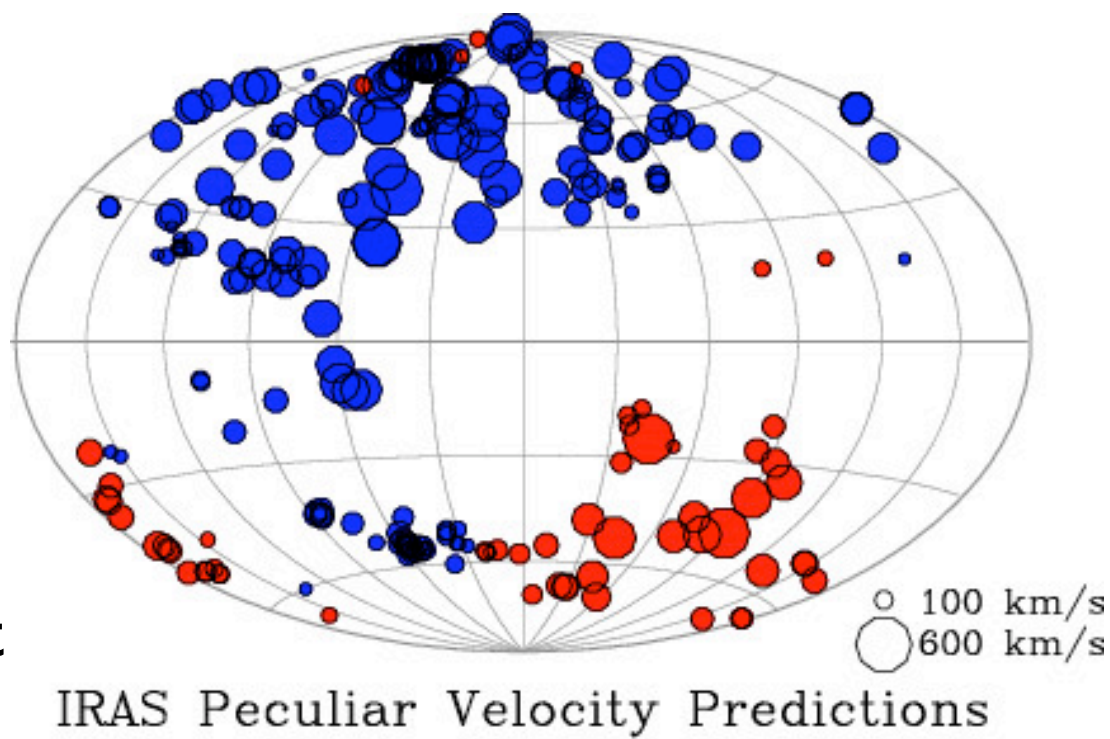
Direct Comparison of Peculiar Velocity Field to the Galaxy Density (and Gravity) Field

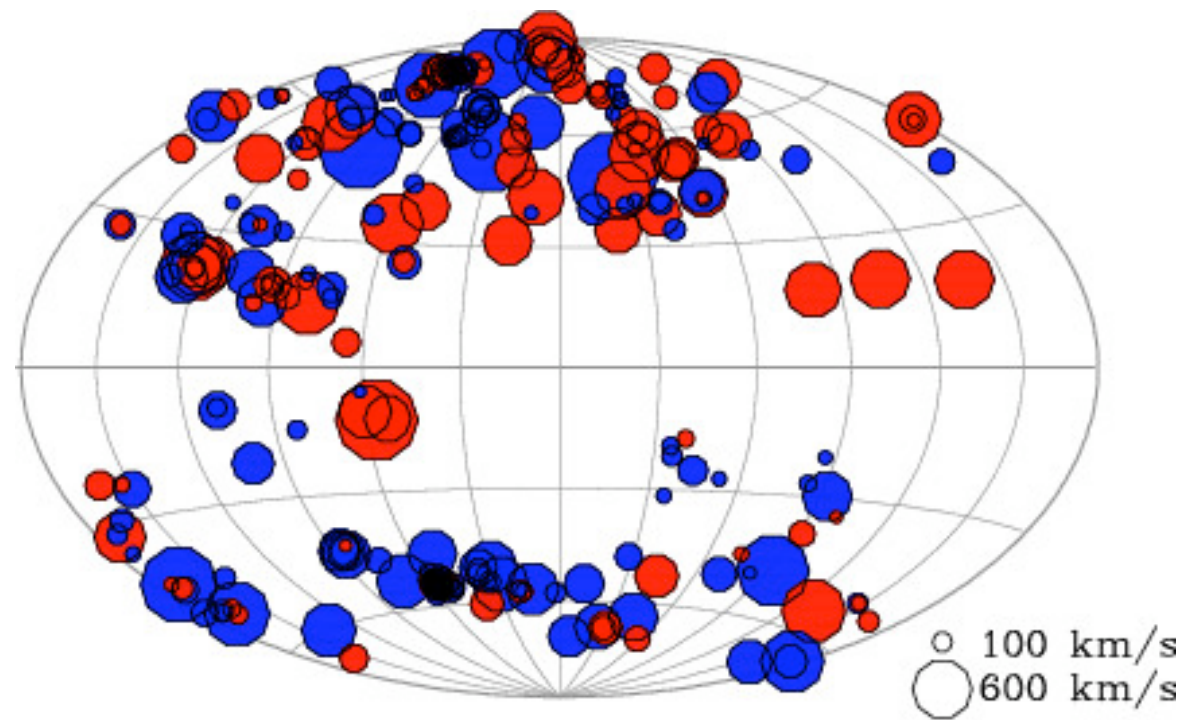
- The present-day peculiar velocity of a *field* galaxy (or group) is equal to the time-averaged gravitational acceleration from all nearby masses times the time since galaxy formation: $v_p = \langle \mathbf{g} \rangle \times t$
- To first order in linear perturbation theory (e.g., Peebles 1980), this can be rewritten to relate v_p to the mass density field:

$$v_p(\mathbf{r}) \approx \frac{\Omega^{0.6} H_0}{4\pi} \int d^3 \mathbf{r}' \delta_m(\mathbf{r}') \frac{\mathbf{r}' - \mathbf{r}}{|\mathbf{r}' - \mathbf{r}|^3}$$

- where Ω is the mean matter density of universe, H_0 is the Hubble constant, and δ_m is the mass density fluctuation field. Thus, peculiar velocities are (to 1st order) independent of Λ , and a good complement to CMB observations (which constrain $\Omega + \Lambda$).
- Usually assume linear biasing: $\delta_m = \delta_g / b$, where δ_g is galaxy number density field (can be found observationally) and b is the galaxy/matter biasing factor (e.g., $b = 1$ is an “unbiased” galaxy distribution).

The Local Group motion is evident in both the galaxy peculiar velocities and density field.

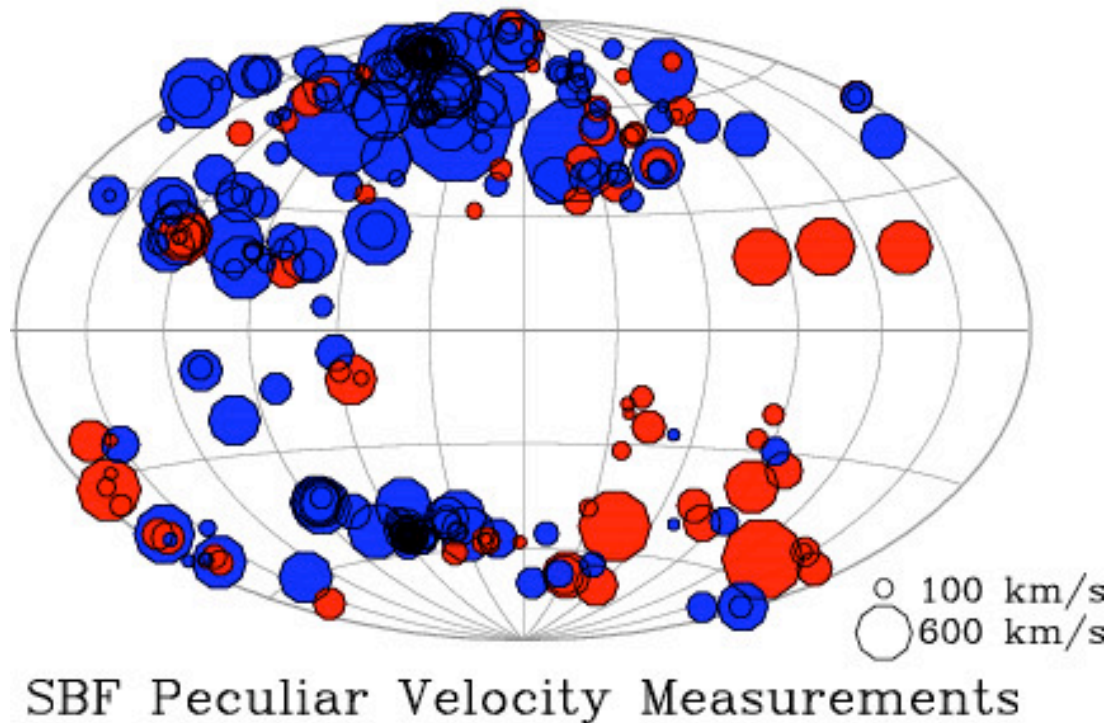
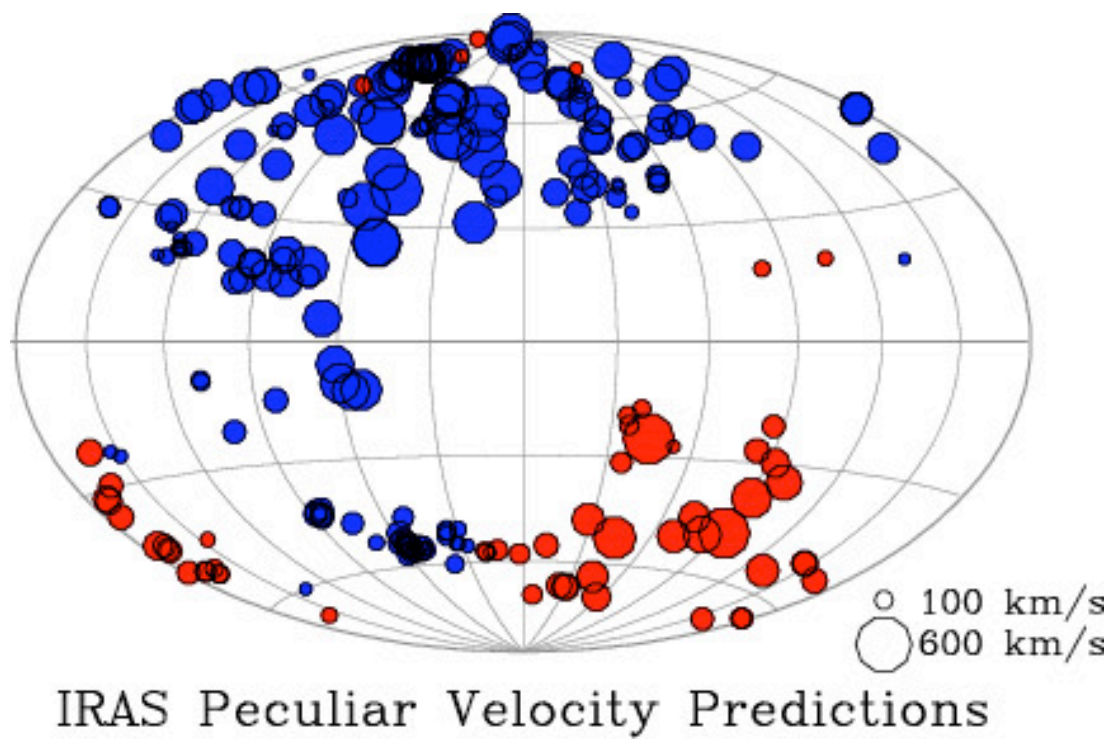




SBF-IRAS Residuals

$$v_p(\mathbf{r}) \approx \frac{\Omega^{0.6} H_0}{4\pi} \int d^3 \mathbf{r}' \delta_m(\mathbf{r}') \frac{\mathbf{r}' - \mathbf{r}}{|\mathbf{r}' - \mathbf{r}|^3}$$

Best fit with a
biasing factor
 $b = 1$ (galaxies
trace mass)
occurs for
 $\Omega_m = 0.25 \pm 0.05$

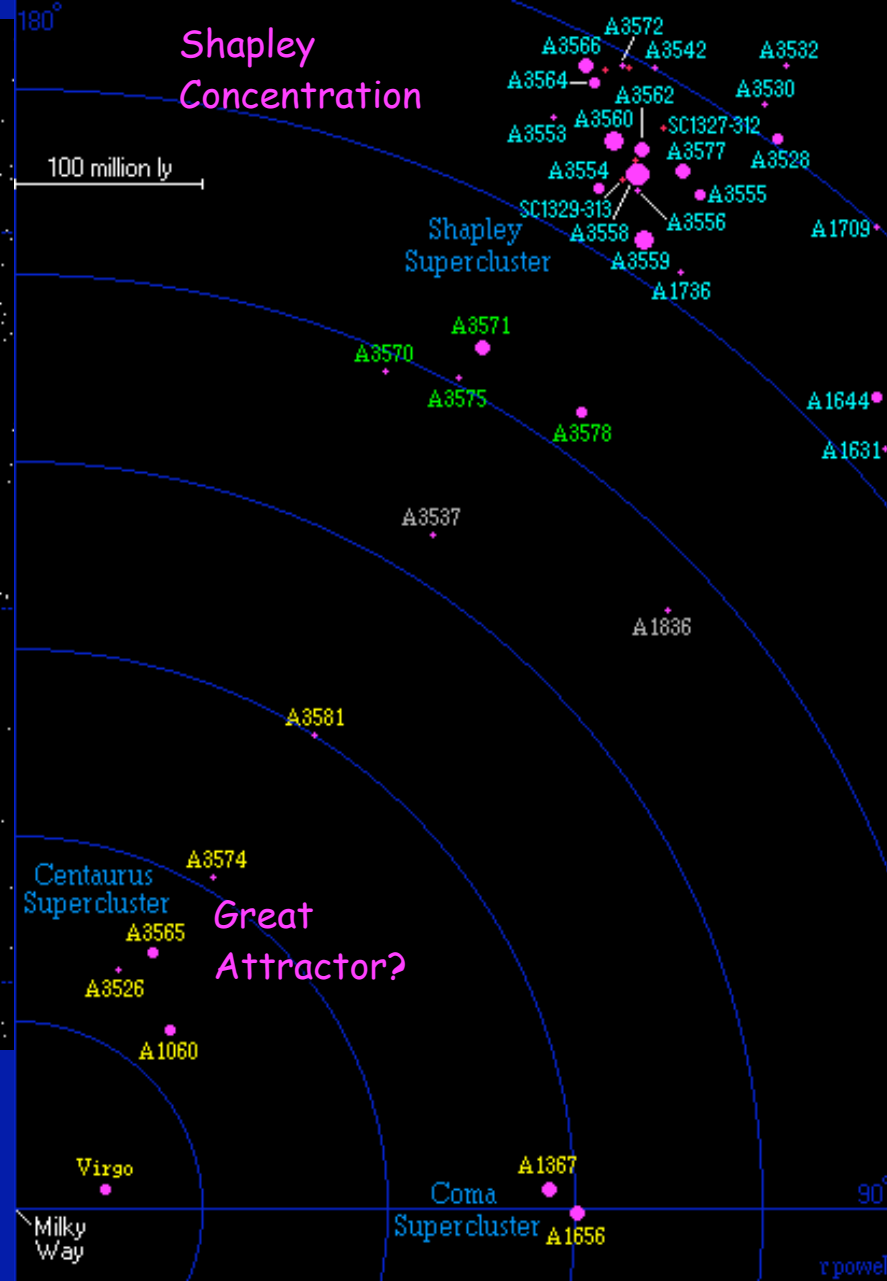
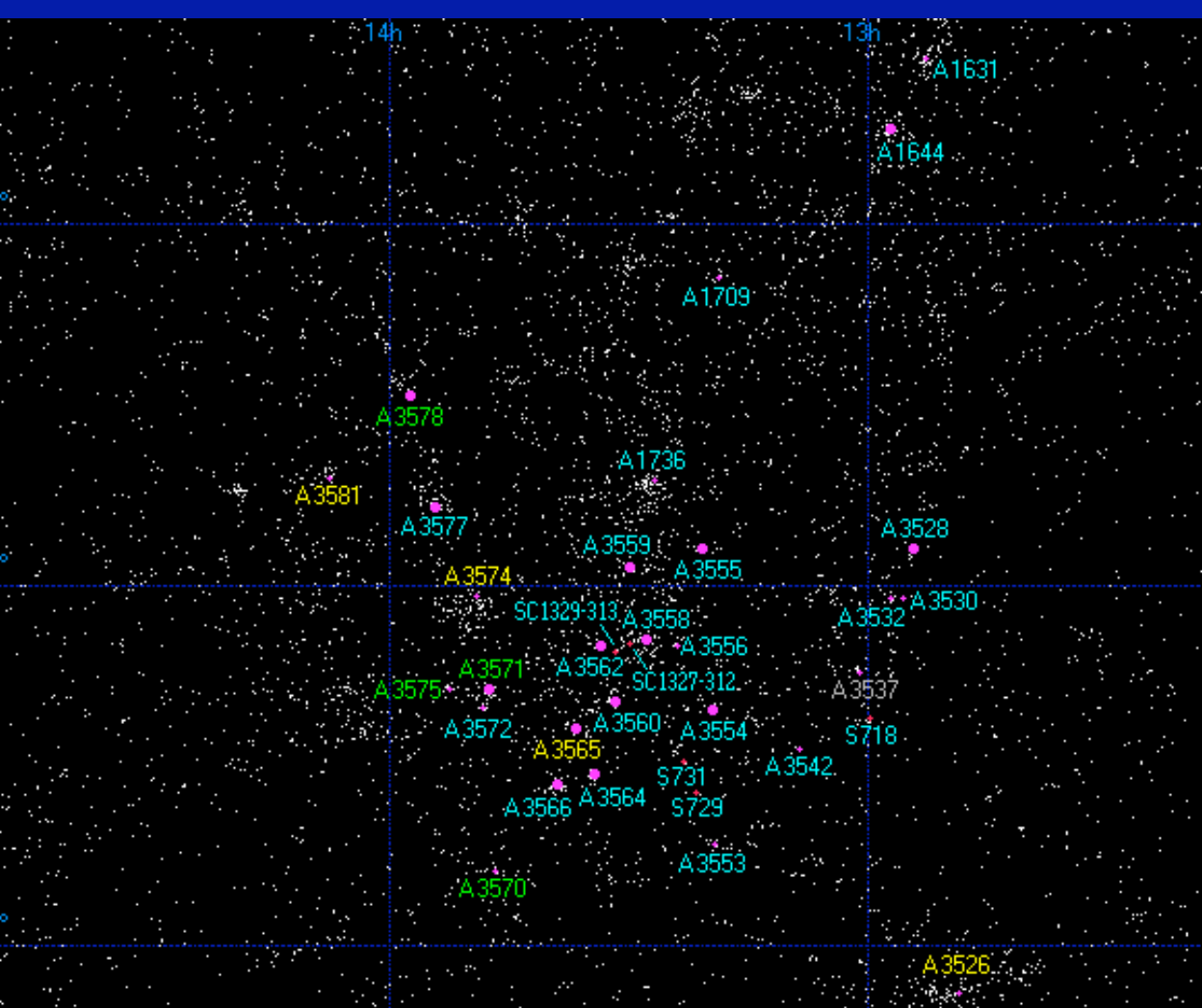


Peculiar Motions and Large Scale Structure

- Large modern redshift surveys provide easier, more direct ways to measure cosmological parameters. For instance, “baryonic acoustic oscillations” (BAO) measure a characteristic size in the large-scale distribution of galaxies, corresponding to the maximum wavelength of sound waves in the hot plasma prior to recombination. For details on BAO, see: <http://cmb.as.arizona.edu/~eisenste/acousticpeak/> .
- Both large-scale motions and BAO are a consequence of structure formation through gravitational instability, which means that initially overdense regions grow by pulling in more matter, which further increases their gravity, causing further mass accretion, and so on. Unlike peculiar velocities, the BAO signature can be measured as a function of redshift, providing a very powerful probe of cosmology.
- But peculiar motions remain the best way to constrain the total $3-D$ large-scale mass distributions of relatively nearby structures. For example, lensing only constrains projected mass and cannot be used very nearby; galaxy redshift surveys only measure galaxies, not the mass distribution; etc. Peculiar velocities can show how the total mass is distributed within the local universe.

How far can we go?

We (you, me, Milky Way, Local Group, etc) are falling towards the constellation Centaurus at 626 km/s (1,410,000 mph).

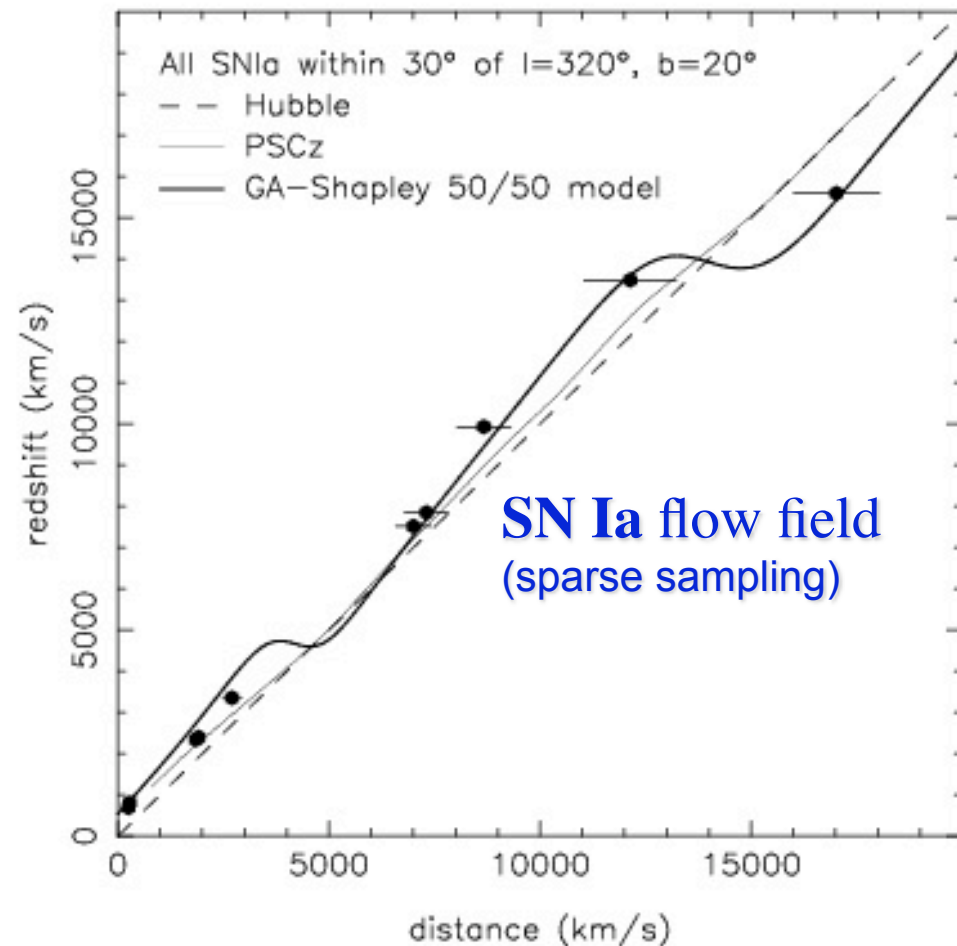
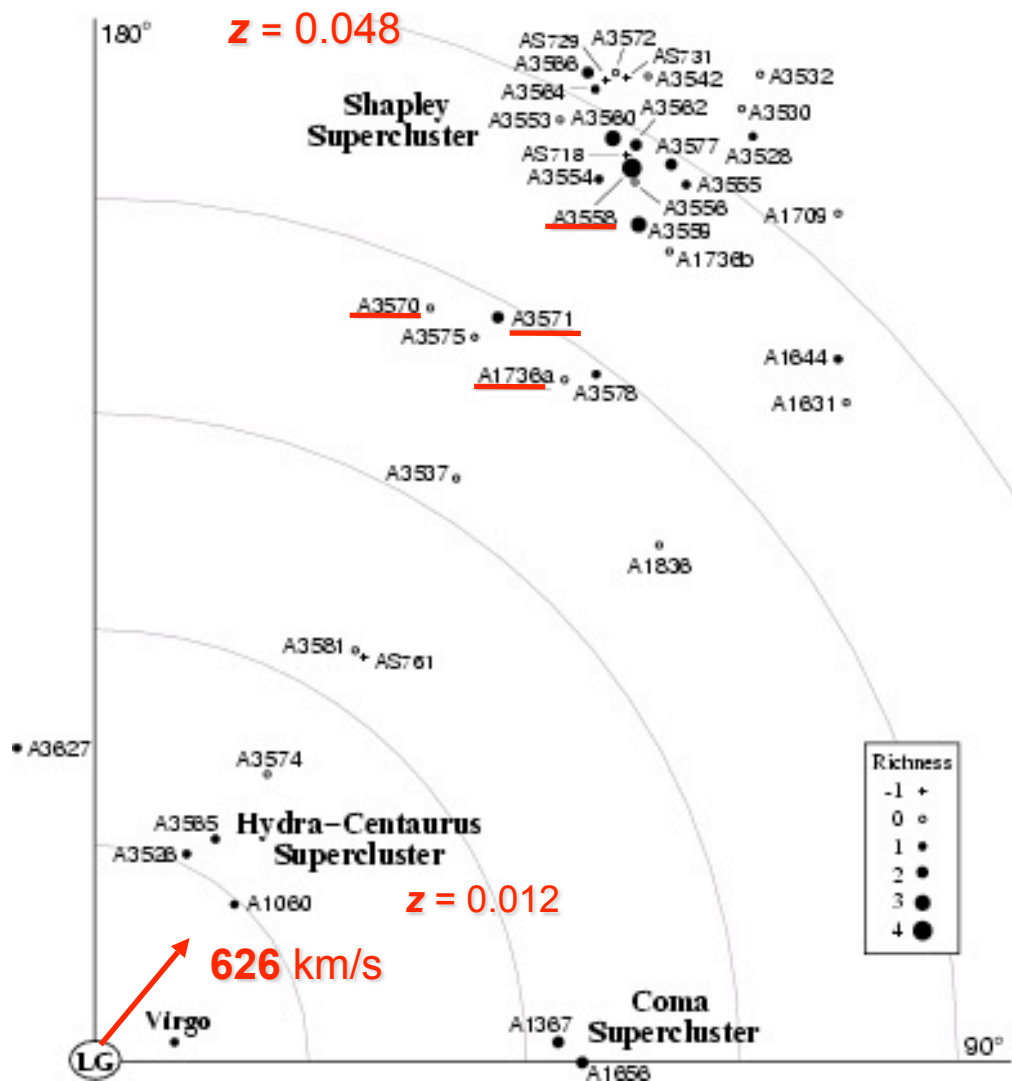


10 clusters in Shapley region are more X-ray luminous any in the “GA” region.

“Streaming Towards Shapley”

114-Orbit Large Program, analysis in progress

(Blakeslee, Lucey, R. Smith, & Tonry)



Determine mass of this extreme supercluster and its influence on Local motion by measuring infall of foreground clusters.

Abell 3558 core



Outlook

- It's an exciting time for cosmology and large-scale structure studies; peculiar velocity surveys remain an interesting way for studying local structure.
- The SBF method provides the best compromise between accuracy and distance range for studying peculiar motions and local structure. It also provides excellent measures of the relative distances to nearby clusters.
- Good near-term prospects for optical SBF with NGVS, Pan-STARRs, etc, which will have good seeing and multi-band coverage to ensure accurate stellar pop calibration.
- The future looks bright, especially for near-IR SBF studies with Gemini+MCAO, hopefully HST+WFC3/IR, JWST & TMT/EELT.